PhD degree in Molecular Medicine (curriculum in Molecular Oncology)

European School of Molecular Medicine (SEMM),

University of Milan and University of Naples "Federico II"

Settore disciplinare: Bio/10

REDUNDANT AND NON-REDUNDANT ROLES OF THE ENDOCYTIC ADAPTOR PROTEINS EPS15 AND EPS15L1 IN MAMMALS

Cinzia Milesi

IFOM, Milan

Matricola n. R10313

Supervisor: Prof. Pier Paolo Di Fiore

IFOM, Milan

Added Supervisor: Dr. Nina Offenhäuser

IFOM, Milan

Anno accademico 2015-2016

TABLE OF CONTENTS

LIST OF ABBREVIATIONS

Abbreviation	Definition
a.a.	arbitrary units
ANK	ankyrin
ANTH	AP180 N-terminal homology
AP-1	adaptor protein 1
AP-2	adaptor arotein 2
BAR	Bin-amphiphysin-RVS
Bd	boundary
BSA	bovine serum albumin
CADASIL	cerebral autosomal dominant arteriopathy with subcortical infarcts and leukoencephalopathy
CD	clathrin-dependent
cDKO	conditional double knockout
cEps15-KO or c15KO	conditional Eps15 knockout
CI	clathrin-independent
CPE	carboxypeptidase E
CCP	clathrin-coated pit
CCV	clathrin-coated vesicle
CDE	clathrin-dependent endocytosis
CF	citofluorimetry
CHC	clathrin heavy chain
CHO	chinese hamster ovary
CIE	clathrin-independent endocytosis

CLASP	clathrin-associated sorting protein
CLC	clathrin light chain
CLIC	clathrin-independent carrier
CLL	chronic lymphocytic leukemia
CMV	cytomegalovirus
Co-A	co-activator
Co-IP	co-immunoprecipitation
Crn7	coronin7
CSL	CBF1/Suppressor of Hairless/Lag-1
CtxB	cholera toxin B
Dx	deltex
ddH_2O	distilled deionized water
DKD	double knock-down
DKO or 15/L1-DKO	double knockout
Dll1	delta-like 1
DMT-1	divalent metal transporter 1
DNA	deoxyribonucleic acid
DOS	delta and OSM-11-like proteins
DOX	doxycycline
Dpc	days post-coitum
DPF	aspartic acid-proline-phenylalanine
DSL	Delta/Serrate/LAG-2
ECGS	endothelial cell growth supplement
ECL	enhanced chemiluminescent
EE	early endosome

EGF	epidermal growth factor
EGFR	epidermal growth factor receptor
EH	Eps15 homology
EHBP-1	Eps15 homology domain containing protein-binding protein 1
ENTH	epsin N-terminal homology
Eps15	epidermal grow factor protein substrate 15
Eps15-KO or 15KO	Eps15 knockout
Eps15L1	epidermal grow factor protein substrate 15-like1
Eps15L1-KO or L1KO	Eps15L1 knockout
ESCRT	endosomal sorting complex required for transport
FACS	fluorescence activated cell sorting
FBS	fetal bovine serum
FEME	fast endophilin-mediated endocytosis
FSC	forward scatter
GEEC	glycosyl phosphatidylinositol-anchored proteins enriched early endosomal compartment
GPCR	G-protein-coupled receptor
GPI-AP	glycosylphosphatidylinositol-anchored proteins
HBSS	Hanks' balanced salt solution
HD	heterodimerization domain
HET	heterozygous
HRP	horseradish peroxidase
HSC-70	heat shock cognate 70
Ht	heart
I	iodinated
IF	immunofluorescence

IL-2R-β	interleukin-2 receptor-β
ILV	intraluminal vesicle
IP	immunoprecipitation
Itsn	intersectin
K_e	endocytic rate constant
KD	knock-down
kDa	kilodalton
KO	knockout
LB	lysogeny broth
Lb	limb bud
LDLR	low-density lipoprotein receptor
LNR	Lin12-Notch repeat
Lqf	liquid facet
MAM	mastermind
MCV	mean corpuscular volume
MEFs	mouse embryonic fibroblast
MetOH	methanol
MHCI	class I major histocompatibility complex
Mib	mind bomb
MW	molecular weight
MVB	multi vesicular body
NECD	Notch extracellular domain
Neur	neuralized
NEXT	Notch extracellular truncation
NICD	Notch intracellular domain

NLS	nuclear localization sequence
NPF	asparagine-proline-phenylalanine
NRAMP-2	natural resistance associated macrophage protein 2
NRR	negative regulatory region
NSCLC	non-small-cell lung carcinomas
NTMIC	Notch transmembrane and intracellular domain
P	phospho
P	p-value
PBS	phosphate-buffered saline
PEST	proline/glutamic acid/serine/threonine
PI3K	phosphoinositide 3-kinase
PIP2	phosphatidylinositol 4,5-bisphosphate
PIP3	phosphatidylinositol 3,4,5-trisphosphate
PK	proteinase K
PLCγ1	phospholipase Cγ1
PM	plasma membrane
PmT	polyoma middle T
PTB	phospho-tyrosine-binding
PTHR	parathyroid hormone receptor
RAM	RBPjk association module
RBC	red blood cells
RDW	red cell distribution width
RNA	ribonucleic acid
RTK	receptor tyrosine kinase
S	site

SNX9	sorting nexin 9
SOP	sensory organ precursor
SSC	side scatter
Su(dx)	suppressor of deltex
SV40	simian virus-40
SVR	synaptic vesicle recycling
TAD	trans-activation domain
TAE	tris-acetate-EDTA
T-ALL	T-acute lymphoblastic leukemia/lymphoma
TBS	tris-buffered saline
TE	tris-EDTA
Tg	transgenic
TetO2	tetracycline operator 2
TetR	tetracycline repressor
Tf	transferrin
TfR	transferrin receptor
TGFβR	tumor growth factor β receptor
TGN	trans-Golgi network
TMD	transmembrane domain
TMX	(Z)-4-hydroxytamoxifen
T-NHL	T-cell non-Hodgkin lymphoma
TMICD	trans-membrane intracellular domain
UAS	upstream activating sequence
UBD	ubiquitin-binding domain
UIM	ubiquitin interacting motif

VacA	vacuolating toxin A
VE	vascular endothelial
VEGF	vascular endothelial growth factor
VEGFR	vascular endothelial growth factor receptor
WB	western blot
WT	wild type
YFP	yellow fluorescent protein
YFP-	negative cells for YFP
YFP+	positive cells for YFP
YFP++	highly positive cells for YFP

FIGURE INDEX

TABLE INDEX

ABSTRACT

Eps15 and Eps15L1 are two endocytic adaptor proteins involved in both clathrin-dependent and clathrin-independent endocytosis of receptor tyrosine kinases. Due to their homology, Eps15 and Eps15L1 are thought to be redundant in several cellular processes. Their redundancy, however, has never been demonstrated in *in vivo* model systems.

Our laboratory has generated genetically engineered mice to unravel the physiological functions of Eps15 and Eps15L1. We found that Eps15-KO (knockout) mice were healthy and fertile, while Eps15L1-KO mice died at birth because of neural defects, showing the specific function of Eps15L1 in neuronal development. Importantly, Eps15/Eps15L1-DKO (double knockout) mice had a more severe phenotype, dying at midgestation, suggesting redundancy in one or more fundamental developmental programs.

The aim of this thesis project was to investigate redundant and non-redundant roles of Eps15 and Eps15L1, with the final goal to unmask the underlying causes of embryo lethality of Eps15/Eps15L1-DKO mice.

Since Eps15/Eps15L1-DKO mice displayed a Notch loss-of-function phenotype, accompanied by a downregulation of Notch target genes, our initial hypothesis was that Eps15 and Eps15L1 were redundantly required in the regulation of the Notch signalling. To address this issue, we set-up a co-culture model system to recapitulate Notch signalling. In detail, we used MEFs (mouse embryonic fibroblasts) derived from Eps15- and Eps15L1-KO mice as a model system for the signal-sending cell and we co-cultured them with CHO (chinese hamster ovary) cells expressing the Notch receptor, as signal receiving cells. We found that Eps15L1, but not Eps15, played a non-redundant role in Notch signalling activation. This finding indicated that impaired Notch signalling was not responsible for the more severe phenotype observed in Eps15/Eps15L1-DKO mice

compared to single KO mice. Whether Eps15 and Eps15L1 are required in signal-receiving cells will be addressed, using MEFs as a model for the signal-receiving cell.

We found that angiogenesis was seriously compromised in Eps15/Eps15L1-DKO mice and, therefore, hypothesized that impaired vascular development might be the major cause of midgestation lethality of these mice. To address this issue, we generated cDKO (conditional Eps15/Eps15L1-DKO mice), which lack Eps15 and Eps15L1 in endothelial and hematopoietic cells. We found that cDKO mice displayed vascular defects but did not recapitulate the severe phenotype of constitutive DKO mice. This finding indicated that impaired angiogenesis was not the major lethality cause of constitutive DKO mice. However, by *in vitro* studies in endothelial cells, we found that Eps15 and Eps15L1 redundantly regulated VEGFR-2 turnover, thus indicating a possible cell-autonomous function of the proteins in vascular homeostasis, even if not sufficient to cause embryo lethality when functionally impaired.

Previous *in vitro* studies have demonstrated a role for Eps15 and Eps15L1 in the CDE (clathrin-dependent endocytosis) of EGFR (epidermal growth factor receptor) and TfR (transferrin receptor). To confirm this role in a clean background, we used MEFs as a model system. By using radioactive assays, we found that Eps15 and Eps15L1 redundantly regulate the CDE of TfR. Indeed, in DKO cells, the K_e (endocytic rate constant) of the TfR was reduced to ~50% and, as a consequence, surface levels of TfR were increased, while single KO cells showed only a minor, if any, defect. Moreover, in DKO cells, we found that the number of AP-2-positive structures (which label clathrin-structures that form during CDE) was increased, but the structures were significantly smaller in size. Whether the maturation of clathrin-coated structures is altered in DKO cells will be addressed by live imaging studies.

Next, we asked whether the role of Eps15 and Eps15L1 in TfR internalization had a physiological relevance *in vivo*. In detail, since TfR is essential for the biology of erythroid cells, we investigated whether erythroid development was impaired in cDKO mice, lacking

Eps15 and Eps15L1 in endothelial and hematopoietic cells. We found that these mice suffered from microcytic hypochromic anemia: RBCs (red blood cells) had reduced MCV (mean corpuscular volume) and high RDW (red blood cell distribution width, index of anisocytosis), and reticulocyte counts were higher. These findings suggest that Eps15 and Eps15L1 redundantly regulate erythroid development. However, since cDKO mice did not recapitulate the severe phenotype of constitutive DKO mice, altered erythroid development *per se* was not the only cause of the early lethality of constitutive DKO mice.

Further studies are required to investigate whether altered development of Eps15/Eps15L1-DKO erytroid cells correlates with increased surface levels of TfR and reduced iron uptake. These findings, combined with previous data generated in our laboratory, highlight that Eps15 and Eps15L1 regulate several cellular processes, both in a redundant and in a non-redundant manner. Functional impairment of these processes, together with other unexplored processes, might addictively contribute to the DKO phenotype.

Chapter 1

INTRODUCTION

1. Endocytosis

1.1. Role of endocytosis

Endocytosis is a mechanism by which eukaryotic cells internalize nutrients and/or other types of molecules, which, at the same time, regulate the composition of the PM (plasma membrane).

Endocytosis initially evolved as a simple process for nutrient uptake. A consequence of endocytosis was the establishment of new endomembrane systems, which lead to cellular compartmentalization and, therefore to the acquisition of the eukaryotic cell plan. Moreover, throughout evolution, an intricacy of entry portals and sorting modalities for different cargoes appeared. Endocytosis was embedded not only with the ability to provide nutrients, but also to regulate the presence of specific proteins and lipids on the PM and to offer new signalling platforms. As discussed in detail later, these new functions allowed endocytosis to act as a master organizer of cell signalling.

To our knowledge, endocytosis permeates every aspect of cell physiology. Indeed, due to its ability to contribute to signalling from membrane receptors, endocytosis regulates fundamental cellular processes such as proliferation, differentiation, apoptosis, metabolism and development. Due to its ability to differentially distribute membrane receptors within the cell, endocytosis controls polarized functions, such as directed cell migration, cell-fate decisions, epithelial-cell polarization, growth cone movement, tissue morphogenesis and cell invasion. Moreover, due to the acquisition of new functions by the endocytic

machinery, endocytosis has become paramount also in cellular programs not directly linked to membrane dynamics, such as mitosis, cellular reprogramming, miRNA biogenesis and transcription (Sigismund, Confalonieri et al. 2012).

The deep intertwining between cell physiology and endocytosis explains why perturbations in the endocytic pathway are responsible for several inherited, neurological, metabolic, autoimmune, infectious and hyperproliferative diseases, among which pathologies of high social impact, such as Alzheimer's disease, diabetes and cancer (Sigismund, Confalonieri et al. 2012).

Deconvolution of the endocytic pathway is therefore important not only for a complete understanding of cellular physiology but also for the development of new strategies in fighting diseases.

1.2. Multiple entry portals and sorting routes

Multiple pathways of endocytosis exist. A rough classification of endocytic paths takes into account cargo size. Large particles (about 500 nm) are taken up by phagocytosis, as it is generally the case for debris, apoptotic cells and pathogens. This type of endocytosis is typical of only few specialized cells (Swanson 2008). Uptake of large amounts of fluid occurs by macropinocytosis, process that it ubiquitous to almost all eukaryotic cells (Kerr and Teasdale 2009). Both phagocytosis and macropinocytosis involve large rearrangements of the PM, which are guided by the remodelling of the actin cytoskeleton and Rho-GTPases (Insall and Machesky 2009). Micropinocytic events, instead, are characterized by smaller invaginations (200 nm) and are classified into two distinct pathways, known as CDE (clathrin-dependent endocytosis) and CIE (clathrin-independent endocytosis) (Doherty and McMahon 2009) (Figure 1).

The CDE is the best characterized pathway and its defining feature is the recruitment of soluble clathrin from the cytoplasm to the PM. PM receptors that enter through the CDE,

may undergo stimulated/ligand dependent-endocytosis, such as EGFR (epidermal growth factor receptor) and GPCRs (G-protein-coupled receptors), or constitutive/ligand-independent endocytosis, such as TfR (transferrin receptor) and LDLR (low-density lipoprotein receptor) (McMahon and Boucrot 2011).

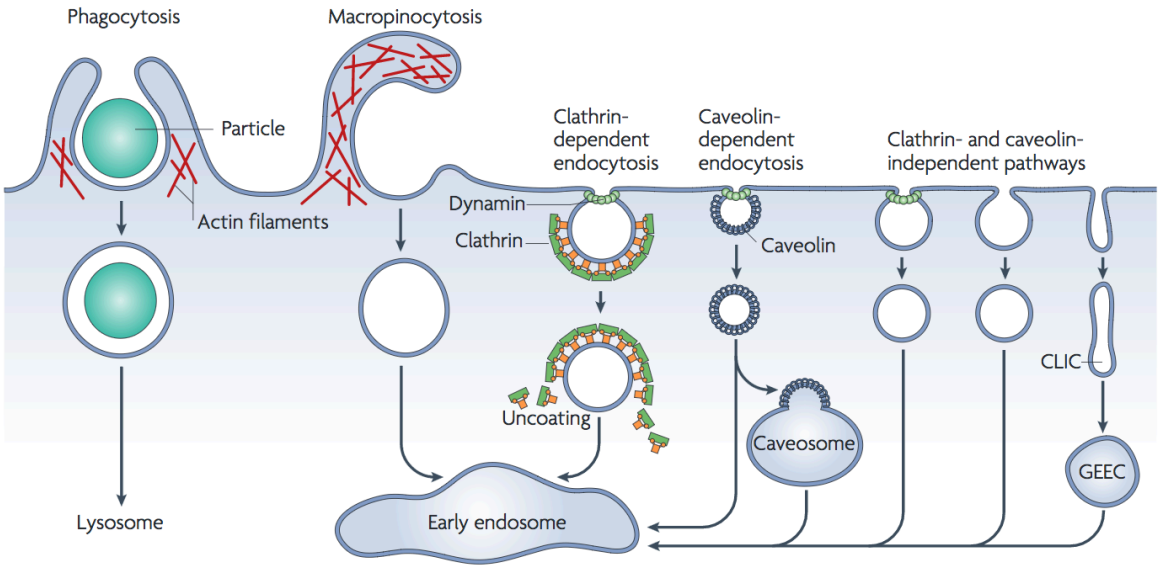

Figure 1. Endocytic pathways**.**

From left to right: large solid particles are internalized through phagocytosis, whereas large fluid particles are taken up through macropinocytosis. Both pathways are actin-dependent. Numerous smaller cargoes, instead, are endocytosed by CD (clathrin-dependent) and/or CI (clathrin-independent) mechanisms. CDE, the best-characterized pathway, involves the coat protein clathrin and the fission GTPase dynamin. CIE, which includes both caveolin-dependent and caveolin-indipendent pathways, instead, may require the GTPase dynamin. While material internalized by phagocytosis is directly transported into lysosomes, most internalized cargoes are delivered to the EE (early endosome) via vesicular (clathrin- or caveolin-coated vesicles) or tubular intermediates (knowns as CLICs, that is clathrin- and dynamin-independent carriers). Before reaching the EE, some cargoes can traffic to intermediate compartments, such as GEECs (glycosyl phosphatidylinositol-anchored proteins enriched early endosomal compartments). Recent findings (Hayer, Stoeber et al. 2010), instead, question the existence of the caveosome as an intermediate compartment of caveolin-dependent endocytosis (from Mayor and Pagano 2007).

The EGFR and the TfR are the most popular experimental systems in the study of mechanisms underlying stimulated and constitutive CDE, respectively. In contrast, the machinery that regulates the different pathways of CIE has only recently started to emerge. Each entry mechanism is related to a specific cellular function. In the case of phagocytosis, for example, material has to be promptly processed. For this reason, the resulting vesicle, named phagosome, is directly fused with lysosomes for degradation (Gagnon, Duclos et al. 2002, Jutras and Desjardins 2005). On the contrary, most of the other entry mechanisms regulate cargo degradation as well as receptor recycling. For this purpose, internalized cargoes are transported to coordinating stations, the EEs (early endosomes), where they are either sorted to the degradative pathway, towards lysosomes, or to the recycling pathway, towards the PM, or retrotransported to the TGN (trans-Golgi network).

The endocytic trafficking across the subcellular compartments is regulated by two main classes of molecules: the Rab (Miaczynska and Zerial 2002, Galvez, Gilleron et al. 2012) (Stenmark 2012) and the Arf families of small GTPases (D'Souza-Schorey and Chavrier 2006).

Rab5 regulates the transport from the PM to the EE (Behnia and Munro 2005), where cargoes are then recycled back to the PM through either a fast Rab4-dependent or a slow Rab8/Rab11-dependent recycling route (Stenmark 2009). In other cases, cargoes are destined to degradation in lysosomes via a route depending on Rab7 (Stenmark 2009).

Arf6, instead, is involved in an additional recycling pathway, which is mainly used by receptors internalized through CIE, such as MHCI (class I major histocompatibility complex), although some CD-internalized cargoes can also be recycled through this pathway (D'Souza-Schorey and Chavrier 2006).

Regarding commitment into the degradative pathway, a key signal to enter this pathway is cargo ubiquitination. Ubiquitinated-cargoes are recognized by protein complexes called ESCRT (endosomal sorting complex required for transport). These complexes, composed of UBD (ubiquitin-binding domains)-containing proteins, act as follows: ESCRT-0, which

is composed of Hrs and STAM, is located in the EE and sequesters ubiquitinated cargoes; ESCRT-I and ESCRT-II mediate invagination of the membrane; ESCRT-III drives the pinching off and the release of the invaginations that will constitute the ILVs (intraluminal vesicles) of the MVB (multivesicular body), an endocytic station that directs cargoes to lysosomes. ESCRT-III, moreover, recruits deubiquitinating enzymes that remove ubiquitin from the cargo, thus allowing the continuous replenishment of the free ubiquitin pool (Raiborg and Stenmark 2009, Hurley and Hanson 2010).

1.3. The CDE

CDE is an important endocytic mechanism that accounts for a large proportion of internalization events. A wide range of molecules, including nutrient-receptor complexes, membrane transporters, adhesion molecules and signalling receptors are endocytosed through CDE. CDE is also involved in SVR (synaptic vesicle recycling). Moreover, CDE is exploited by pathogens, such as toxins, viruses and bacteria, to entry into cells. Anthrax, for example, is one of the larger toxins entering the cells through CDE (Doherty and McMahon 2009).

In CDE, cargoes are recruited into PM invaginations called CCPs (clathrin-coated pits). Several adaptor proteins, among which AP-2, bridge the cargo to clathrin, whose polymerization drives the progressive invagination of the pit. The CCP is then released into the cytoplasm as a CCV (clathrin-coated vesicle) trough the action of the GTPase dynamin.

1.3.1. The main components of CDE: clathrin, AP-2 and CLASPs

Clathrin, AP-2 and CLASPs are the main components of CDE (Figure 2). The defining feature of CDE is the recruitment of soluble clathrin from the cytoplasm to the PM, where it assembles into a polygonal lattice to coat intracellular membrane surface (McMahon and

Boucrot 2011). The assembly subunit of a clathrin coat is a three-legged structure referred to as triskelion, which is composed of three copies of the CHC (clathrin heavy chain), with a mass of 180 kDa, and three copies of the CLC (clathrin light chain), with a mass of 25 kDa. While CHCs provide the structural backbone of the clathrin lattice, CLCs seem to regulate the formation and the disassembly of the clathrin lattice (Brodsky, Chen et al. 2001). In a CCP, polymerization of clathrin results in the stabilization of membrane curvature and displacement of cargoes and adaptor proteins to the edge of the forming vesicle (Tebar, Sorkina et al. 1996, Saffarian, Cocucci et al. 2009). In some cell types, a substantial pool of clathrin can also be found as flat lattices, referred to as clathrin plaques. Clathrin plaques are mostly found at the adherent membrane surface and are longer-lived than CCPs (Saffarian, Cocucci et al. 2009). The exact function of clathrin plaques is still under investigation.

Other actors of CDE are the endocytic adaptor proteins, whose function is to bridge cargoes with clathrin. To achieve bridging with clathrin, adaptors proteins establish multiple and redundant interactions with some or all of the four types of binding partners: lipids, cargoes, clathrin and other adaptor proteins. Endocytic adaptor proteins are divided into two main groups: multimeric adaptor proteins (e.g., AP-2) and monomeric adaptor proteins, also called CLASPs (clathrin-associated sorting proteins).

AP-2 is the most abundant non-clathrin constituent of purified CCVs and it is the prototypal and best characterized multimeric endocytic adaptor. It consists of two large subunits (α, β2), one medium subunit (μ2) and one small subunit (σ2). The large subunits can be subdivided into a trunk domain (70–75 kDa) and an appendage domain (~30 kDa), which are connected by an extended, proteolytically sensitive, flexible linker (Zaremba and Keen 1985, Kirchhausen, Nathanson et al. 1989). The large subunit trunk domains plus the medium and small subunits represent the biochemically stable AP-2 core domain. AP-2 has the ability to interact with membrane lipids, clathrin, cargoes and CLASPs. Cargoes, specifically, can be bound directly, through the recognition of a tyrosine- or a di-leucine-

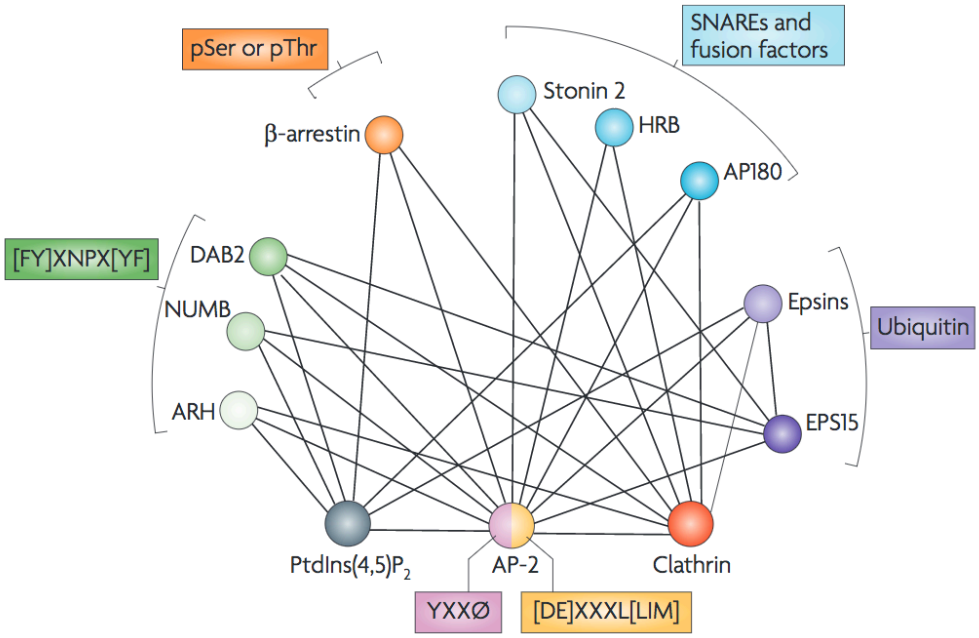

Figure 2. The endocytic clathrin interactome**.**

A network of interactions is assembled during CDE. The core adaptor AP-2 connects transmembrane cargoes to the clathrin coat. Cargoes are then recognized either directly, through their tyrosine- (YXX∅) or di-leucine- ([DE]XXXL[LIM]) based motifs, or indirectly, through several accessory adaptor proteins, named CLASPs. Each class of accessory adaptor proteins decodes a specific cargo signal: ARH, Numb and Dab2 recognize the peptide sequence [FY]XNPX[YF]; epsin and Eps15 proteins bind to ubiquitinated cargoes; β-arrestins internalize phosphorylated receptors. In contrast to these mechanisms, little is known about the packaging of SNAREs, which generally lack known sorting signals and do not seem to be ubiquitinated (from Traub 2009).

based motif, or indirectly, through CLASPs (Traub 2009). The μ2-domain recognizes PIP2 (phosphatidylinositol 4,5-bisphosphate) and the YXX∅ (X is any amino acid and ∅ is a bulky hydrophobic amino acid) sorting signal in the TfR, while the σ2-subunit binds to the acidic di-leucine internalization signal, [DE]XXXL[LIM]. The α and β2 subunits, instead, bind to CLASPs, which, as discussed later, regulate assembly and budding of CCPs. Among these, AP-2 interacts with the scaffolding proteins Eps15 and Itsn (intersectin),

with the membrane bending/curvature-sensing epsin, endophilin and FCHo1/2 proteins, with the phosphoinositide phosphatase sinaptojanin and with the GTPase dynamin. Due to its ability to interact with different molecules, AP-2 is considered the hub of the endocytic clathrin interactome (Traub 2009, McMahon and Boucrot 2011). The observation that the number of CCPs is strongly decreased (by >90%) upon KD (knock-down) of its expression (Hinrichsen, Harborth et al. 2003, Motley, Bright et al. 2003) further supports the central role of AP-2 in CDE. Nevertheless, AP-2 does not account for all CD-endocytic events. More recently, indeed, other adaptor proteins, such as epsins and β-arrestins, due to their ability to interact with both PM cargoes and clathrin, have been proposed to work as AP-2 substitutes for certain receptors (Sigismund, Confalonieri et al. 2012).

CLASPs absolve two main functions: i) they drive efficient sorting of specific cargoes into CCPs, thus preventing competition and allowing plasticity in the selection of cargoes for internalization, and ii) are involved in the formation and maturation of CCVs. They can be classified on the basis of the motif recognized on the cargo. PTB (phospho-tyrosine-binding) domain-containing CLASPs, for example, recognize the [FY]XNPX[YF] cargo signal. The PTB domain is able to bind PIP2 and cargo, simultaneously. Examples of PTB domain-containing CLASPs are Dab2, ARH and Numb (Maurer and Cooper 2006). Other CLASPs, such as Eps15 and epsin proteins, mediate the recruitment of ubiquitinated cargoes (Wendland 2002, Sorkina, Miranda et al. 2006). Neuronal AP180 and its ubiquitous counterpart CALM, known as PICALM, instead, do not bind directly to the cargo, but link clathrin to membrane phospholipids. These proteins possess an ANTH (AP180 N-terminal homology) domain, which binds PIP2, and a binding site for clathrin (Norris, Ungewickell et al. 1995, Ye and Lafer 1995). Binding sites for AP-2 and Eps15 proteins are also present (Figure 3). N-BAR (Bin-amphiphysin-RVS) and BAR domain-containing proteins, such as SNX9 (sorting nexin 9) and amphiphysin, generate and stabilize membrane curvature, bind both clathrin and AP-2, and recruit dynamin to the

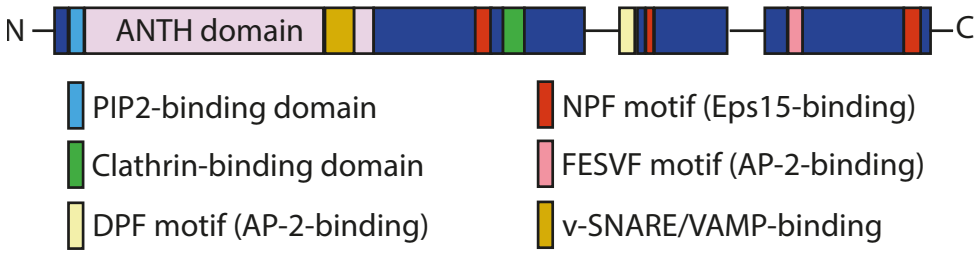

Figure 3. Structure of the human PICALM protein.

The figure depicts the structure of the human protein PICALM, an accessory endocytic adaptor protein. PICALM contains several binding motifs that allow its interaction with membrane phospholipids, clathrin, AP-2 and other CLASPs, such as Eps15. Domains are coloured-coded and indicted below the scheme.

neck of the budding vesicle (Lundmark and Carlsson 2003, Peter, Kent et al. 2004). Due to their overlapping binding abilities, CLASPs often play redundant roles in CDE. Indeed, Eps15 and epsin proteins are redundantly necessary in the CDE of EGFR (Sigismund, Woelk et al. 2005). Similarly, Eps15 and Itsn proteins are redundantly involved in the internalization of both TfR and EGFR (Henne, Boucrot et al. 2010). To complicate the picture even more, the cell may use the same CLASPs to trigger different intracellular routes. This is the case of Eps15 and epsin proteins, which have been demonstrated to participate also in the CIE of EGFR (Sigismund, Woelk et al. 2005).

1.3.2. The steps of CDE

CDE proceeds through five steps: initiation, cargo selection, coat assembly, scission and uncoating (McMahon and Boucrot 2011). Theses processes involve a hierarchy of molecular events (i.e., spatial/temporal cues and cargo-dependent accessory factors) and are governed by a checkpoint system that determines the fate of the pit between a progressive and an abortive state.

The nucleation of productive CCPs at the PM appears to be a stochastic process (Ehrlich, Boll et al. 2004, Banerjee, Berezhkovskii et al. 2012). According to a different model, there are selected regions of the PM in which assembly and disassembly of CCVs is more frequent. Actin participates in the formation of these regions referred to as hot spots (Gaidarov, Santini et al. 1999).

Regardless of how the nucleation of a CCP starts, specific adaptor proteins are recruited to the PM that trigger the formation of the pit during the initiation step. These proteins include AP-2, FCHo1/2, Eps15 and Itsn proteins (McMahon and Boucrot 2011). Different models have been proposed to delineate the functional timing of the mentioned endocytic adaptor proteins during CCP initiation, which will be discussed in section "4.2. The role of Eps15 and Eps15L1 in CD- and CI-endocytosis".

After initiation, endocytic adaptor proteins drive cargo recruitment and clathrin assembly to form a CCP, which is then pinched off from the PM to form a CCV. Scission of the coated pit is mediated by the GTPase dynamin. Dynamin is recruited by N-BAR domain-containing proteins (Ferguson, Raimondi et al. 2009, Sundborger, Soderblom et al. 2011), among which amphiphysin, endophilin and SNX9, which have a preference for the curvature of the vesicle neck. Coordinated dynamin oligomerization and GTP hydrolysis mediate membrane scission (Roux, Uyhazi et al. 2006, Bashkirov, Akimov et al. 2008). In mammals, three genes encoding for dynamin exist: dynamin1, 2 and 3. Dynamin1 is exclusively expressed in the brain, where it is required for efficient SVR during intense activity. Dynamin1-KO (knockout) mice die two weeks after birth (Ferguson, Brasnjo et al. 2007). Dynamin2 is ubiquitously expressed. Dynamin2-KO mice are early embryonic lethal due to the house-keeping functions of dynamin2 (Ferguson, Raimondi et al. 2009). Dynamin3 is selectively expressed in the brain and in testis. Dynamin3-KO mice do not exhibit obvious neurological or male fertility defects (Raimondi, Ferguson et al. 2011).

When CCVs are in the cytoplasm, the clathrin coat is disassembled by the ATPase HSC70 (heat shock cognate 70) and its cofactor auxilin, allowing the vesicles to travel and to fuse

with their target endosome. Changes in the phosphoinositide composition of CCVs, mediated by the phosphatase synaptojanin, are also required for uncoating of the vesicles (McMahon and Boucrot 2011), but whether synaptojanin acts by facilitating auxilin recruitment (Massol, Boll et al. 2006) or via another mechanism is still unclear.

1.4. The CIE

CIE is a heterogeneous group of pathways that share the common property of being insensitive to clathrin depletion. These pathways are frequently formed from membrane microdomains known as lipid rafts, which are enriched in cholesterol, glycosphingolipids, GPI-APs (glycosylphosphatidylinositol-anchored proteins) and signalling molecules. Since they depend on colestherol-rich PM microdomains, another common feature of these pathways is their sensitivity to pharmacological cholesterol depletion (Le Roy and Wrana 2005).

Due to the heterogeneity of CIE, attempts to classify these pathways rely on three major criteria: 1) dependency on dynamin for vesicle release; 2) presence of "coat-like" proteins involved in membrane curvature and stabilization, such as caveolins or flotillins, as in the case of caveolin-mediated or flotillin-mediated internalization, respectively; and 3) dependency on small GTPases. Figure 4 reports the classification scheme proposed by Mayor and Pagano (Mayor and Pagano 2007).

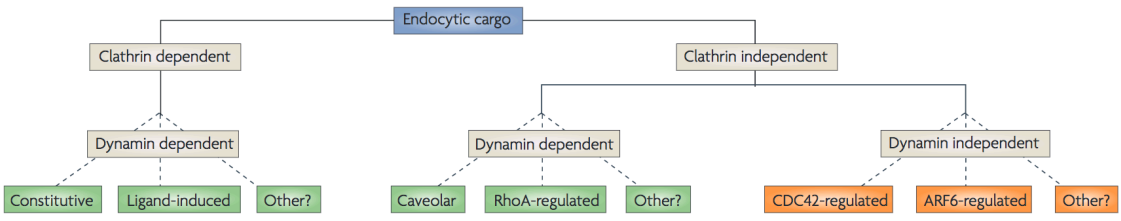

Figure 4. Pathways of CD- and CI-endocytosis**.**

Molecules are internalized through CDE and/or CIE. CDE requires the fission protein dynamin and can be constitutive or induced by ligand binding to the receptor. CIE can either be dynamin-dependent or dynamin-independent. Clathrin-independent and dynamin-dependent pathways encompass caveolin-dependent endocytosis and RhoA-dependent endocytosis, whereas clathrin- and dynamin-independent pathways include CDC42-dependent endocytosis and Arf6-dependent endocytosis. Other unexplored mechanisms might exist (from Mayor and Pagano 2007).

In this scheme, CI-endocytic events are firstly subdivided into dynamin-dependent and dynamin-independent pathways. A second degree of classification takes into account their dependency on a specific small GTPase, so that they are classified as RhoA-, CDC42- or Arf6-dependent. Caveolin-mediated endocytosis is the best-characterized dynamin-dependent endocytic route. Caveolin is an integral membrane protein that induces the formation of flask-like invaginations at the PM, named caveolae. Caveolar cargoes are diverse, ranging from lipids, proteins and lipid-anchored proteins to pathogens, like SV40 (simian virus 40) and CtxB (cholera toxin B) (Mayor and Pagano 2007). These cargoes, however, can be internalized also via other pathways. Another dynamin-dependent endocytic pathway involves the small GTPase RhoA, which is responsible for the internalization of IL-2R-β (interleukin-2 receptor-β). In contrast to these pathways, CDC42- and Arf6-dependent endocytic pathways are dynamin-independent. CDC42-dependent endocytosis is involved in the uptake of CtxB, the plant protein ricin and the *Helicobacter pylori* VacA (vacuolating toxin A). This route also carries fluid-phase markers and GPI-APs. Cargo molecules internalized through Arf6-dependent endocytosis include MHCI, β1-integrin, CPE (carboxypeptidase E), E-cadherin and GPI-APs (Mayor and Pagano 2007).

More recently, a new CI-endocytic pathway, called FEME (fast endophilin-mediated endocytosis), has been identified. This CI-endocytic route requires dynamin activity and is characterized by the formation of fast-acting tubulovesicular structures marked and

controlled by endophilin. FEME mediates the internalization of several GPCRs, numerous RTKs (receptor tyrosine kinases), among which EGFR, cholera and shiga toxins and IL-2R (Boucrot, Ferreira et al. 2015).

1.5. Regulation of cell signalling by endocytosis

Endocytosis has the ability to orchestrate biochemical pathways by coordinating cell signalling variables, such as duration, intensity, integration and spatial distribution (Polo and Di Fiore 2006). A first tier of regulation is achieved through the control, by internalization itself, of the availability on the PM of all the components participating in a specific biochemical pathway, including receptors, ligands, substrates and mediators (Sigismund, Confalonieri et al. 2012).

Cell signalling can be modulated by controlling the number of PM receptors. Regarding this point, the classical function of endocytosis is the attenuation of the signal, which occurs when activated receptors are degraded through lysosomes. Nevertheless, endocytosis can also sustain the signal by moving receptors trough the recycling pathway towards the PM, to differently redistribute the proteins.

The fate of the receptor often depends on the endocytic route through which it is internalized. This is the case of EGFR, which, when stimulated with low doses of the EGF ligand, is almost exclusively internalized through CDE and then recycled to the PM. At higher doses of EGF, instead, EGFR is internalized through CIE. This shift at higher doses of EGF correlates with the monoubiquitination of EGFR and its degradation in the lysosomes, an event that avoids excessive stimulation (Sigismund, Woelk et al. 2005, Polo and Di Fiore 2006).

Cell signalling can also be modulated by the regulation of ligand accessibility, as exemplified by the Notch receptor system, which will be discussed in section “2.4. Regulation of Notch signalling by endocytosis”.

Another mechanism to achieve signal modulation is the physical separation of the receptor from its substrates or mediators located at the PM. As an example, GPCR signalling through PM potassium channels requires that receptors and G proteins are present in the same membrane (Mathie 2007). Similarly, PLCγ1 (phospholipase Cγ1) and PI3K (phosphoinositide 3-kinase) signalling by EGFR are inhibited by receptor internalization due to the lack of their lipid substrate, PIP2, in endosomes (Haugh and Meyer 2002).

Cargo trafficking control is not the only mechanism through which the cell regulates signalling. Indeed, a second tier of cell signalling regulation is achieved within endosomes. In detail, it has become evident in recent studies that endosomes have numerous unique properties that allow them to serve as internal signalling platforms (Sorkin and von Zastrow 2009). These properties include: i) a small volume that favours ligand-receptor association; ii) a relatively longer resident time of activated receptors here compared to the PM; iii) the ability to move long distances (for example towards nucleus); iv) a scaffold-promoting microenvironment, due to the presence of specific lipids, such as PIP3 (phosphatidylinositol 3,4,5-trisphosphate), and proteins which favour selected signallings; v) an acidic pH that favours specific reactions, such as proteolysis of signalling molecules (Sorkin and von Zastrow 2009). Thanks to these properties, endosomes impact on signalling mainly in two ways: by sustaining signals originating from the PM or by assembling specific signalling complexes that are prohibited at the PM (Sadowski, Groen et al. 2008, Gould and Lippincott-Schwartz 2009, Scita and Di Fiore 2010). An example of sustained signal is promoted by several RTKs and their ligands, including EGF-EGFR, which remain bound and active after internalization in endosomes. Also GPCR signalling is sustained in endosomes, via β-arrestins or through cAMP production. In detail, it has been shown that β-arrestin act as a specific scaffold protein that anchors ERK1/2 to the endosome (DeWire, Ahn et al. 2007), thus sustaining signalling from GPCRs. Moreover, it has been demonstrated that some GPCRs, such as PTHR (parathyroid hormone receptor), are internalized together with the Gα protein that, in the EE, continues to produce cAMP

(Calebiro, Nikolaev et al. 2009, Ferrandon, Feinstein et al. 2009). TGFβR (tumor growth factor β receptor) internalization, instead, offers an example of an endosome-specific signalling: when internalized, it interacts with the FYVE domain-containing adaptor SARA, which is located in EEs. Subsequent interaction of SARA with SMAD2 allows the phosphorylation of SMAD2 by the receptor in endosomes. Then, SMAD2 dissociates and interacts with SMAD4, forming a complex that translocates into the nucleus to regulate gene transcription (Tsukazaki, Chiang et al. 1998).

2. The Notch signalling pathway

2.1. The importance of studying the Notch signalling pathway

Notch is the receptor of an evolutionarily conserved signalling pathway involved in metazoan development and in tissue renewal. Notch allows short-range communication between cells and, in a context-dependent manner, can promote or suppress cell proliferation, cell death, acquisition of specific cell fates or activation of differentiation programs (Kopan and Ilagan 2009).

Due to the critical function covered by Notch in cellular physiology, it is not surprising that aberrant gain or loss of Notch signalling components are linked to multiple human disorders. These disorders include developmental syndromes (such as Alagille syndrome, Tetralogy of Fallot, syndactyly, spondylocostal dysostosis and familial aortic valve disease), adult-onset diseases (for example CADASIL, acronym for cerebral autosomal dominant arteriopathy with subcortical infarcts and leukoencephalopathy) and cancer (Kopan and Ilagan 2009). Concerning cancer, depending on the tumor type, Notch can act as an oncogene or a tumor suppressor and can also serve as a cancer stem cell factor (Roy, Pear et al. 2007). The clearest example in which Notch acts as an oncogene is represented by T-ALL (T-acute lymphoblastic leukemia/lymphoma), an aggressive neoplasm of immature T-cells. Recent studies have revealed a role for Notch also in human breast cancer and lung cancer (Pece, Serresi et al. 2004, Roy, Pear et al. 2007, Westhoff, Colaluca et al. 2009). Moreover, Notch signalling is altered in primary human melanomas and in solid tumours, such as medulloblastoma and ovarian cancer (Roy, Pear et al. 2007). It seems that the list of neoplasms involving alterations in Notch signalling will continue to grow. Since Notch signalling plays such a relevant role in disease, understanding the biochemical mechanisms involved in its regulation is of growing interest.

2.2. Players of the Notch signalling pathway

Both Notch receptors and Notch ligands are transmembrane proteins expressed on the PM. Cells expressing Notch receptors are called signal-receiving cells, while cells expressing Notch ligands are referred to as signal-sending cells. Notch ligands can be presented either by a neighbouring cell or the Notch-expressing cell, thus allowing trans- or cis-interactions, respectively.

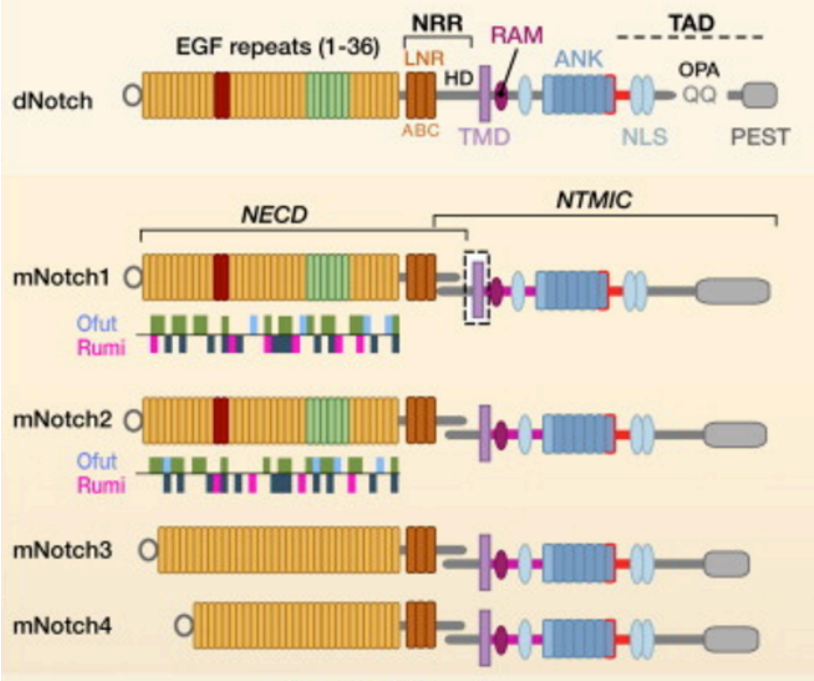

Figure 5. Structure of Notch receptors.

Drosophila melanogaster possesses only one Notch receptor (dNotch), whereas mammals have four Notch paralogs (mNotch1-4). The figure shows the domain organization of Notch receptors that is similar both in *Drosophila melanogaster* and in mammals. They differ only in the number of EGF repeats. EGF repeats 11-12 (red) mediate productive interactions with the ligand presented by a neighboring cell (trans interactions), whereas EGF repeats 24-29 (green) are involved in cis-inhibition by ligands expressed on the same cell. EGF repeats may contain consensus motifs for fucosylation by O-fut1 and for glucosylation by Rumi. The putative distribution of fucosylation sites (common in green, unique in light blue) and glucosylation sites (common in dark blue, unique in magenta) are shown for mNotch1 and mNotch2 (adapted from Kopan and Ilagan 2009).

Domain organization of Notch receptors is similar in *Drosophila melanogaster*, in *Caenorhabditis elegans* and in mammals. However, whereas *Drosophila melanogaster* possesses only one Notch receptor (dNotch) and *Caenorhabditis elegans* possesses two redundant Notch receptors, mammals have four Notch paralogs (mNotch1-4) with both redundant and unique functions (Figure 5) (Kopan and Ilagan 2009). The extracellular domain of all Notch proteins contains 29-36 tandem EGF-like repeats, some of which mediate interactions with Notch ligands. Moreover many EGF repeats bind to calcium ions, affecting the structure and the affinity with ligands. EGF repeats are then followed by the NRR (negative regulatory region) sequence, which is composed of three cysteine-rich LNR (Lin12-Notch repeats) sequences and a HD (heterodimerization domain). The function of HD is to prevent receptor activation in the absence of ligand. In mammals, the HD contains a cleavage site, S1 (site 1), which is recognized by a furin-like convertase. The proteolytic cleavage of Notch at S1 results in a NECD-NTMIC (Notch extracellular domain-Notch transmembrane and intracellular domain) heterodimer held together by non-covalent interactions. Inside the cell, after the TMD (transmembrane domain), there is a RAM (RBPjk association module) domain, which is connected by a NLS (nuclear localization sequence) to seven ANK (ankirin) repeats. At the C-terminus there is a TAD (trans-activation domain) that contains two NLS and conserved PEST (proline/glutamic acid/serine/threonine)-rich motifs. The PEST region harbours degradation signals, known as degrons, which regulate the stability of the effector of the Notch signalling, e.g., the NICD (Notch intracellular domain). In *Drosophila melanogaster*, inside the TAD, there is also an OPA region (polyglutamine-repeat containing region) (Kopan and Ilagan 2009).

Notch ligands differ in domain composition. The largest class of Notch ligands is characterized by three related structural motifs: an N-terminal DSL (Delta/Serrate/LAG-2) motif, the DOS (Delta and OSM-11-like proteins) domain, composed of specialized tandem EGF repeats, and EGF-like repeats, which can bind or not calcium ions (Figure 6). Both DSL and DOS domains are involved in receptor binding.

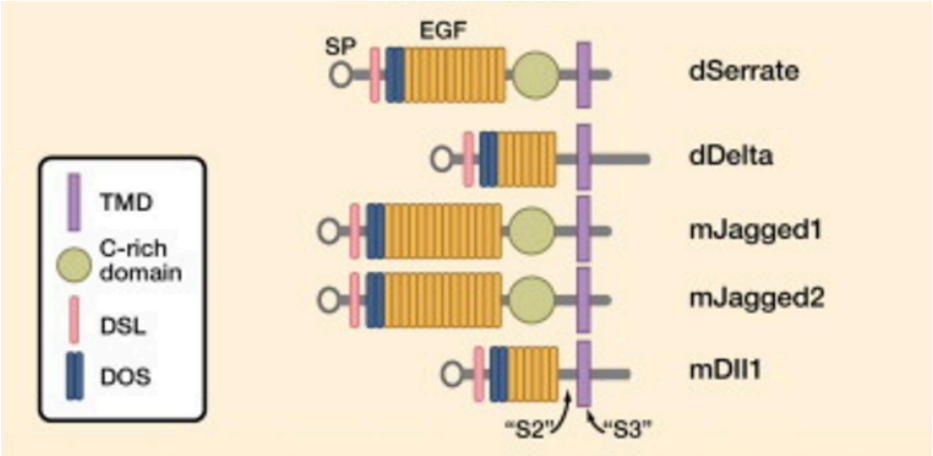

Figure 6. Classical DSL ligands.

Classical DSL ligands contain DSL and DOS domains and EGF motifs. Some of them possess also a C-rich domain. S2 and S3 represent sites in which cleavage may occur (adapted from Kopan and Ilagan 2009).

Nevertheless, not all Notch ligands possess these sequences: the mammal ligands Dll3 and Dll4, indeed, lack the DOS motif. These molecules act alone (this is the case of Dll4) or in combination with DOS co-ligands (probably Dll3). All these ligands are called canonical DSL ligands and differ from non-canonical ligands, which are a group of structurally diverse proteins that lack the DSL domain and that presumably have a role in the modulation of Notch receptor activity (Kopan and Ilagan 2009).

2.3. Overview of the Notch signalling pathway

Activation of the Notch receptor consists of a series of regulated proteolytic events that result in the release of the NICD, which travels to the nucleus, where it assembles a transcription complex for the activation of downstream target genes (Figure 7). The first cleavage occurs during the biosynthetic route at S1 and leads to the formation of NECD-NTMIC, which is subsequently trafficked to the PM.

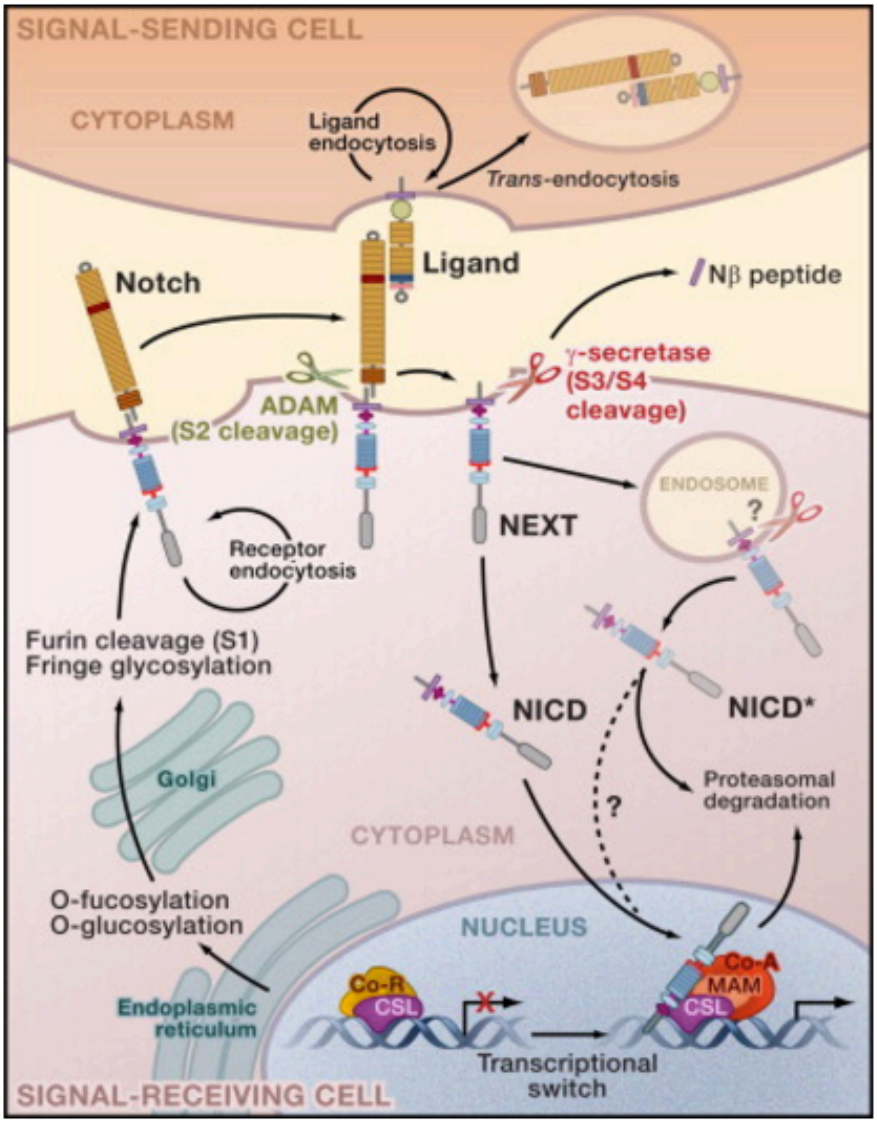

Figure 7. The Notch signalling pathway.

The figure shows the steps that lead to the maturation and activation of the Notch receptor in the signal-receiving cell. The newly translated Notch receptor is glycosylated in the endoplasmic reticulum by the enzymes O-fut and Rumi. When it reaches the Golgi, the Notch receptor is cleaved by furin at S1 and O-fucose is extended by Fringe. Mature Notch receptor is then targeted to the cell surface, where it is activated by binding to a ligand presented on the signal-sending cell. After ligand binding, S2 is cleaved by ADAM metalloproteases and the NEXT fragment is generated. The NEXT fragment is subsequently cleaved by γ-secretase complex from S3 to S4, with the release of NICD and Nβ peptide. γ-secretase cleavage can occur either on the cell surface or in endosomal compartments. Active NICD specie enters the nucleus where it associates with

CSL, MAM and additional Co-A proteins to activate transcription. Endocytosis of Notch receptors and ligands plays a key role in signal modulation (from Kopan and Ilagan 2009).

After ligand binding, Notch receptor is cleaved by ADAM metalloproteases at S2 (site 2), with the formation of the membrane-anchored NEXT (Notch extracellular truncation) fragment.

Two models have been proposed to explain how S2 is exposed to the proteolytic activity of ADAM: the mechano-transduction model and the allosteric model. The first model proposes that, after ligand binding, the receptor undergoes trans-endocytosis, generating a mechanical strain that exposes S2. According to the second model, ligand binding leads to an allosteric change in the NRR from a protease-resistant to a protease-sensitive conformation (Kopan and Ilagan 2009).

When the NEXT fragment is formed, it is cleaved by γ-secretase complex from S3 (site 3) to S4 (site 4), with the release of NICD and Nβ peptide. γ-secretase cleavage can occur at the PM or in endosomal compartments, but cleavage at the membrane favours the production of more stable forms of NICD (Kopan and Ilagan 2009). In detail, γ-secretase cleavage leads to the formation of NICD variants with diverse N-termini: NICD-V starting with valine 1744, NICD-L starting with lysine 1745 or 1746, and NICD-S starting with serine 1747. While NICD-S and NICD-L molecules are created in endosomes and then rapidly degraded, NICD-V, which is generated at the PM, is stable (Kopan and Ilagan 2009). Stable NICD, subsequently, enters the nucleus to activate transcription, together with the DNA-binding protein CSL (CBF1, Suppressor of Hairless, Lag-1), the transcriptional co-activator MAM (Mastermind) and other Co-A (co-activator) proteins. Signal downregulation is mediated by the kinase CDK8, which phosphorylates the PEST domain, and by E3 ubiquitin ligases (including Sel10/Fbw7), which targets NICD for proteasomal degradation (Kopan and Ilagan 2009).

2.4. Regulation of Notch signalling by endocytosis

Endocytosis plays a critical role in the modulation of Notch signalling (Le Borgne 2006). The classic function of endocytosis is the downregulation of the signal by sending the receptor, the ligand or both towards degradation. However, it has become clear that endocytosis can also contribute to signal activation (Le Borgne 2006). Endocytosis of DSL ligands, for example, promotes ligand-dependent Notch activation. The key regulators of the endocytosis of DSL ligands are Lqf (liquid facet, the *Drosophila melanogaster* epsin gene), Neur (neuralized) and Mib (mind bomb) (Le Borgne 2006). Epsins are part of CLASPs (see section "1.3.1. The main component of CDE: clathrin, AP-2 and CLASPs") that bind PIP2, clathrin, AP-2 and other accessory proteins in coated pits. Neur and Mib, instead, are two RING-finger-containing E3 ubiquitin ligases that cause the ubiquitination of DSL ligands. Ubiquitination is an internalization signal that is recognized by adaptor proteins containing UBDs, such as Lqf itself. Monoubiquitinated transmembrane receptors are usually targeted to lysosomes for degradation. In the case of Notch signalling, ubiquitinated DSL ligands are thought to be targeted to endosomes for their activation and then recycled back to the PM (Le Borgne 2006).

Two alternative, but not exclusive, models have been proposed to explain the requirement of Lqf, Neur and Mib in Notch activation. The first model proposes that Lqf targets ubiquitinated DSL ligands to a particular subclass of coated pits that have special properties for Notch activation. This model is compatible with the hypothesis that S2 (the cleavage site that is recognized by ADAM) of ligand-bound Notch becomes unmasked when the formation of endocytic pits in the signal-sending cell promotes pulling forces on NECD. In the second model, Lqf is proposed to target ubiquitinated DSL ligands, initially inactive, to an endocytic recycling pathway where they are converted into active ligands (Le Borgne 2006). Different mechanisms have been proposed to explain how ligand activation occurs: proteolytic modifications, pH-dependent change of conformation, packaging into lipid rafts or targeting into secreted vesicles.

Also the Notch receptor undergoes endocytic trafficking, which can promote either positive or negative regulation of the pathway, in a context-dependent manner. Notch internalization is mediated by Numb, a conserved membrane-associated protein that acts upstream of the γ-secretase cleavage to block Notch signalling. Numb is an endocytic adaptor that interacts with Notch and AP-2. Numb interacts also with the E3 ubiquitin ligase AIP/Itch (in *Drosophila melanogaster* Su(dx), suppressor of deltex, member of Nedd4 family) to promote ubiquitination, endocytosis and degradation of Notch. However ubiquitination is not always a signal that leads to Notch degradation. Indeed, when the receptor is ubiquitinated by Dx (deltex, an E3 ubiquitin ligase that acts as an antagonist of Su(dx)), Notch is protected from entering the degradative pathway (Le Borgne 2006).

3. The TfR and its physiological role

3.1. The CDE of the TfR

The TfR mediates the internalization of iron in complex with the plasma glycoprotein Tf (transferrin). Figure 8 depicts the main actors involved in the internalization of TfR. As shown, two ions of ferric iron bind to Tf, thus generating differic Tf. When differic Tf binds to the TfR, the complex is internalized through CDE into the early endosomal compartment. In this compartment, the low pH allows iron to be released from Tf. Within the lumen, iron is reduced from ferric iron to ferrous iron by a ferrireductase and then delivered to the cytoplasm by NRAMP-2 (natural resistance associated macrophage protein 2), otherwise called DMT1 (divalent metal transporter 1). In the cytoplasm, iron is used for metabolic functioning, that is, for the synthesis of heme and non-heme iron containing proteins, or stored in ferritin. The TfR, instead, is recycled to the PM where the neutral pH favors the release of iron-free Tf (apo Tf) back into the circulation (Ponka and Lok 1999).

As previously mentioned, the TfR is the most popular experimental system used to unravel the molecular details of constitutive CDE.

Several proteins regulate the CDE of TfR, as well as the CDE of EGFR and LDLR. Other proteins, instead, act as specific adaptor proteins. RNA interference experiments in HeLa cells identified clathrin and dynamin2 as common and essential actors in the internalization of both TfR and EGFR: the internalization rates of these receptors, indeed, were strongly reduced in cells depleted of CHC (but not CLC) or dynamin2. Another common actor was AP-2: the internalization rates for both receptors were ~50% reduced in cells depleted of β2- or μ2-adaptin. Other endocytic adaptors had a less strong effect.

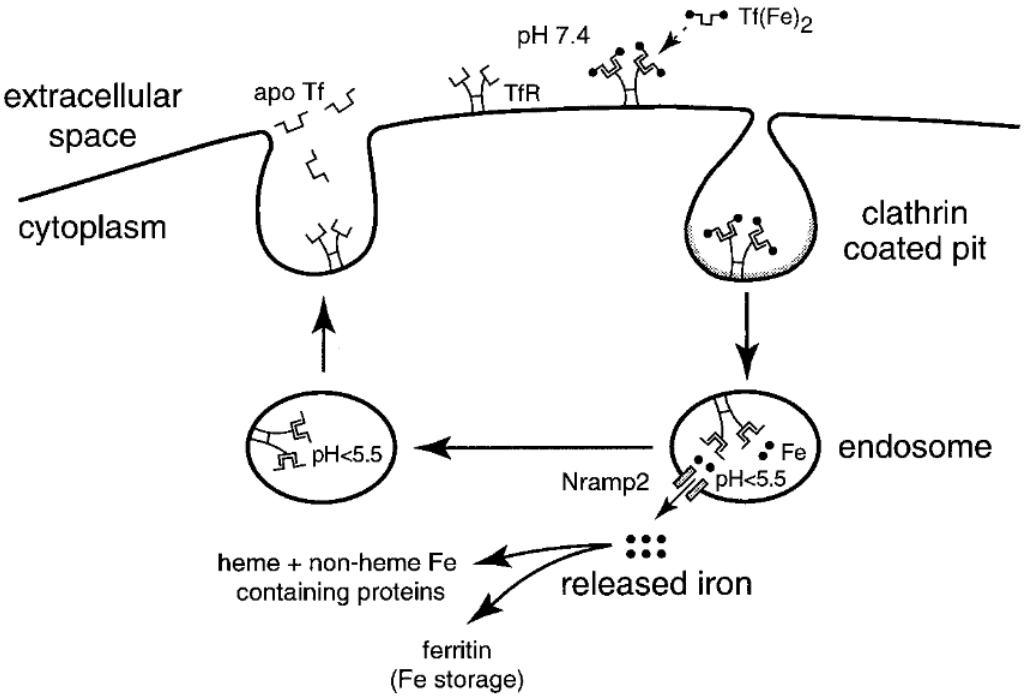

Figure 8. The CDE of the TfR.

The figure depicts cellular iron uptake via CDE of the TfR, as explained in the text (adapted from Ponka and Lok 1999).

For example, in cells depleted of Eps15 or Eps15L1, the internalization rates were reduced to 15-30%; however, when both proteins were depleted, the internalization rates were reduced to 40%, suggesting a redundant role of these proteins. Depletion of Grb2 or CALM, instead, did not affect internalization of TfR but decreased the internalization rate of EGFR to 70% and 45%, respectively (Huang et al., 2004), suggesting a role for these proteins as specific adaptor proteins in EGFR internalization. TTP, instead, an endocytic adaptor protein able to interact with AP-2, clathrin and Eps15, was identified as a specific adaptor protein in the internalization of TfR: when TTP was knocked-down in HeLa cells, the internalization of TfR, but neither of EGFR or LDLR, was reduced 3-fold (Tosoni, Puri et al. 2005). RNA interference experiments in BSC1 cells (monkey kidney epithelial cells) identified FCHo1/2 as other common endocytic adaptor proteins in CDE: KD of these proteins, indeed, reduced the number of CCPs and almost completely inhibited the

internalization of TfR, EGFR and LDLR (Henne, Boucrot et al. 2010). Studies in HeLa cells found that TfR did not require the endocytic adaptor protein Dab2, in contrast to β1-integrin. Eps15 and Itsn proteins, instead, were required for internalization of both TfR and β1-integrin: KD of Eps15 plus Eps15L1 or Itsn1 plus Itsn2 reduced internalization of TfR, as well as of β1-integrin, to 40%; quadruple KD of all four proteins further reduced internalization of both receptors, but not to the same extent as KD of CHC. Moreover, quadruple KD of these proteins caused, at the ventral surface of HeLa cells, a decrease in the number of CCPs and plaques, and an increase of the median size of plaques (Teckchandani, Mulkearns et al. 2012). To complicate the picture even more, some endocytic adaptor proteins participate in the internalization of TfR in some cell lines but not in others. This is the case of CALM, whose downregulation by RNA interference in HeLa cells does not affect TfR internalization (Huang, Khvorova et al. 2004), while KO of the protein in murine erythroblasts reduces TfR internalization (Ishikawa, Maeda et al. 2015). These results indicate the existence of a cell-type specific machinery, besides a common one, regulating internalization of receptors.

3.2. Importance of the TfR in the physiology of RBCs

The TfR plays a fundamental role in cell physiology, as it provides cells with iron. Iron is an essential mineral that serves critical cellular functions, such as oxygen transport (as heme in hemoglobin), DNA biosynthesis (as a cofactor of ribonucleotide reductase) and ATP generation (as a cofactor for proteins involved in the citric acid cycle and electron transport chain).

Due to its broad spectrum, with the exception of mature RBCs (red blood cells), also called erythrocytes, and other terminally differentiated cells, TfR is expressed on all cells. Among these, cells and tissues with the highest density of TfR are immature RBCs, placental tissues and rapidly dividing cells.

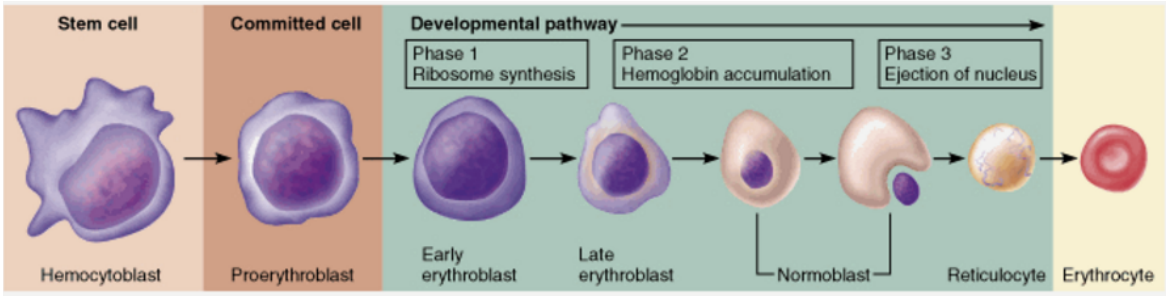

Figure 9. Erythropoiesis.

RBCs are produced from precursor cells in the bone marrow. Here a stem cell called hemocytoblast is transformed into a committed cell, the proerythroblast, which in turn gives rise to the early (basophilic) erythroblast. The early erythroblast produces huge numbers of ribosomes that are necessary for hemoglobin synthesis. The synthesis of hemoglobin starts as early as the erythroblast is transformed into the late erythroblast and proceeds until the conversion of the late erythroblast into a normoblast. After hemoglobin accumulation, most of the organelles are ejected, leading to the conversion of a normoblast into a reticulocyte, which is considered a young RBC still containing a network of clumped ribosomes and rough endoplasmic reticulum. The reticulocyte is then released in the blood stream, where it completes its maturation into an erythrocyte. All the development process from the hemocytoblast to the reticulocyte stage takes around 3 to 5 days to occur, while the reticulocyte becomes a fully matured erythrocyte within 2 days from its release in the blood stream (from Human Anatomy & Physiology, published by Benjamin Cummings; Addison Wesley Longman, 2001)

In immature RBCs, in detail, high expression of TfR correlates with their high demand of iron for hemoglobin production: in a normal adult, indeed, iron hemoglobin accounts for as much as 70% of the total iron content (Ponka and Lok 1999). In the organism, therefore, immature RBCs are the most avid consumers of iron. Mature RBCs, instead, loose the ability to internalize iron: in these cells, the TfR is downregulated, since all the hemoglobin necessary for their functioning has been synthesized and accumulated throughout the developmental pathway.

Some of the molecular details regarding the developmental pathway of RBCs are described here below.

Mature RBCs are highly specialized cells involved in hemoglobin transport and gas exchange in the lungs and peripheral tissues. They have no organelles in their cytoplasm and develop directly from reticulocytes, which are defined as erythroid cells that have lost their nucleus but still retain residual ribosomes and rough endoplasmic reticulum that will be eliminated as the reticulocyte becomes a mature RBC. Reticulocytes, instead, derive from precursor cells generated in the bone marrow (Figure 9).

Throughout their entire maturation process, RBCs undergo an extensive process of cell remodelling, during which all the unnecessary proteins and structures are eliminated, in order to optimize their function in hemoglobin transport, gas diffusion and deformability. The structures that are lost during maturation include the nucleus, the mitochondria, the endoplasmic reticulum, the Golgi apparatus, ferritin particles and ribosomes. Moreover, several unnecessary proteins are downregulated during the developmental pathway. The TfR is one of the proteins that are downregulated during maturation. Downregulation of the TfR occurs through exocytosis, a process consisting in the release of exosomes (vesicles derived from the ILVs of MVBs) into the extracellular space and regulated by ESCRT complexes. Besides TfR, other PM proteins are downregulated by exocytosis, such as glucose, nucleoside and amino acid transporters, the Na/K-ATPase and aquaporin1 (Ney 2011). Also unnecessary cytoplasmic proteins are downregulated during maturation. Among these, the one worth mentioning is the endocytic adaptor AP-2, which is degraded by the proteasome system. Being necessary for CDE of TfR, downregulation of AP-2 is intimately linked to TfR: indeed, it has been suggested that reduction of AP-2 levels favors the binding of TfR to the ESCRT machinery (in detail, with Alix) and its secretion via exosomes (Geminard, De Gassart et al. 2004).

3.3. The role of the TfR in anemia

As reported in the previous section, immature RBCs express high levels of TfR to sustain their high demand of iron for hemoglobin production. Therefore, *in vivo* disruption of proteins participating in iron uptake by TfR has a great impact on the physiology of RBCs. The most severe phenotype is observed in TfR-null mice, which die before embryonic day 12.5 (Levy, Jin et al. 1999). These mice present both erythropoiesis and neural defects. In detail, they have signs of fetal hydrops with growth retardation, severe pallor and pericardial effusions. Embryonic erythrocytes have an increased frequency of multinuclearity (sign of stressed erythropoiesis) and cultured yolk-sac hematopoietic progenitors produce smaller erythroid colonies. In the organism the neural tube architecture is distorted and exhibits signs of apoptosis. Defective development of the nervous system might be secondary to hypoxia and/or directly caused by an inadequate supply of iron for its activities (Levy, Jin et al. 1999).

Reduction of TfR levels or perturbations in other proteins participating in iron uptake by TfR, instead, are compatible with life, but are responsible for the onset of an anemic condition, referred to as microcytic hypochromic anemia (Levy, Jin et al. 1999, Zhu, McLaughlin et al. 2008, Ishikawa, Maeda et al. 2015). This condition, as the nomenclature suggests, is characterized by the presence of microcytic and hypochromic RBCs, e.g., of RBCs with reduced MCV (mean corpuscular volume) and reduced hemoglobin content, as a consequence of impaired iron availability. Microcytic hypochromic anemia is also characterized by an increase in the number of immature RBCs and of RDW (red cell distribution width) index. High RDW index indicates a high degree of aniso-poikilocytosis, e.g. a high variation in RBC size.

Heterozygous mice for TfR, for example, have a less severe phenotype compared to TfR-null mice: they survive to adulthood and are indistinguishable from WT (wild type), but suffer from microcytic hypochromic anemia due to reduced membrane levels of the TfR. In the whole organism hematocrits and hemoglobin levels are normal due to a

compensatory increase in RBC number. Moreover, while iron saturation of serum Tf is normal, total body iron accumulation is reduced, as indicated by reduced iron in the liver and in the spleen, probably due to reduced intestinal iron absorption (Levy, Jin et al. 1999). Also hematopoietic-specific null mice for the transcription factors Stat5a/b exhibit microcytic hypochromic anemia (Zhu, McLaughlin et al. 2008). In these mice protein levels of TfR are reduced to 50%, indicating that Stat5a/b participate in the regulation of TfR expression. In contrast to heterozygous mice for TfR, these mice have a decreased RBC count, hemoglobin and hematocrit, and an increased iron deposition in the liver. The lack of Stat5a/b in the whole organism leads to a more severe anemia compared to hematopoietic-specific Stat5a/b-null mice and animals die perinatally.

More recently, another protein has been found to be essential for the proper development of RBCs: the clathrin adaptor protein PICALM (Ishikawa, Maeda et al. 2015). Inactivation of PICALM in the hematopoietic system of adult mice leads to anemia, as evidenced by a reduced RBC number, hemoglobin and hematocrit. Anemia is microcytic and hypochromic, with a high RDW. In these mice, an increased number of reticulocytes in the blood and of immature erythroblasts in the spleen has also been found. These phenotypes are indicative of a maturation defect, confirmed through the observation that hematopoietic progenitor cells KO for PICALM barely develop into an erythroid lineage when cultured *in vitro*. This maturation defect has been linked to reduced TfR internalization due to a role for PICALM in the maturation of CCPs: PICALM-KO splenic erythroblasts have increased amounts of surface-bound Tf and impaired TfR internalization, which correlate with a reduced number of CCPs (Ishikawa, Maeda et al. 2015).

4. Eps15 and Eps15L1

4.1. Structure and binding partners of Eps15 and Eps15L1

In the beginning of the nineties, several proteins were found to be tyrosine phosphorylated upon EGF stimulation of NIH EGFR cells (NIH 3T3 mouse fibroblasts overexpressing human EGFR) (Fazioli, Bottaro et al. 1992). A screening on a λgt11 cDNA expression library prepared from NIH 3T3 fibroblasts led to the identification of a partial cDNA encoding for a new protein. Being tyrosine phosphorylated upon EGF stimulation, this new protein was named Eps15 (from EGFR pathway substrate 15) (Fazioli, Minichiello et al. 1993). In order to obtain the full-length sequence of Eps15, the partial cDNA was used as a probe to screen a mouse keratinocytes cDNA library (Fazioli, Minichiello et al. 1993). Subsequently, using a specific probe derived from the cDNA encoding for the first domain of Eps15, another EGFR substrate was identified. Because of its homology to Eps15, the new protein was designed as Eps15R (for Eps15-related) (Wong, Schumacher et al. 1995) and later, according to the official nomenclature, as Eps15L1 (for Eps15-like1). Further studies addressed their biochemical features and functions.

The structure of Eps15 and Eps15L1 and their binding partners are described here below.

Eps15 and Eps15L1 are 47% identical and share high co-linearity and homology (Wong, Schumacher et al. 1995). The two proteins are characterized by a modular structure composed of three main domains. Through their domains, Eps15 and Eps15L1 bind to a number of different partners, thus taking part in several intermolecular networks and serving diverse cellular functions (Figure 10).

Eps15 has a predicted molecular weight of 142-kDa and is composed of 897 amino acids, while Eps15L1 is predicted to be a 125-kDa protein of 907 amino acids.

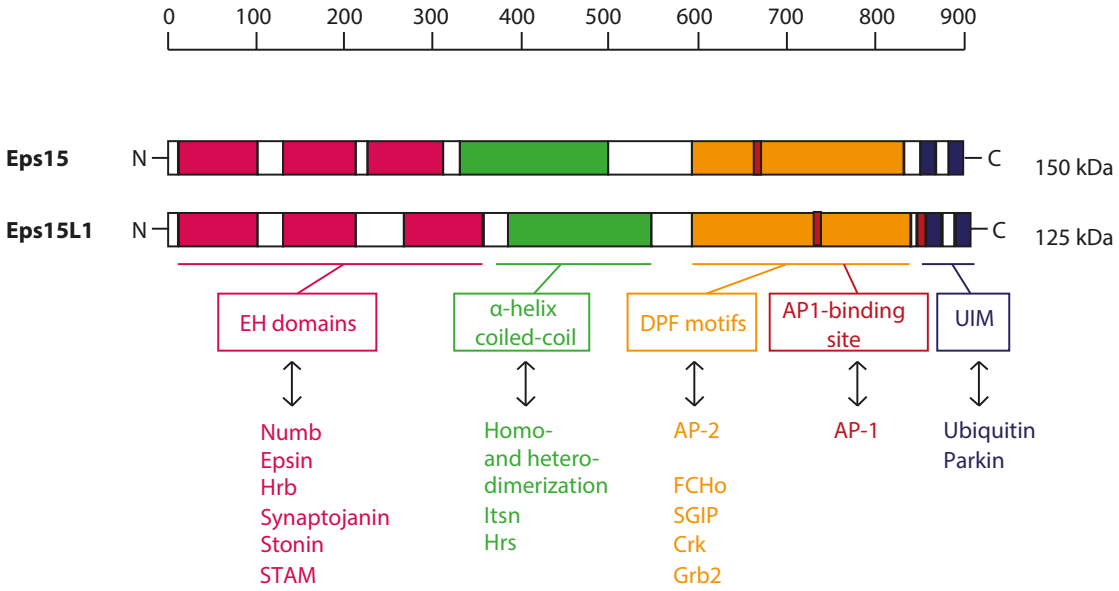

Figure 10. Structure of murine Eps15 and Eps15L1.

Eps15 and Eps15L1 are modular proteins displaying 47% identity and composed of three EH domains at the N-terminus (magenta), a central α-helical coiled-coil region (green) and a C-terminal domain containing several DPF motifs (orange), an AP-1-binding domain (red) and two UIMs (blue). For each domain, the main binding partners of Eps15 and Eps15L1 are indicated.

The first domain is located in the N-terminal region and includes three imperfect repeats of 95 to 97 amino acids, corresponding to a protein-protein interaction domain that was first identified in Eps15: the EH domain (for Eps15 homology). EH domains mediate binding with NPF (asparagine-proline-phenylalanine)-containing proteins, such as the endocytic proteins Numb, epsin, Hrb, synaptojanin, stonin, STAM and others.

The second domain of Eps15 and Eps15L1 contains 24 heptad repeats and has a α-helical coiled-coil structure. This structure, commonly found in cytoskeleton-related proteins, serves as a dimerization interface: through it, Eps15 and Eps15L1 form hetero- or homo-dimers and oligomers (Cupers, ter Haar et al. 1997, Tebar, Confalonieri et al. 1997, Coda, Salcini et al. 1998). Moreover, this region mediates binding with other endocytic adaptor proteins, such as Hrs and Itsn. The third domain is located in the C-terminal region and

contains a proline-rich domain and several DPF (aspartic acid-proline-phenylalanine) repeats. The proline-rich domain mediates interaction with Crk and Grb2 (van Bergen En Henegouwen 2009). The DPF motifs mediate binding with AP-2 (through α-adaptin), SGIP1 and FCHo. SGIP1 and FCHo bind to Eps15 proteins through their μ–homology domain (Uezu, Horiuchi et al. 2007, Hollopeter, Lange et al. 2014, Ma, Umasankar et al. 2016). The C-terminus of Eps15 and Eps15L1 harbours two UIMs (ubiquitin interacting motif), which are shared by other endocytic proteins, such as epsins and Hrs. These motifs, which mediate the binding to ubiquitin, allow endocytic proteins to interact with ubiquitinated receptors and to be ubiquitinated in a process called coupled ubiquitination (Polo, Sigismund et al. 2002).

Since the discovery of Eps15 and Eps15L1 in 1993 as substrates of the tyrosine kinase activity of the EGFR, several studies delineating their cellular functions have arisen. Taken together, it emerges that Eps15 and Eps15L1 are two accessory adaptor/scaffolding proteins that serve pleiotropic functions within the endocytic machinery: they regulate the early events of CDE and CIE of several cargo molecules, their sorting in the EEs and protein trafficking from the TGN to the PM.

4.2. The role of Eps15 and Eps15L1 in CD- and CI-endocytosis

Eps15 and Eps15L1 were initially proposed to participate in endocytosis. Indeed, it was known that other EH-containing proteins were involved in endocytosis, like End3p and Pan1p, the yeast homologs of Eps15. Moreover, they were found to interact with several endocytic proteins, such as epsin1 and epsin2 (Chen, Fre et al. 1998), AP-2 (Benmerah, Begue et al. 1996), Grb2 (Schumacher, Knudsen et al. 1995), Itsn, dynamin (Sengar, Wang et al. 1999) and Numb (Salcini, Confalonieri et al. 1997).

Many evidences pointed to a major role for Eps15 and Eps15L1 as scaffolding proteins involved in the CDE of EGFR, prototype of ligand-dependent endocytosis, and TfR,

prototype of constitutive endocytosis: i) Eps15 was found to ubiquitously and constitutively bind AP-2 (Benmerah, Gagnon et al. 1995); ii) Eps15 and Eps15L1 co-localized with AP-2 and clathrin (Tebar, Sorkina et al. 1996, vanDelft, Govers et al. 1997, Coda, Salcini et al. 1998); iii) membrane-associated Eps15 was located at the rims of CCPs (Tebar, Sorkina et al. 1996); iv) antibodies blocking Eps15 or Eps15L1 inhibited endocytosis of EGFR and TfR in CV-1 cells (monkey kidney cells) (Carbone, Fre et al. 1997); v) fragments encompassing the C-terminal region of Eps15 inhibited endocytosis of EGFR in CV-1 and COS-7 cells (monkey kidney cells); vi) fragments encompassing either the EH domains or the C-terminal region of Eps15 inhibited infection by Sindbis virus in NIH 3T3 cells (Carbone, Fre et al. 1997); vii) mutant forms of Eps15 containing only the C-terminal region inhibited internalization of TfR in HeLa cells and of EGFR and TfR in A431 cells (human squamous carcinoma cells) (Benmerah, Lamaze et al. 1998, Benmerah, Bayrou et al. 1999). The effects on EGFR and TfR internalization have been recently revisited and quantified through radioactive internalization assays, following KD of Eps15 and Eps15L1, alone or in combination, in HeLa cells (Huang, Khvorova et al. 2004). As reported in section "3.1. The CDE of the TfR", it emerges that Eps15 and Eps15L1 have a less drastic effect on the internalization of these receptors: indeed, it has been reported that in HeLa cells depleted of Eps15 or Eps15L1, the internalization rates of TfR and EGFR were reduced to 15-30%; when both proteins were depleted, the internalization rates were decreased to 40%, thus suggesting a redundant role of these proteins (Huang, Khvorova et al. 2004).

Targeting of Eps15 to CCPs has long been described to be AP-2-dependent (Benmerah, Poupon et al. 2000), in line with the traditional view that CCP initiation is triggered by the recruitment to the PM of AP-2 as a first adaptor protein. This view has been challenged by a model according to which initiation of a CCP requires the formation of a putative nucleation module that defines the sites on the PM where AP-2 will be recruited. This putative nucleation module is composed of FCHo, Eps15 and Itsn proteins (Stimpson,

Toret et al. 2009, Henne, Boucrot et al. 2010). However, a more recent study has taken advantage of live-cell TIRF imaging to reconstruct, at high temporal resolution, the initial events of CCP formation. According to this study, pits are initiated by clathrin and AP-2, which arrive concomitantly at the PM. In detail, the initial molecular complex is composed of one triskelion and two AP-2 complexes, followed by another similar complex, which binds to the membrane through interaction of AP-2 with PIP2. In this scenario, FCHo1/2, and probably also Eps15 and Itsn proteins, are not essential for initiation but are required for sustained growth of CCPs (Cocucci, Aguet et al. 2012).

Besides playing a role in CDE, it has been demonstrated that Eps15 and Eps15L1 take part also in the CIE of EGFR (Sigismund, Confalonieri et al. 2012). Indeed, triple KD of Eps15, Eps15L1 and epsin1 in HeLa cells results in the inhibition of this pathway.

4.3. Post-translational modifications of Eps15 and Eps15L1

During endoytosis, Eps15 undergoes a serie of post-translational modifications. Upon EGF stimulation, Eps15 is tyrosine phosphorylated. This event is essential for EGFR internalization but not for constitutive uptake of the TfR (Confalonieri, Salcini et al. 2000). Phosphopeptide experiments demonstrate that phosphorylated tyrosines in Eps15 likely serve as binding sites for PTB domain-containing proteins (Confalonieri, Salcini et al. 2000).

Eps15 is also monoubiquitinated upon EGF stimulation (vanDelft, Govers et al. 1997) via a mechanism called coupled monoubiquitination (Polo, Sigismund et al. 2002), where monoubiquitination depends on a functional UIM domain. The precise role of adaptor monoubiquitination in RTK endocytosis is still a matter of debate. Monoubiquitination of adaptors might permit the formation of several tiers of ubiquitin-dependent interactions, resulting in the progression of ubiquitinated cargoes along the endocytic pathway. Alternatively, it has been proposed that ubiquitination (coupled monoubiquitination) could

represent a signal to "switch off" the binding activity of the adaptor by allowing intramolecular interactions between the UBD and the ubiquitin moiety present in cis (Hoeller, Crosetto et al. 2006). This mechanism could cause the release of the ubiquitinated cargo that, thus, becomes available for other interactions along the endocytic route. Nevertheless, the hypothesis that adaptor monoubiquitination inhibits the cargo binding has recently been challenged by the finding that monoubiquitination of Eps15 does not change its ability to interact with EGFR and that it is necessary for EGFR internalization, already at low doses of EGF ligand when EGFR is internalized only by CDE (Savio, Wollscheid et al. 2016).

Finally, it has also been demonstrated that Eps15, together with epsin, is phosphorylated during mitosis. This phosphorylation inhibits the interaction of the two proteins with AP-2 and causes dissociation of the two proteins from CCPs, thus resulting in the mitotic block of endocytosis (Chen, Slepnev et al. 1999).

4.4. Other cellular functions of Eps15 and Eps15L1

In the literature, there are reports revealing that Eps15 proteins participate also in late endocytic events. Indeed, the finding that Eps15 co-localizes with EGFR in the early and late endosomes suggests that Eps15 is involved not only in the early steps of EGFR internalization, but also in the sorting of the receptor at the EE (Torrisi, Lotti et al. 1999). Further studies found that protein sorting was regulated by two different isoforms of Eps15, Eps15b and Eps15s. In detail, Eps15b, an Eps15 isoform lacking the EH domains, was shown to interact with the ubiquitin-binding proteins Hrs and STAM at the EE and to form a complex (ESCRT-0) responsible for receptor degradation (Roxrud, Raiborg et al. 2008). Instead, Eps15s, an Eps15 isoform lacking the 111 terminal amino acids, including the UIM domains, was shown to co-localize with Rab11 in recycling endosomes (Chi, Cao et al. 2011).

Other studies unmasked a role for Eps15 in the secretory pathway: Eps15 was found to interact with AP-1 (Kent, McMahon et al. 2002, Chi, Cao et al. 2008) trough a 14 aminoacid motif located immediately C-terminally from the AP-2 binding site. In the TGN, Eps15 promotes the formation of tubular-carrier precursors by targeting polyubiquitinated coronin7, a stabilizer for F-actin, at the TGN (Yuan, Lee et al. 2014).

More recent studies have dissected the role of Eps15 in the internalization of other proteins rather than the EGFR and the TfR. Indeed, it has been demonstrated that Eps15 proteins participate in the CDE of β1-integrin through an AP-2-independent and Dab2-dependent mechanism (Teckchandani, Mulkearns et al. 2012), and in the internalization of connexin43, a base component of gap-junctions (Girao, Catarino et al. 2009). These studies, therefore, unveil a role for Eps15 proteins in cell adhesion and cell-cell contact.

Due to the ability of Eps15 to interact with Hrb, a protein involved in nuclear import/export, a role for Eps15 proteins has also been postulated in the nucleus, similar to other endocytic adaptors. However, whether they function in nucleocytoplasmic transport or transcriptional regulation still remains to be elucidated (Doria, Salcini et al. 1999, Vecchi, Polo et al. 2001, Poupon, Polo et al. 2002, Pilecka, Banach-Orlowska et al. 2007).

4.5. The functions of Eps15 in lower organisms

Some *in vitro* studies suggest a function for Eps15 proteins in the regulation of signalling pathways of the nervous system. Eps15 proteins, indeed, were found to interact with neural endocytic proteins, such as sinaptojanin (Haffner, Takei et al. 1997), parkin (Fallon, Belanger et al. 2006), spartin (Bakowska, Jenkins et al. 2005) and stonin2 (Martina, Bonangelino et al. 2001). Moreover, Eps15 was found to be enriched at the presynaptic nerve terminals, the site of a specialized form of CDE (Chen, Slepnev et al. 1999), necessary to efficiently recycle synaptic vesicle proteins (De Camilli and Takei 1996).

In line with these findings, studies in lower organisms, where only one Eps15 gene exists, pointed to a major role for Eps15 proteins in the development of synaptic structures and in SVR.

Studies in *Caenorhabditis elegans* revealed that ehs-1, the orthologue of Eps15, was essential in synaptic transmission under unfavourable conditions (Salcini, Hilliard et al. 2001). Deletion of the gene caused uncoordinated movements and reduction in the number of synaptic vesicles in a temperature-sensitive manner. Interestingly, ehs-1 mutants displayed also reduced levels of Itsn1 (Rose, Malabarba et al. 2007, Wang, Bouhours et al. 2008), suggesting a role for Eps15 in the stabilization of this endocytic protein.

In *Drosophila melanogaster*, deletion of Eps15 causes lethality during the pupal stage. Eps15-null mutants have defects in the development of synaptic structures, which exhibited an extra number of boutons and branches (Koh, Korolchuk et al. 2007). Both electron microscopy analyses and dye uptake experiments revealed that the number of recycled vesicles was reduced in Eps15-null mutants (Koh, Korolchuk et al. 2007). Because of SVR impairment, Eps15-null mutants exhibit cisternae and large invaginations still associated with the PM (Koh, Korolchuk et al. 2007). Of note, Eps15-null mutants have reduced levels of Itsn and dynamin and, in a subtle way, of AP-2, stonedB, synaptotagmin and endophilin1 (Koh, Korolchuk et al. 2007).

5. Physiological functions of Eps15 and Eps15L1 in mammals

5.1. Eps15, Eps15L1 and Eps15/Eps15L1 KO mice

In order to characterize the physiological functions of Eps15 and Eps15L1 in mammals, single and double KO (DKO) mice for Eps15 and Eps15L1 were previously generated in our laboratory. Both the Eps15 and Eps15L1 null alleles were generated by deletion of the first exon and the upstream region of each gene. In detail, the Eps15 null allele was obtained by homologous recombination. Instead, the Eps15L1 null allele was obtained by homologous recombination combined with the Flp-FRT and the Cre-loxP strategy.

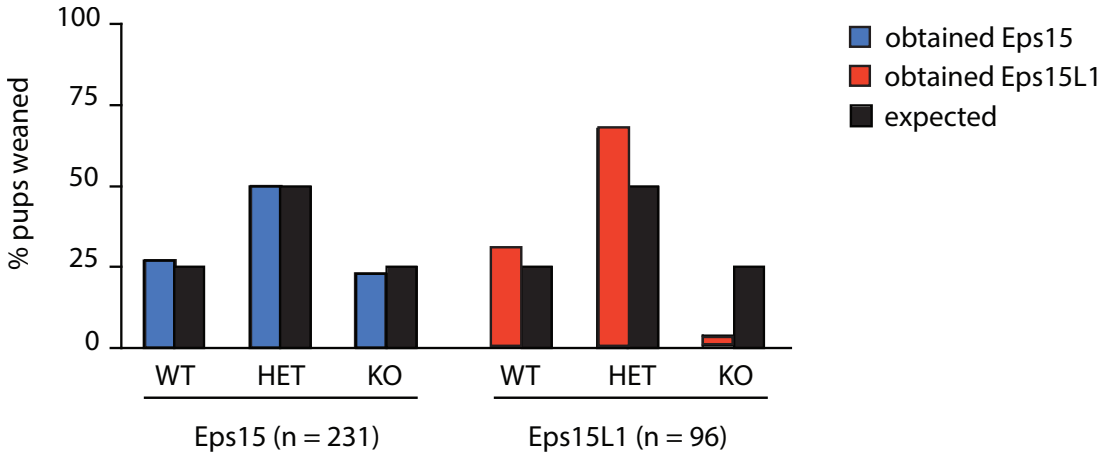

Figure 11. Eps15-KO mice, but not Eps15L1-KO ones, survive at weaning according to the expected Mendelian ratio.

The bar graph depicts the percentage of wild type (WT), heterozygous (HET) and knockout (KO) pups for Eps15 (blue bars) and Eps15L1 (red bars) that survived at weaning, compared to the expected Mendelian ratio (black bars).

Eps15-KO mice were viable, healthy and fertile, with no obvious phenotype, except for a defect in B cell lymphopoiesis (Pozzi, Amodio et al. 2012). In contrast, Eps15L1-KO mice

were postnatal lethal, with only 10% of the pups surviving to adulthood (Figure 11). Newborn Eps15L1-KO mice had no obvious morphological defects, but the great part of them had no milk in the stomach. Moreover, Eps15L1-KO mice displayed neurological deficits, as assessed by reduced reactivity in any neurological tests and by difficult respiratory activity. Deeper investigations highlighted a fundamental role of Eps15L1 in the nervous system. In detail, biochemical analysis of newborn brain lysates revealed that Eps15L1-KO mice had reduced levels of the endocytic proteins synaptophysin and Itsn1. Moreover, ultrastructure analysis of *in vitro* cultured hippocampal neurons showed that the lack of Eps15L1 led to a reduced number of synaptic vesicles, thus indicating a defect in SVR (Alberici et al., unpublished results).

Eps15/Eps15L1-DKO displayed a more severe phenotype than single KO mice: they died at midgestation between 10.5 and 11.5 dpc (days post coitum) (Table 1) and had severe developmental defects. At 9.5 dpc, more severely affected embryos had growth defects and absence of turning. All embryos, moreover, had an open neural tube, an enlarged pericardium and the limb bud was absent (Figure 12A). Less severely affected embryos had also reduced vascularization, as assessed by PECAM-1 staining (Figure 12B, C).

dpc	Litters	Eps15-KO/ Eps15L1-WT	Eps15-KO/ Eps15L1-HET	Eps15-KO/ Eps15L1-KO	Total
9.5	19	39 (27%)	75 (53%)	28 (20%)	142
10.5	2	1 (7%)	11 (78%)	2 (14%)	14
11.5	1	4 (57%)	3 (43%)	0	7
12.5	2	8 (40%)	12 (60%)	0	20

Table 1. Eps15/Eps15L1-DKO mice die between 9.5 and 11.5 dpc.

The table represents the number and the percentage of Eps15-KO/Eps15L1-WT, Eps15-KO/Eps15L1-HET and Eps15-KO/Eps15L1-KO embryos, from different litters, which were found viable from 9.5 to 12.5 dpc.

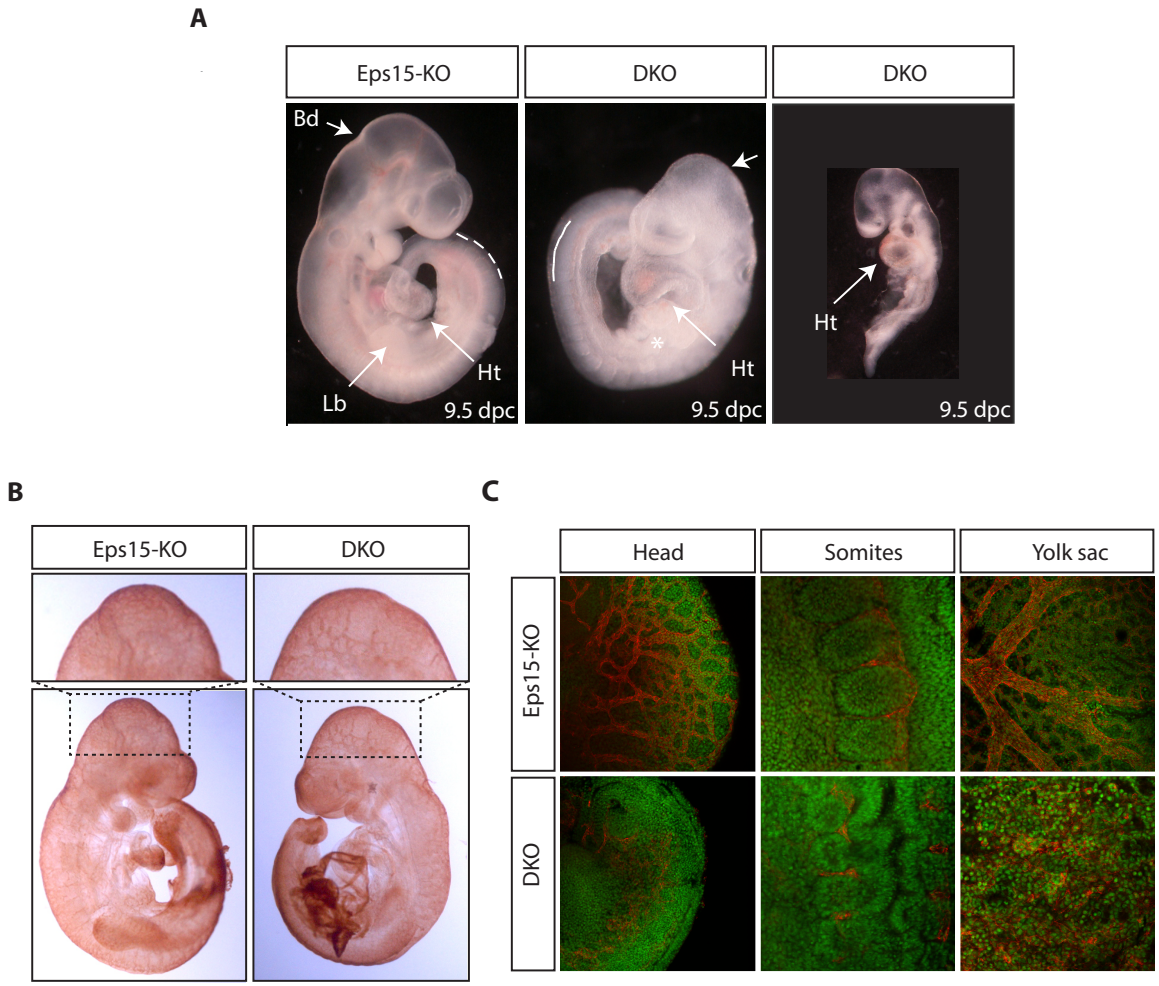

Figure 12. 9.5 dpc Eps15/Eps15L1-DKO have severe development defects.

A. The photographs compare 9.5 dpc DKO and Eps15-KO mice. White arrows indicate midbrain/hindbrain boundary (Bd), lim bud (Lb) and heart (Ht). Star indicates absence of forelimb bud in DKO mice. **B.** Immunohistochemical staining with the endothelial marker PECAM-1 of 9.5 dpc DKO and Eps15-KO mice. Magnifications represent portions of the head. **C.** IF staining with the endothelial marker PECAM-1 (red) of 9.5 dpc DKO and Eps15-KO mice. The head, somitic and yolk sac regions are shown.

5.2. Functions of Eps15 and Eps15L1 in mammals: hypothesis on Notch signalling regulation

Studies from Eps15/Eps15L1-DKO mice revealed that lack of both proteins lead to morphological defects that phenocopyed characteristics of Notch signalling loss-of-function mutants, such as Notch1-KO (Swiatek, Lindsell et al. 1994, Limbourg, Takeshita

et al. 2005), Notch1/Notch4-DKO (Krebs, Xue et al. 2000), Dll1-KO (Hrabe de Angelis, McIntyre et al. 1997), Dll4-KO (Duarte, Hirashima et al. 2004), Jagged1-KO (Xue, Gao et al. 1999), Numb-KO (Zilian, Saner et al. 2001), epsin1/2-DKO (Chen, Ko et al. 2009) and Mib1-KO (Koo, Lim et al. 2005) (Table 2).

Gene Name	Receptor/ ligand/ other	KO lethality	Cardiovascular defects	Placental and yolk sac defects	Defects in nervous system	Reference
Notch1	Receptor	< 11.5 dpc	YES	YES	YES	(Swiatek, Lindsell et al. 1994)
Tie2Cre/ Notch1	Receptor	< 11.5 dpc	YES	YES	YES	(Limbourg, Takeshita et al. 2005)
Notch1/ Notch4	Receptor	< 11.5 dpc	YES	YES	YES	(Krebs, Xue et al. 2000, Krebs, Xue et al. 2000)
Dll1	Ligand	< 11.5 dpc	YES	/	YES	(Hrabe de Angelis, McIntyre et al. 1997)
Dll4	Ligand	< 11.5 dpc	YES	YES	/	(Duarte, Hirashima et al. 2004)
Jag1	Ligand	< 11.5 dpc	YES	/	/	(Xue, Gao et al. 1999)
Numb	Endocytic adaptor	< 11.5 dpc	YES	YES	YES	(Zilian, Saner et al. 2001)
Epsin1/2	Endocytic adaptors	< 11.5 dpc	YES	YES	YES	(Chen, Ko et al. 2009)
Mib1	E3 ligase	< 11.5 dpc	YES	YES	/	(Koo, Lim et al. 2005)
Eps15/Eps15L1	Endocytic adaptors	< 11.5 dpc	YES	YES	YES	(unpublished)

Table 2. Notch loss-of-function mutants.

The table summarizes the main phenotypic defects (lethality and presence of cardiovascular, placental, yolk sac and neural defects) of embryos KO for the principal components of the Notch signalling pathway.

To understand whether and which signalling pathways were deregulated in the absence of Eps15 and Eps15L1, a microarray analysis was performed on 9.5 dpc Eps15-KO, Eps15L1-KO and Eps15/Eps15L1-DKO embryos.

The majority of genes that were altered in DKO mice recapitulated the morphological changes in the embryos. Indeed, genes involved in cardiac and neural development, in hematopoiesis and in metabolism were deregulated. Numerous genes were also found altered in the signalling category. Major signalling pathways, such as SMAD, β-catenin and hedgehog, were not deregulated (data not shown). However, the Notch target genes HES1, HES5 and NRARP were downregulated in DKO embryos. To confirm these findings, a QPCR analysis of 9.5 dpc embryos was performed, using epsin1/2-DKO embryos as a control. The Notch target genes HES1, HES5 and NRARP were confirmed to be downregulated in Eps15/Eps15L1-DKO to the same extent as in epsin1/2-DKO mice (Figure 13). Taken together, these observations suggest that loss of both Eps15 and Eps15L1 correlate with a Notch loss-of-function phenotype.

Besides morphological defects and downregulation of the Notch target genes HES1, HES5 and NRARP in Eps15/Eps15L1-DKO mice, previous data pointed to a role for Eps15 and Eps15L1 in the endocytic regulation of Notch signalling: i) Eps15 and Eps15L1 physically interact with Numb and epsin (Salcini, Confalonieri et al. 1997, Chen, Fre et al. 1998), key regulators of Notch receptor and ligand activity, respectively; ii) Eps15 and Eps15L1 act in complex with epsin1 to modulate EGFR endocytosis (Chen, Fre et al. 1998, Sigismund, Woelk et al. 2005); iii) Eps15 and Eps15L1 possess two UIM domains, one of the two essential domains needed for epsin-dependent activation of Notch ligands (Xie, Cho et al. 2012).

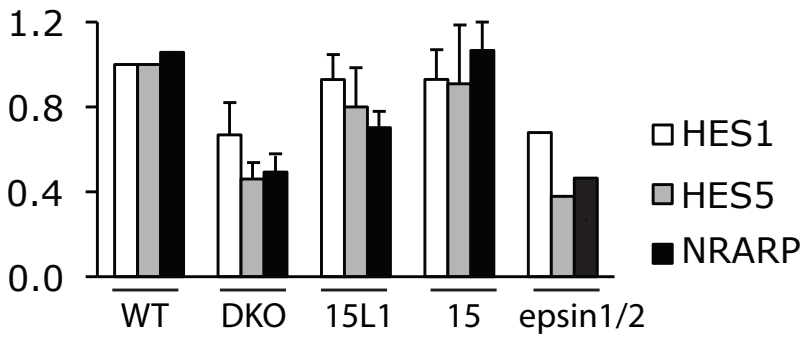

Figure 13. Downregulation of Notch target genes in 9.5 dpc Eps15/Eps15L1-DKO mice.

The bar graph depicts the relative expression levels of the Notch target genes HES1 (white bars), HES5 (grey bars) and NRARP (black bars) in wild type (WT), Eps15/Eps15L1-DKO (DKO), Eps15L1-KO (15L1), Eps15-KO (15) and epsin1/2-DKO (epsin1/2) embryos at 9.5 dpc, as determined by QPCR. All values were normalized on GAPDH and on the relative expression levels of WT embryos. At least 3 independent embryos were analysed for each gene, except for epsin1/2-DKO (n=1). Results are expressed as mean ± standard deviation.

These observations lead to the hypothesis that Eps15 and Eps15L1 might regulate Notch signalling, either in the signal-sending or in the signal-receiving cell.

To study the biology of Notch ligands and receptors *in vitro*, our laboratory employed a luciferase-based co-culture cell model system in which a signal-sending cell, expressing a Notch ligand, and a signal-receiving cell, expressing a Notch receptor, come into close contact (Lucano et al., unpublished results). As a model for the signal-sending cell, the bone marrow, stromal, murine cell line OP9, overexpressing the Notch ligand Dll1 (OP9-Dll1 cells) was used. The OP9-Dll1 cell line was generated in 2002 by Schmitt and Zuniga-Pflucker as a tool to study the role of Dll1 in thymocyte development *in vitro* (Schmitt and Zuniga-Pflucker 2002). As a model for the signal-receiving cell, the murine, myoblast cell line C2C12, a subclone of the myoblast cell line established by Yaffe and Saxel (Yaffe and Saxel 1977), constitutively expressing the Notch1 receptor (C2C12-Notch1 cells), was used. In this co-culture cell model system, it was found that transient KD of Eps15 and Eps15L1, alone or in combination, in OP9-Dll1 cells lead to a ~50% reduction of Notch activation. On the contrary, no effect was observed when Eps15 and Eps15L1 were knocked-down, alone or in combination, in the signal-receiving cell. Of note, no further reduction of Notch signalling was observed when Eps15 and Eps15L1 were knocked-down in combination both in the signal-sending and in the signal-receiving cell. This *in vitro* work suggests that Eps15 and Eps15L1 regulate Notch signalling in the signal-sending cell.

6. Aims of this project

Most of the *in vitro* studies found in literature have been focused on Eps15, while fewer studies have addressed the *in vitro* functions of Eps15L1. The reason of this discrepancy resides on the fact that Eps15 and Eps15L1 have always been thought to be redundant in several cellular processes, due to their homology, their common binding partners and their similar cellular localization. Nevertheless, this redundancy has not always been demonstrated by *in vitro* studies. In addition, their role in a physiological setting has never been investigated.

Our laboratory addresses whether Eps15 and Eps15L1 exert redundant and/or non-redundant roles in mammals, using genetically engineered mice as a model system. In these organisms, the genetical removal of components of endocytosis rarely impinges on its efficiency, likely because functionally redundant proteins or pathways compensate for their lack. This is the case for Eps15, whose removal has no evident effect (Pozzi, Amodio et al. 2012), suggesting that other proteins, more likely its homologous Eps15L1, could absolve its functions. Nevertheless, during evolution, homologous proteins are differently shaped, so that some functions can be lost and others acquired.

Up to now, studies in genetically engineered mice indicate that while Eps15 functions can be redundantly compensated by Eps15L1 and/or other endocytic proteins, Eps15L1 plays a non-redundant role in the regulation of SVR, which is reminiscent of the role played by its orthologous in lower organisms (Alberici et al., unpublished results). Since studies in single KO mice indicate that Eps15 and Eps15L1 have both redundant and non-redundant functions, the severe phenotype of Eps15/Eps15L1-DKO might result from the impairment of a redundant function that is essential for embryo development or from the combined impairment of redundant and non-redundant functions, which, even if not essential, might addictively contribute to embryo lethality.

The aim of this project was to investigate redundant and non-redundant functions of Eps15 and Eps15L1 in order to unmask the underlying causes of embryo lethality in Eps15/Eps15L1-DKO mice.

To this end, by combining *in vivo*, *in vitro* and *ex vivo* approaches, we have investigated whether: i) Eps15 and Eps15L1 play a role in the regulation of Notch signalling in mouse embryonic fibroblasts (MEFs) derived from KO mice for Eps15 and Eps15L1, in order to extend previous findings (see section "5.2. Functions of Eps15 and Eps15L1 in mammals: hypothesis on Notch signalling regulation"); ii) whether midgestation lethality of DKO mice is caused by impaired vascular development; iii) whether Eps15 and Eps15L1 play a role in EGFR and TfR internalization in MEFs, due to the extensive literature claiming their role in the internalization of these receptors in various cellular systems; iv) whether Eps15 and Eps15L1 affect RBC development, similarly to other endocytic adaptor proteins, such as PICALM (Ishikawa, Maeda et al. 2015).

Chapter 2

MATERIALS AND METHODS

1. Materials

1.1. Solutions

Gietscher buffer 10X

NH_4SO_4	166 mM
Tris-HCl pH 8.8	670 mM
β-Mercaptoethanol	5 mM
EDTA pH 8.0 10 mM	67 µM

Store at -20 °C.

JS buffer 1X

HEPES, pH 7.4	50 mM
NaCl	150 mM
Glycerol	1%
Triton X-100	1%
$MgCl_2$	1.5 mM
EGTA	5 mM

Just before use, add the following phosphatase and protease inhibitors: PMSF 1

mM, sodium orthovanadate 10 mM, sodium fluoride 50 mM and Protease inhibitor cocktail Set III 100X (Calbiochem).

Laemmli buffer 5X

SDS	10%
Tris HCl, pH 6.8	250 mM
DTT	500 mM
Glycerol	50 %
Bromophenol blue	0.005 %

Store at -20 °C.

Paraformaldehyde 4%

Paraformaldehyde	4 gr
PBS 1X	100 ml

Store at -20 °C.

Phosphate-buffered saline (PBS) 1X

NaCl	137 mM
KCl	2.7 mM
Na_2HPO_4	10 mM
KH_2PO_4	2 mM

Ponceau S

Ponceau	0.1% (w/v)
Acetic acid	5%

RIPA lysis buffer 1X

Tris HCl, pH 7.6	50 mM
NaCl	150 mM
NP-40	1%
SDS	0.1%
Deoxycholic acid	0.5%

Just before use, add the following phosphatase and protease inhibitors: PMSF 2 mM, sodium orthovanadate 10 mM, sodium pyrophosphate pH 7.5 20 mM, sodium fluoride 50 mM and Protease inhibitor cocktail Set III 200X (Calbiochem).

SDS-PAGE running buffer 10X

Glycine	192 mM
Tris HCl, pH 8.3	250 mM
SDS	1%

Tail buffer

Gietscher buffer	1X
Triton X-100	0.5%
Proteinase K (PK)	500 μg/ml

Tris-Acetate-EDTA (TAE) 50X

Tris base	2 M
Acetic acid	1 M
EDTA, pH 8	10 mM

Adjust the pH to 8.5 with HCl.

Tris-EDTA (TE) 1X

Tris base	10 mM
EDTA	1 mM

Adjust the pH to 8 with HCl.

Tris-buffered saline (TBS) 1X

NaCl	137 mM
KCl	2.7 mM
Tris HCl pH 7.4	25 mM

Adjust the pH to 7.4 with HCl.

Tris-HCl 1 M

Tris base	121.1 gr
ddH_2O	to 1 L

Adjust the pH to 7.4, 7.6 or 8.0 with HCl.

Western transfer buffer 10X

Glycine	192 mM
Tris HCl, pH 8.3	250 mM

For Western transfer buffer 1X, dilute the 10X stock 1:10 with ddH_2O and 20% v/v methanol or ethanol.

1.2. Reagents

The manufacture has been indicated for each reagent used in this thesis project.

1.3. Antibodies

The antibodies used in this thesis project are listed in Table 3.

Home made antibodies were raised as indicated:

- rabbit polyclonal anti-Eps15, home made against full-length murine Eps15 protein fused to GST;
- rabbit polyclonal anti-Eps15L1, home made against the N-terminal region of murine Eps15L1 (aminoacids: 216-266) between the EH2 and EH3 fused to GST;
- rabbit polyclonal anti-Itsn1, home made against the central region of human Itsn1 (aminoacids: 583-888), kindly provided by Simona Polo.

1.4. RNAi oligos

The sequence of the scrambled Stealth RNAi siRNA oligo (Invitrogen) used in this thesis project is: AGACGAACAAGUCACCGAC.

The sequence of the Stealth RNAi siRNA oligo against murine Mib1 (Invitrogen) used in this thesis project is: GGUGCUAAGCUAGACAUUCAGGAUA.

1.5. Constructs and plasmids

pLenti TetR Blast was purchased from Addgene (Plasmid #17492).

pcDNA5/TO-Delta-mCherry was kindly provided by Elowitz MB (Sprinzak, Lakhanpal et al. 2010).

pBABE-mycEps15L1 has been previously described (Coda, Salcini et al. 1998).

2. Methods

2.1. Cloning techniques

2.1.1. Agarose gel electrophoresis

DNA samples were loaded on 0.8%-2% agarose gels along with DNA markers (1 kb DNA Ladder, Promega). Gels, containing Gel Red (Biotium), were run in TAE buffer 1X at 80 Volts, until desired separation was achieved. DNA bands were visualized under a UV lamp.

2.1.2. Minipreps

Individual colonies were used to inoculate 10 ml LB (lysogeny broth) medium (containing the appropriate antibiotic) and grown overnight at 37°C. Bacteria were centrifuged for 5 minutes at 16,000 x g using a 5415 R centrifuge (Eppendorf). Minipreps were performed with the Wizard Plus SV Minipreps Kit (Promega), according to manufacturer's instructions. The plasmids were eluted in 50 µl nuclease-free H_2O.

2.1.3. Diagnostic DNA restriction

0.5 µg DNA were digested for 2 hours at 37 °C with 10-20 units of restriction enzyme (New England Biolabs). For digestion, the volume was made up to 20 µl with the appropriate buffer and ddH_2O.

2.1.4. Large scale plasmid preparation

Bacterial competent DH5α, transformed with the desired plasmid DNA, were grown

overnight at 37 °C into 250 ml LB medium (containing the appropriate antibiotic). Plasmid DNA was isolated with the Qiagen Maxi-prep kit, according to manufacturer's instructions.

2.1.5. Transformation of bacterial competent cells

An aliquot of bacterial competent cells DH5α (Invitrogen) was thawed on ice and incubated with the desired plasmid DNA for 30 minutes on ice. Cells were then subjected to a heat shock for 45 seconds at 42 °C and returned to ice for additional 5 minutes. 300 µl of SOC were added and the cells were left at 37 °C for further 60 minutes before plating onto LB agar plates containing the appropriate antibiotic. Two plates for each reaction were used, one plated with 100 µl of the transformed bacterial cells and the other one with the rest. Plates were incubated overnight at 37 °C.

2.2. Cell culture techniques

2.2.1. Cell lines and culture conditions

MEFs were generated from 13.5 dpc $Eps15^{flp/flp}/Eps15L1^{+/+}/tg^{CreERT2}$ and $Eps15^{flp/flp}/Eps15L1^{-/-}/tg^{CreERT2}$ mice, as described in section "2.8.3. Preparation of MEFs" of this chapter. MEFs were used for radioactive assays, Co-IP and IF analysis. They were grown in HEPES buffered GlutaMAX-DMEM (Gibco Invitrogen), supplemented with 10% FBS (fetal bovine serum) south american (HyClone).

MEFs were immortalized upon continuing passaging in sub-confluent conditions. Immortalized MEFs were used as a model for the signal-sending cell. In detail, for the generation of immortalized MEFs expressing doxycycline-inducible Dll1-mCherry (MEF-Dll1 cells), cells were firstly transduced with pLenti TetR Blast by lentiviral particles and selected for 15 days with 1 µg/ml blasticidin (Thermo Fisher Scientific). Cells were then

transfected with pcDNA5/TO-Delta-mCherry using Lipo2000 reagent (Invitrogen), according to the manufacturer's instructions, and selected with 75 μg/ml hygromycin (Thermo Fisher Scientific) for 5 days. Cells, stably expressing doxycycline-inducible Dll1-mCherry, were sorted by FACS after induction of Dll1-mCherry expression by treatment with 50 ng/ml doxycycline for 24 hours. KD in MEF-Dll1 cells was performed by transfection of 10 nM Stealth RNAi siRNA oligos (Invitrogen) with Lipofectamine RNAiMAX transfection reagent (Invitrogen), according to the manufacturer's instructions. MEF-Dll1 cells were grown in HEPES buffered GlutaMAX-DMEM (Gibco Invitrogen), supplemented with 10% tetracycline-free FBS (HyClone).

Deletion of Eps15 in primary and immortalized fibroblasts was obtained by treatment of the parental cell line ($Eps15^{flp/flp}/Eps15L1^{+/+}/tg^{CreERT2}$ and $Eps15^{flp/flp}/Eps15L1^{-/-}/tg^{CreERT2}$) with 250 nM (Z)-4-hydroxytamoxifen (Sigma) for 10 days.

CHO-hN1Gal4 cells were a gift from Elowitz MB (Sprinzak, Lakhanpal et al. 2010).

CHO and CHO-hN1Gal4 cells were grown in GlutaMAX-MEMα (Gibco Invitrogen), supplemented with 10% tetracycline-free FBS (HyClone). CHO-hN1Gal4 cells were cultured in the presence of the following antibiotics: 10 μg/ml blasticidin (Thermo Fisher Scientific), 400 μg/ml zeocin (Thermo Fisher Scientific) and 600 μg/ml geneticin (Thermo Fisher Scientific).

Immortalized endothelial cells were generated from lungs of $Eps15^{flp/flp}/Eps15L1^{-/-}$ newborn mice by Polyoma middle T (PmT) infection, as described in section "2.8.4 Preparation of endothelial cells" of this chapter (Balconi, Spagnuolo et al. 2000). Cells were grown on culture dishes coated with 0.1% gelatin (Sigma), in the presence of HEPES buffered GlutaMAX-DMEM (Gibco Invitrogen), supplemented with 20% FBS north american (HyClone), 50 μg/ml ECGS (endothelial cell growth supplement) (Sigma) and 100 μg/ml heparin (Sigma). To obtain endothelial cells stably expressing myc-Eps15L1, cells were transduced with pBABE-mycEps15L1 by retroviral particles and selected for three days with 1 μg/ml puromycin (Thermo Fisher Scientific). Deletion of Eps15 was obtained by

treatment, for two consecutive days, with 100 μg/ml Tat-Cre recombinase for 1 hour at 37 °C.

All cell lines used in this thesis project were cultured under sterile conditions in a humidified incubator at 37 °C and 5% CO_2. Culturing media were changed every 2/3 days. Cells were harvested at 80-90% confluency and plated at a ratio of 1:5/1:10 for CHO and CHO-hN1Gal4 cells, and 1:2/1:3 for all the other cell lines. Harvesting of the cells was performed as follows: cells were washed twice with sterile PBS 1X, without calcium and magnesium, and subsequently incubated with 0,05% trypsin/0,02% EDTA solution in PBS 1X (EuroClone) at 37 °C for 5 minutes. After the detachment of the cells, trypsin was inhibited by addition of the appropriate medium supplemented with FBS. Cells were diluted to the desired concentration in growth medium and plated.

For long-term storage, cells were frozen and stored in liquid nitrogen as follows: after trypsinization, 1 million of cells was suspended in 1 ml of freezing solution, composed of 90% FBS (HyClone) and 10% DMSO (Sigma), and placed in cryovials (Nalgene). Vials were immediately placed at -80 °C in a cryobox and, after overnight storage, transferred to liquid nitrogen.

2.2.2. Transfections

RNAi transfection

MEF-Dll1 cells were transfected with 10 nM Stealth RNAi siRNA oligos (Invitrogen) through Lipofectamine RNAiMAX transfection reagent (Invitrogen), according to the manufacturer's instructions. Lipofectamine RNAi Max is a cationic lipid, optimized for RNA molecules transfection. Cationic lipids establish electrostatic bonds with the negative charges of the nucleic acid and the negative charges of PM, thus facilitating the entry of the nucleic acid into the cell.

To perform RNAi transfection, on day 1 cells were detached from the plate, counted and

suspended in fresh medium at $0{,}5x10^5$ cells/ml concentration. 2 ml of cell suspension (for a total of $1x10^5$ cells) were transferred in a sterile 15 ml falcon. 500 µl of transfection mix were added dropwise to the cell suspension and the content of the falcon was then plated in 1 well of a 6-well plate.

Transfection mix was prepared as follows:

- Mix 1: 5 µl of Lipofectamine RNAi MAX (Invitrogen) in 250 µl of Opti-MEM fresh medium (Gibco).
- Mix 2: Oligos at the desired final concentration in 250 µl of Opti-MEM fresh medium (Gibco).
- Transfection mix: mix 1 was added to mix 2 and incubated 20 minutes at room temperature before use.

RNA interfered cells were transferred in a humidified incubator at 37 °C and 5% CO_2 for 24 hours. On day 2 the culture medium was changed and transfection was repeated, as described before, on adherent cells. On day 3 cells were used for the co-culture assay experiment, until day 5. KD efficiency was evaluated by WB at the fifth day.

DNA transfection

Immortalized MEFs were transduced with pcDNA5/TO-Delta-mCherry using Lipo2000 reagent (Invitrogen), according to the manufacturer's instructions. In detail, cells were plated in 10 cm plates so that they were 90% confluent on the day of transfection. The day after, the culture medium was replaced by 7.5 ml of complete medium plus 2.5 ml of transfection mix.

Transfection mix was prepared as follows:

- Mix 1: 10 µg DNA in 1250 µl of Opti-MEM fresh medium (Gibco).
- Mix 2: 30 µl Lipo2000 reagent in 1250 µl of Opti-MEM fresh medium (Gibco).
- Transfection mix: mix 1 was added to mix 2 and incubated 20 minutes at room temperature before use.

Transduced cells were transferred overnight in a humidified incubator at 37 °C and 5% CO_2. On day 2 the culture medium was changed. 24 hours after transfection, cells were selected with 75 μg/ml hygromycin (Thermo Fisher Scientific) for 5 days and continuously cultured in the presence of the antibiotic.

2.2.3. Infection

Retroviral infection

Endothelial cells were transduced with murine Eps15L1 by retroviral infection. Retroviruses were produced by overnight transfection of the Phoenix helper cell line with 10 μg of pBABE-mycEps15L1 DNA. In detail, Phoenix cells were plated in 10 cm plates so that they were 70-80% confluent on the day of transfection. The day of transfection, the medium was replaced by 9 ml of complete medium, 20 μM cloroquine and 1 ml of transfection mix.

Transfection mix was prepared as follows:

- Mix 1: 500 μl of HBSS (Hanks' balanced salt solution) 2X.
- Mix 2: 10 μg pBABE-mycEps15L1, 61 μl $CaCl_2$ 2M, ddH_2O up to 500 μl.
- Transfection mix: mix 2 was added to bubbling mix 1 and incubated 5 minutes at room temperature before use.

On day 2, endothelial cells were plated on 6-well plates. 48 hours after transfection of the Phoenix helper cell line, supernatant was collected and passed through a 0.45 μm filter. After the addition of 8 μg/ml polybrene (Sigma), the supernatant was added to endothelial cells. Cells were then centrifuged for 45 minutes at 18,000 rpm. After infection, the viral supernatant was replaced with the standard medium (see section "2.2.1. Cell lines and culture conditions"). 48 hours after infection, infected cells were selected with 1 μg/ml puromycin (Thermo Fisher Scientific) and continuously cultured in the presence of the antibiotic.

Lentiviral infection

Immortalized MEFs were transduced with pLenti TetR Blast by lentiviral particles. Lentiviruses were produced by overnight transfection of the 293T helper cell line with 10 µg of pLenti TetR Blast DNA. In detail, on day 1, 293T cells were plated in 10 cm plates at $5x10^6$ cells/plate. In the evening, the medium was replaced by 9 ml of complete medium and 1 ml of transfection mix.

Transfection mix was prepared as follows:

- Mix 1: 500 µl of HBSS 2X.
- Mix 2: 10 µg pLenti TetR Blast DNA, 2.8 µg ENV, 5 µg pMDL, 2.5 µg REV, 62.4 µl $CaCl_2$ 2M, sterile TE 0.1X up to 500 µl.
- Transfection mix: mix 2 was added to bubbling mix 1 and incubated 5 minutes at room temperature before use.

On day 2, target cells were plated on 6-well plates. On day 3, supernatant from 293T cells was collected and passed through a 0.45 µm filter. After the addition of 8 µg/ml polybrene (Sigma), the supernatant was added to MEFs. Cells were then centrifuged for 45 minutes at 18,000 rpm. After infection, the viral supernatant was replaced with the standard medium (see paragraph "2.2.1. Cell lines and culture conditions"). 48 hours after infection, infected cells were selected with 10 µg/ml blasticidin (Thermo Fisher Scientific) for 15 days and continuously cultured in the presence of the antibiotic.

2.3. Protein procedures

2.3.1. Cell lysis

Cell culture plates were put on ice, washed with PBS 1X and then lysed in JS or RIPA buffer with a cell-scraper. Lysates were clarified by centrifugation at 13,000 rpm for 20 minutes at 4 ºC, using a 5415 R centrifuge. Protein concentration was measured by BCA

Protein assay (Thermo Fisher Scientific), according to manufacturer's instructions, using BSA (bovine serum albumin) as standard.

2.3.2. WB (Western blot)

Proteins were dissolved in Laemli buffer 1X, boiled at 95 °C for 5 minutes and spun. Desired amounts of proteins were loaded onto 4-20% Criterion TGX Stain-Free precast gels (Biorad) for electrophoresis, together with a WesternC Western Blotting Protein Standard (Biorad) for MW (molecular weight) determination. Gels were run at 200 Volts in running buffer 1X within a Criterion electrophoresis cell (Biorad). After electrophoresis, proteins were transferred to a nitrocellulose membrane by a Trans-Blot Turbo blotting apparatus (Biorad). Ponceau staining was used to determine the efficiency of protein transfer onto the filters. Filters were blocked for 1 hour in 5% BSA-TBST 1X, where TBST 1X is TBS 1X supplemented with 0.1% Triton X-100. After blocking, filters were incubated overnight at 4 °C with the primary antibody diluted in 5% BSA-TBST 1X and then washed in TBST 1X (three washes of 5 minutes each). Filters were then incubated with the appropriate HRP (horseradish peroxidase)-conjugated secondary antibody diluted in TBST 1X for 1 hour at room temperature. After incubation with the secondary antibody, filters were washed in TBST 1X (three washes of 5 minutes each). The bound secondary antibody was revealed under a ChemiDoc Imaging System, after incubation with SuperSignal West Femto Maximum Sensitivity Substrate (Thermo Fisher Scientific), an ultra-sensitive ECL (enhanced chemiluminescent) substrate. Quantification of blots was performed with ImageJ Software. All statistical analyses were performed using Excel. The statistical significance was obtained applying t-test.

2.3.3. IP (Immunoprecipitation)

WT, Eps15-KO, Eps15L1-KO and Eps15/Eps15L1-DKO MEFs were generated from $Eps15^{flp/flp}/Eps15L1^{+/+}/tg^{CreERT2}$ and $Eps15^{flp/flp}/Eps15L1^{-/-}/tg^{CreERT2}$ cells. In detail, $Eps15^{flp/flp}/Eps15L1^{+/+}/tg^{CreERT2}$ were used as WT, while $Eps15^{flp/flp}/Eps15L1^{-/-}/tg^{CreERT2}$ were used as Eps15L1-KO. By (Z)-4-hydroxytamoxifen treatment, Eps15-KO and Eps15/Eps15L1-DKO cells were generated from WT and Eps15L1-KO cells, respectively. Cells of each genotype were lysed in JS buffer for 10 min at 4 ºC. Lysates were centrifuged for 30 minutes at 4 ºC at 13,000 rpm and then ultra-centrifuged for 1 hour at 4 ºC at 45,000 rpm. After protein determination with BCA protein assay, one part of the lysates was collected as input, while another part was used for IP. In detail, same amounts of proteins from each genotype were incubated overnight at 4 ºC, under rotation, with mouse anti-alpha Adaptin antibody [AP6] (0.5 ug antibody/100 ug proteins) or home made rabbit anti-Itsn1 antibody (1.2 ug antibody/100 ug proteins). The following day lysates were incubated with Dynabeads Protein G (Invitrogen) (300 ug beads/100 ug proteins), previously washed with JS buffer, for 1 hour at 4 ºC, under rotation. The beads, bound to mouse anti-alpha Adaptin antibody [AP6] or home made rabbit anti-Itsn1 antibody, were then separated from supernatant with the magnetic particle concentrator DynaMag-2 (Invitrogen) and washed with JS buffer. The supernatants, containing unbound proteins, were collected as post-immunoprecipitated. Proteins bound to beads were eluted in Laemmli Buffer 2.5X, boiled at 95 ºC, separated from the beads with the magnetic particle concentrator and then processed for WB analysis, together with input and post-immunoprecipitated.

2.4. Analysis of the Notch signalling pathway

2.4.1. Measurement of Dll1 levels in MEF-Dll1 cells by FACS analysis

Flow cytometry assay is a technique for counting, examining and sorting cells suspended

in a stream of fluid. It allows simultaneous multi-parametric analysis of the physical and/or chemical characteristics of single cells flowing through a fluidic, optical and electronic detection apparatus. A beam of laser light of a determined single wavelength is directed onto a hydro-dynamically focused stream of fluid. Each suspended cell passes through a small nozzle, one cell at a time, and scatters the light in a certain way. Moreover fluorescent chemicals found in the cell or attached to the cell membrane can be excited into emitting light at a higher wavelength than the light source. The detectors pick up this combination of scattered and fluorescent light and, by analyzing fluctuations in brightness at each detector (one for each fluorescent emission peak), it is then possible to derive information about the physical and chemical structure of each individual cell. FSC (forward scatter) correlates with the cell size and SSC (side scatter) depends on the inner density and granularity of the cell (e.g. shape of the nucleus, the amount and type of cytoplasmic granules or the membrane roughness).

WT, Eps15L1-KO, Eps15-KO and Eps15/Eps15L1-DKO MEF-Dll1 cells were used. Eps15-KO and Eps15/Eps15L1-DKO MEF-Dll1 cells were generated from WT ($Eps15^{flp/flp}/Eps15L1^{+/+}/tg^{CreERT2}$) and Eps15L1-KO ($Eps15^{flp/flp}/Eps15L1^{-/-}/tg^{CreERT2}$) cells, respectively, by treatment with 250 nM (Z)-4-hydroxytamoxifenefore for 10 days. WT MEF-Dll1 cells were treated with different amounts of doxycycline (50, 100, 150 ng/ml) for 24, 48 and 72 hours, in order to determine the optimal mode for Dll1-mCherry induction. Since Dll1-mCherry induction was similar in all conditions, for further experiments, MEF-Dll1 cells of each genotype were treated with 50 nM doxycycline for 48 hours. To measure surface levels of Dll1-mCherry, cells were washed with PBS 1X without calcium and magnesium, trypsinized for 3 minutes with 0.05% trypsin/0.02% EDTA, suspended in complete medium and counted. For each staining, $1x10^5$ cells were blocked for 1 hour in 10% BSA-PBS 1X on ice. Cells were then stained overnight at 4 °C with 1 µg/ml anti-Dll1 HMD1-3 Alexa Fluor 647 (Biolegend) in 100 µl of 5% BSA-PBS 1X. After staining, cells were washed in cold PBS 1X, suspended in 2% BSA-PBS 1X and

immediately analyzed using flow cytometer. Data generated by flow-cytometer were analyzed by FlowJo (version 10.1) and plotted in two dimensional dot plots. In detail, cells were first gated based on the size (FSC) and on density and granularity of the cells (SSC). Next, cells were gated into four subpopulations: cells not expressing Dll1-mCherry (double negative cells for mCherry and Alexa Fluor 647 and single negative cells for mCherry), cells expressing Dll1-mCherry but not exposing the ligand on the PM (single positive cells for mCherry) and cells expressing Dll1-mCherry that was exposed on the PM (double positive cells for mCherry and Alexa Fluor 647). These gates were defined by fluorescence analysis of mCherry and Alexa Fluor 647, after surface-staining, of the parental MEF cell line not expressing doxycycline-inducible Dll1-mCherry: being this cell line double negative for both mCherry and Alexa Fluor 647, it was used to determine background fluorescence intensities for mCherry and Alexa Fluor 647.

2.4.2. Co-culture assay among MEF-Dll1 and CHO-hN1Gal4 cells

MEF-Dll1 cells were co-cultured with CHO-hN1Gal4 cells in a 24-well plate. For each well, $6x10^4$ MEF-Dll1 and $4x10^4$ CHO-hN1Gal4 cells were mixed and plated. Control experiments were performed with WT MEF-Dll1 cells previously transfected with a siRNA oligo against Mib1 or a scrambled siRNA oligo, as above described (the sequence of siRNA oligos and technical procedures are reported in sections “1.4. RNAi oligos” and “2.2.2. Transfections” of this chapter, respectively). To investigate the role of Eps15 and Eps15L1 in Notch signalling activation, WT, Eps15L1-KO, Eps15-KO and Eps15/Eps15L1-DKO MEF-Dll1 cells were used. Co-culture was performed for 48 hours in presence or absence of 50 ng/ml doxycycline. In control experiments, co-culture was also performed in presence of 1 μM of the Notch signalling inhibitor DAPT (Sigma) or 0.01% DMSO vehicle (Sigma). Drugs were administered for the total co-culture time. 48 hours after co-culture, cells were trypsinized and collected for cytofluorimetric analysis. In

detail, cells where washed 3 times in PBS 1X (containing calcium and magnesium) and trypsinized with 0.25% trypsin without EDTA for 10 minutes. After centrifugation at 2,500 rpm for 5 minutes at 4 °C, cells were suspended in 200 µl of PBS 1X containing 2% tetracycline-free serum and transferred into FACS tubes for detection of mCherry and YFP fluorescence. Data generated by flow-cytometer were analyzed by FlowJo and plotted in two dimensional dot plots. In detail, mixed MEF-Dll1 and CHO-hN1Gal4 cells were firstly gated based on the size (FSC) and on density and granularity of the cells (SSC). To determine Notch induction through YFP fluorescence, negative and positive cells for YFP (YFP- and YFP+, respectively), among CHO-HN1Gal4 cells, were gated based on the FACS analysis of the parental CHO cell line, which was used to define background fluorescence intensity of YFP. Among YFP positive cells (YFP+), cells expressing high levels of YFP (YFP++) were defined based on the shift of the cellular cloud. To determine Dll1 induction in MEF-Dll1 cells, negative and positive cells for mCherry were gated based on the FACS analysis of the parental MEF cell line, which was used to define background fluorescence intensity of mCherry.

2.5. Analysis of Notch and VEGFR-2 signalling pathways in endothelial cells

For the analysis of the Notch signalling pathway, confluent endothelial cells were treated with 10 µM of the Notch signalling inhibitor DAPT (Sigma) or 0.1% DMSO vehicle (Sigma) for 24 hours, followed by a second drug dose for other 8 hours. Cells where then lysed in JS buffer for WB analysis of NICD levels.

For the analysis of the VEGFR-2 signalling pathway, endothelial cells were plated in sub-confluent conditions in 6-well plates. Cells were then starved overnight in MCDB 131 medium (Gibco Invitrogen) containing L-glutamine and 1% BSA. The day after, cells were

stimulated with 80 ng/ml VEGF (PeproTech) for 0, 5, 15 and 30 minutes and then lysed in JS buffer for analysis of VEGFR-2 signalling pathway by WB.

2.6. Radioactive assays with ^{125}I-EGF and ^{125}I-Tf

2.6.1. Radioactive internalization assays with ^{125}I-EGF and ^{125}I-Tf

Radioactive internalization assays with ^{125}I-EGF or ^{125}I-differic Tf (Perkin Elmer) were performed in WT, Eps15L1-KO, Eps15-KO and Eps15/Eps15L1-DKO MEFs. Eps15-KO and Eps15/Eps15L1-DKO cells were derived by (Z)-4-hydroxytamoxifen treatment of $Eps15^{flp/flp}/Eps15L1^{+/+}/tg^{CreERT2}$ (WT) and $Eps15^{flp/flp}/Eps15L1^{-/-}/tg^{CreERT2}$ (Eps15L1-KO) cells, respectively. The day before experiment, cells were plated in a 24-well plate in order to have 90% of confluency the day after ($9x10^4$ cells/well). Cells were plated in the presence of HEPES buffered GlutaMAX-DMEM, supplemented with 10% FBS. The following day cells were serum starved in HEPES buffered GlutaMAX-DMEM supplemented with 0.1% BSA for 2 hours. For the analysis of internalization kinetics of the TfR, cells were incubated at 37 °C with 1 ug/ml ^{125}I-differic Tf for 2, 4 or 6 minutes. Unspecific was determined by incubation of cells with excess of cold ligand (500 X). For the analysis of internalization kinetics of the EGFR, cells were incubated at 37 °C with high doses and low doses of EGF ligand for 2, 4 or 6 minutes, in order to follow CDE and CIE of EGFR, respectively. For stimulation at high doses, 3 ng/ml of ^{125}I-EGF were combined to 27 ng/ml of cold ligand, for a total of 30 ng/ml of EGF. For stimulation at low doses, 1.5 ng/ml of ^{125}I-EGF were used. Unspecific was determined by incubation of cells with excess of cold ligand (300 X). After internalization, cells were put on ice, washed with cold PBS 1X and incubated for 5 minutes with an acid wash solution, pH=2.5 (0.2M acetic acid, 0.5M NaCl), to remove the quote of ligand bound on the membrane receptors. The acid wash solution was removed from the cells for radioactivity measurements. This sample represented the amount of ^{125}I-EGF or ^{125}I-differic Tf bound to the receptors on the cell surface (Bound).

Cells were then dried at room temperature and lysed with 300 µl of a solution containing 1N NaOH. The lysates, representing the amount of internalized ^{125}I-EGF or ^{125}I-differic Tf, were collected for radioactivity measurements. After being corrected for non-specific binding, the ratio between Internalized and Bound was determined for each time point. These data were used to obtain the internalization curves, representing the time in minutes and Internalized/Bound ratios on the x- and y-axis, respectively. The K_e (endocytic rate constant) were extrapolated from the internalization curves and correspond to the slopes of the best-fitting curves.

2.6.2. Measurement of the number of EGFR and TfR at the cell surface by saturation binding with ^{125}I-EGF and ^{125}I-Tf

For the count of PM receptors/cell, after serum starvation, cells were cooled on ice and incubated at 4 °C for 5 hours in the presence of 50 ng/ml EGF (HOT/COLD=1/9) or 2 µg/ml Tf (HOT/COLD=1/3). Unspecific binding of EGF or Tf to cell surface was determined by incubation of cells with excess of cold ligand (300 X and 500 X, respectively). After incubation at 4 °C, cells were put on ice, washed with cold PBS 1X, dried at room temperature and lysed with 300 µl of a solution containing 1N NaOH. The lysates were collected for radioactivity measurements. This sample represented the amount of ^{125}I-EGF and ^{125}I-Tf bound at equilibrium, which is dependent on the number of EGFR or TfR on the cell surface. After correction for non-specific binding, the assay provided the quantitative measurement of the number of EGFR or TfR for each well and, by counting the number of cells plated in each well, the number of surface EGFR or TfR for each cell.

2.7. IF (immunofluorescence)

WT, Eps15L1-KO, Eps15-KO and Eps15/Eps15L1-DKO MEFs were used for IF analysis. Eps15-KO and Eps15/Eps15L1-DKO cells were generated by (Z)-4-hydroxytamoxifen

treatment of $Eps15^{flp/flp}/Eps15L1^{+/+}/tg^{CreERT2}$ (WT) and $Eps15^{flp/flp}/Eps15L1^{-/-}/tg^{CreERT2}$ (Eps15L1-KO) cells, respectively. All cells were plated on glass coverslips at a density of $1x10^4$ cells/cm^2. The following day cells were put on ice, fixed in cold 4% paraformaldehyde for 10 minutes and then washed with PBS 1X. After fixation, cells were incubated in blocking solution (TBS 1X, enriched with 0.05% Triton-X100 and 5% BSA) for 1 hour at room temperature in the dark. Cells were then stained overnight at 4 ºC in the dark with the following primary antibodies diluted in blocking solution supplemented with 3% normal donkey serum: mouse anti-Adaptin alpha antibody, together with rabbit anti-Eps15, anti-Eps15L1 or anti-Itsn1 antibody. The next day, cells were washed with TBS 1X-0.05% Triton-X100 and then incubated with the following secondary antibodies in TBS 1X: donkey anti-mouse antibody conjugated with Alexa Fluor 488 and donkey anti-rabbit antibody conjugated with Alexa Fluor 647. Cells were then washed with TBS 1X-0.05% Triton-X100 and stained with DAPI for 5 minutes in the dark at room temperature. After being washed with ddH_2O, coverslips were mounted with mowiol on glass slides and then analysed with a SP5 inverted confocal.

For the detection of endothelial markers, endothelial cells were plated on 8 well µ-slides (Ibidi) coated with 0.1% gelatin (Sigma). Cells were stained, as before described, with the following primary antibodies: anti-PECAM-1 and anti-VE-cadherin. The following secondary antibodies were used: donkey anti-mouse or donkey anti-rabbit antibody conjugated with Alexa Fluor 647. Stained cells were examined under a wide-field fluorescence microscope (Olympus) with the help of the associated software MetaMorph (Molecula Devices).

Confocal and wide-field images were further processed with the ImageJ software.

2.8. *In vivo* methods

2.8.1. Maintenance and generation of the mouse strains

Generation and description of breedings necessary for this study are listed in Table 4.

Mice were kept at the following stabulation conditions:

• temperature: 22±2 °C;

• humidity: 55±10 %;

• light/dark cycle of 12 hours (light from 7 a.m. to 19 p.m.);

• standardized diet with pellets (Harland tekland) and *ad libitum* H_2O.

Experiments involving animals were performed in accordance with the Italian Laws (D.L.vo 116/92 and following additions), which enforce EU 86/609 Directive (Council Directive 86/609/EEC of 24 November 1986 on the approximation of laws, regulations and administrative provisions of the Member States regarding the protection of animals used for experimental and other scientific purposes).

2.8.2. DNA extraction for genotyping

Genomic DNA was isolated from head regions or tail biopsies of mouse embryos or newborn mice, respectively, as follows: head regions or 2-3 mm tail biopsies were digested overnight at 56 °C (optimal temperature for PK activity), in 100 µL of tail buffer. Following short agitation, the mixtures were centrifuged for 5 seconds at 13,000 rpm. To inactivate the PK, digested tissues were left 5 minutes at 95 °C and then centrifuged for 5 seconds at 13,000 rpm, after short shaking. Digested tissues were stored at 4 °C until genotyping. The components of the tail buffer serve the following functions: NH_4SO_4 to precipitate proteins; tris pH 8.8 as solution buffer; β-mercaptoethanol to inactivate cellular enzymes; EDTA pH 8.0 to inactivate proteinases and DNAses depending on divalent ions; Triton X-100 to solubilize; PK for digestion.

2.8.3. Preparation of MEFs

Pregnant mice were sacrificed at 13.5 dpc by CO_2 asphyxia. Embryos were separated from the placenta and the yolk sac and sacrificed by decapitation. The head was used for genotyping. For the isolation of MEFs, the belly was cut and internal organs were removed. Embryos were dissociated with a blade, transferred in 1 ml of 0.05% trypsin/0.02% EDTA and incubated for 10 minutes at 37 °C, under agitation. Embryos were incubated for additional 10 minutes after addition of 100 μg/ml DNase I (Roche). Digested tissues were passed three times through a 1 ml syringe with a 18 gauge needle. After addition of complete medium, cells were passed through a 70 μm cell strainer and plated in 10 cm petri dishes. Cells were grown at 37 °C in 9% CO_2.

MEFs were immortalized upon continued passaging at 37 °C, in 5% CO_2, under sub-confluent conditions: most of them underwent senescence by passage 17, while immortal clones, which overcome senescence, were propagated and expanded in culture.

2.8.4. Preparation of endothelial cells

Endothelial cells were prepared from lungs of $Eps15^{flp/flp}/Eps15L1^{-/-}$ newborn mice. Newborn mice were sacrificed by decapitation. Tail biopsies were cut for genotyping. Lungs were extracted, dissociated with a blade and transferred in 1 ml of DMEM containing 1.5 mg/mL collagenase A and 25 μg/mL DNase (Boehringer-Mannheim GmbH). Lungs were then incubated in this solution for 30 minutes at 37 °C, under agitation. The resulting cell suspension was passed through a 70 μm cell strainer and centrifuged for 5 minutes at 16,000 rpm. Cells were then plated in complete medium in a 24-well plate coated with 0.1% gelatin and incubated at 37 °C. 48 hours later, the cells were immortalized with PmT. In detail, cells were incubated with 1 mL of complete medium containing ~10^5 neomycin-resistant colony-forming units of the retrovirus vector N-TKmT, in the presence of 8 μg/mL polybrene (Sigma). The virus-containing medium

was replaced 4 hours later with fresh complete medium. Fresh medium was replenished three times per week. Colonies of endothelial cells, usually observed after 20 to 30 days, were detached, pooled and reseeded in wider wells. PmT specifically immortalizes endothelial cells and not any other cell type (Garlanda, Parravicini et al. 1994), which are lost within 2 or 3 passages.

2.8.5. Whole mount staining with PECAM-1 primary antibody

$Eps15^{flp/flp}/Eps15L1^{+/-}/tg^{Tie2Cre}$ adult male mice and $Eps15^{flp/flp}/Eps15L1^{+/-}$ adult female mice were crossed to generate $Eps15^{flp/flp}/Eps15L1^{+/+}$ (WT), $Eps15^{flp/flp}/Eps15L1^{+/+}/tg^{Tie2Cre}$ (conditional Eps15-KO, referred to as cEps15-KO), $Eps15^{flp/flp}/Eps15L1^{-/-}$ (constitutive Eps15L1-KO) and $Eps15^{flp/flp}/Eps15L1^{-/-}/tg^{Tie2Cre}$ (conditional DKO, referred to as cDKO) embryos. Embryos were collected at 9.5 dpc and fixed overnight at 4 °C in 100% MetOH (methanol). After fixation, whole mount staining with PECAM-1 was performed as follows: embryos were rehydrated through series of diluted MetOH in PBS 1X (75% MetOH, 50% MetOH, 25% MetOH) for 15 minutes each. Embryos where then blocked overnight at 4 °C in PBS 1X containing 5% donkey serum, 1% BSA and 0.5% Triton-X100. After blocking, embryos were washed with PBS 1X and incubated overnight at 4 °C in a rocking platform with PECAM-1 primary antibody, diluted 1:3 in PBS 1X containing 0.5% BSA and 0.25% Triton-X100. Embryos were washed three times (each wash of 15 minutes) at room temperature in PBS 1X containing 0.01% Triton-X100. Embryos were then incubated for 2 hours at room temperature with anti-rat Alexa 488, diluted 1:500, and TO-PRO-3 (Thermo Fisher Scientific), diluted 1:1000, in PBS 1X containing 0.5% BSA and 0.25% Triton-X100. Embryos were then washed three times (each wash of 15 minutes) in PBS 1X containing 0.01% Triton-X100. Embryos were post-fixed in 4% paraformaldehyde for 15 minutes on ice and then washed with PBS 1X. Post-fixed embryos were mounted with ProLong Gold and analyzed by confocal microscope.

2.8.6. Blood collection and May-Grünwald Giemsa staining of blood smears from newborn mice

$Eps15^{flp/flp}/Eps15L1^{+/-}/tg^{Tie2Cre}$ adult male mice and $Eps15^{flp/flp}/Eps15L1^{+/-}$ adult female mice were crossed to generate $Eps15^{flp/flp}/Eps15L1^{+/+}$ (WT), $Eps15^{flp/flp}/Eps15L1^{+/+}/tg^{Tie2Cre}$ (cEps15-KO), $Eps15^{flp/flp}/Eps15L1^{-/-}$ (constitutive Eps15L1-KO) and $Eps15^{flp/flp}/Eps15L1^{-/-}/tg^{Tie2Cre}$ (cDKO) newborn mice. At birth, these mice were sacrificed by decapitation for blood collection. Collected blood (50 µl from each newborn) was diluted 1:5 with an EDTA solution containing 18,6% EDTA and 2% NaOH (EDTA final concentration was 100 mM). One part of the blood was analyzed in a hemocytometer (Beckman Coulter), while another part was smeared on glass slides and stained for May-Grünwald Giemsa (Sigma). May-Grünwald-Giemsa staining is the stain usually employed for blood and bone marrow films. It consists of a mixture of methylene blue (which dyes acidic cell components blue), azure (which dyes basic cell components red and violet) and eosin (which dyes alkaline cell components orange-red). The cellular components are stained as follows: residual RNA, cytoplasm and nucleoli are blue; DNA and primary granula are red and violet; hemoglobin and eosinophilic granula are orange-red. Among RBCs, reticulocytes are identified due to the presence in their cytoplasm of dark blue dots and curved linear structures, stained by methylene blue and corresponding to the reticular network of ribosomal RNA present in these cells. May-Grünwald Giemsa staining was performed according to the manufacturer's instructions, as follows: blood smears were incubated for 5 minutes in May-Grünwald solution (Sigma), washed for 1,5 minutes in PBS 1X, incubated for 20 minutes in 0.4% p/v Giemsa solution (Sigma) diluted 1:20 in ddH_2O, and briefly washed with ddH_2O. After staining, blood smears were air-dried and examined under a stereomicroscope (Leica).

Antibody	Species	Company	WB	IF	CF	IP
anti-Adaptin alpha	mouse	BD Bioscience (610501)	1:1000	1:500		
anti-AKT	rabbit	Cell Signalling Technology (9272)	1:1000			
anti-alpha adaptin [AP6]	mouse	Abcam (ab2730)				0.5
anti-Cleaved Notch1 (Val1744)	rabbit	Cell Signalling Technology (2421)	1:1000			
anti-Dll1 HMD1-3 conjugated to Alexa Fluor 647	armenian hamster	Biolegend (128311)			1:250	
anti-Eps15	rabbit	home made (130820A)		1:500		
anti-Eps15 (H896)	rabbit	Santa Cruz (sc-1840)	1:1000			
anti-Eps15L1	rabbit	home made (130821A)	1:1000	1:500		
anti-Itsn1	rabbit	home made (130131)	1:1000	1:500		1.2
anti-Mib1	rabbit	Sigma (M5948)	1:1000			
anti-mouse conjugated to Alexa Fluor 488	donkey	Jackson Immuno Research (715-545-150)		1:400		
anti-mouse conjugated to Alexa Fluor 647	donkey	Jackson Immuno Research (715-605-151)		1:400		
anti-mouse IgG linked to HRP	horse	Cell Signalling Technology (7076)	1:10000			
anti-PECAM-1	rat	home made (Mec 13.3)		1:3		
anti-phospho-AKT (Ser473)	rabbit	Cell Signalling Technology (9271)	1:1000			
anti-phospho-p44/42 MAPK (Erk1/2) (Thr202/Tyr204) (D13.14.4E) XP	rabbit	Cell Signalling Technology (4370)	1:1000			
anti-phospho-VEGF Receptor2 (Tyr1175) (19A10)	rabbit	Cell Signalling Technology (2478)	1:1000			
anti-p44/42 MAPK (Erk1/2) (137F5)	rabbit	Cell Signalling Technology (4695)	1:1000			
anti-rabbit conjugated to Alexa Fluor 647	donkey	Jackson Immuno Research (711-605-152)		1:400		

anti-rabbit IgG linked to HRP	goat	Cell Signalling Technology (7074)	1:10000	
anti-α-Tubulin	mouse	Sigma (T9096)	1:5000	
Anti-VE-cadherin	rabbit	Abcam (ab33168)		1:400
anti-VEGF Receptor2 (D5B1)	rabbit	Cell Signalling Technology (9698)	1:1000	
anti-Vinculin	mouse	Sigma (V9131)	1:5000	

Table 3. List of antibodies.

The table reports the antibodies that were used in this thesis project. Numbers in WB (western blot), IF (immunofluorescence) and CF (cytofluorimetry) columns refer to antibody dilution (v/v). Numbers in IP (immunoprecipitation) column refer to μg of antibody used to immunoprecipitate 100 μg of total proteins.

Mouse strain	Description of the strain	Reference or Company
General Deleter Cre	Expression of Cre recombinase in the germline.	(Schwenk, Baron et al. 1995)
General Flp Recombinase	Expression of Cre recombinase in the germline.	(Rodriguez, Buchholz et al. 2000)
Rosa26^{CreERT2}	Knock-in of the (Z)-4-hydroxytamoxifen-inducible Cre recombinase in the Rosa26 locus.	(Ventura, Kirsch et al. 2007)
Tie2-Cre	Expression of Cre recombinase in endothelial and hematopoietic cells.	(Kisanuki, Hammer et al. 2001)
Eps15-KO	KO of Eps15 was obtained by replacing the first coding exon and 2 kb of the 5' promoter region with a neomycin cassette.	(Pozzi, Amodio et al. 2012)
Eps15L1-KO	KO of Eps15L1 was obtained by inserting a PGK-neo cassette next to the first coding exon. Both were then removed by crossing with general deleter Cre mice. The Cre transgene was removed by subsequent breedings.	Unpublished (Ozgene)
Eps15$^{tm1a(KOMP)Wtsi}$ (=Eps15$^{flp/flp}$)	The PGK-neo cassette was removed by breeding to General Flp recombinase mice. The Flp transgene was removed by subsequent breedings. LoxP sites flank the 10th exon of Eps15.	Unpublished (Sanger Institute)

Table 4. List of murine strains.

The table reports the murine strains that were used for this thesis project.

Chapter 3

RESULTS

1. Eps15L1 regulates Dll1 biology in MEFs

1.1. The FACS-based co-culture assay

Since Eps15/Eps15L1-DKO mice phenocopy Notch loss-of-function mutants and the Notch target genes HES1, HES5 and NRARP are downregulated in these mice, we hypothesized that Eps15 and Eps15L1 redundantly regulate the Notch signalling pathway. Previous work in our laboratory exploited a luciferase-based co-culture assay to directly test whether Eps15 and Eps15L1 regulate the Notch signalling pathway either in the signal-sending cell or in the signal-receiving cell. Through this assay, in which OP9-Dll1 and C2C12-Notch1 were used as signal-sending and signal-receiving cells, respectively, it was found that, in contrast to what we expected, Eps15 and Eps15L1 are required in a non-redundant manner in the signal-sending cell to allow activation of the Notch signalling (Lucano et al., unpublished results). These findings were derived by siRNA interference of Eps15 and Eps15L1, alone or in combination, in OP9-Dll1 or C2C12-Notch1 cells.

To confirm this finding in a cleaner and physiological setting, we decided to use, as signal-sending cells, MEFs generated from KO mice for Eps15 and Eps15L1 and expressing inducible Dll1-mCherry as Notch ligand (MEF-Dll1 cells). Moreover, to increase the reproducibility of the read-out of the co-culture assay, we set-up a new co-culture cell model system, based on a FACS-assay, to measure Notch activity (Figure 14A).

As a model system for the signal-sending cell, we generated two different cell lines of MEF-Dll1: $Eps15^{flp/flp}/Eps15L1^{+/+}/tg^{CreERT2}$ and $Eps15^{flp/flp}/Eps15L1^{-/-}/tg^{CreERT2}$. In absence of (Z)-4-hydroxytamoxifen treatment, these cell lines were used as WT and Eps15L1-KO, respectively. When treated with (Z)-4-hydroxytamoxifen, deletion of Eps15 in WT cells lead to the generation Eps15-KO cells, while deletion of Eps15 in Eps15L1-KO cells lead to the generation of Eps15/Eps15L1-DKO cells (Table 5).

Cell line	- TMX	+ TMX
$Eps15^{flp/flp}/Eps15L1^{+/+}/tg^{CreERT2}$	WT	Eps15-KO
$Eps15^{flp/flp}/Eps15L1^{-/-}/tg^{CreERT2}$	Eps15L1-KO	DKO

Table 5. Generation of WT, single and double Eps15 and Eps15L1 KO MEF-Dll1 cells.

$Eps15^{flp/flp}/Eps15L1^{+/+}/tg^{CreERT2}$ and $Eps15^{flp/flp}/Eps15L1^{-/-}/tg^{CreERT2}$ untreated with (Z)-4-hydroxytamoxifen (-TMX) were used as WT and Eps15L1-KO cells, respectively. Eps15-KO and DKO cells were generated by (Z)-4-hydroxytamoxifen treatment (+TMX) of WT and Eps15L1-KO cells, respectively,

In all these cells, the expression of Dll1-mCherry was induced by doxycycline treatment, according to the T-Rex system (Figure 14B).

As a model system for the signal-receiving cell, we used CHO cells expressing hN1Gal4 (CHO-hN1Gal4 cells), generated in Michael B. Elowitz's laboratory (Sprinzak, Lakhanpal et al. 2010). hN1Gal4 is a fusion protein between the extracellular portion of the human Notch1 receptor (NECD) and the transcription factor Gal4, which substitutes the NICD. When CHO-hN1Gal4 cells are co-cultured with signal-sending cells (in our case MEF-Dll1 cells), binding of hN1Gal4 to the Notch ligand leads to the activation of the receptor, which undergoes two proteolytic cleavages.

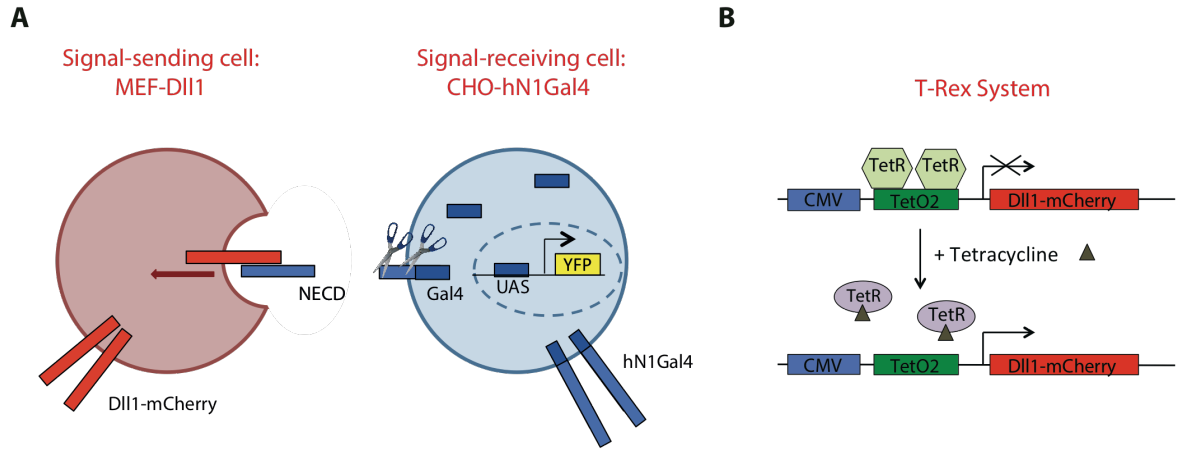

Figure 14. The FACS-based co-culture assay.

A. The figure depicts the FACS-based co-culture assay used to investigate the requirement of Eps15 and Eps15L1 in the regulation of Notch signalling. MEF-Dll1 and CHO-hN1Gal4 cells were used as signal-sending and signal-receiving cells, respectively. Notch signalling induction by Dll1-mCherry is measured as expression of YFP in signal-receiving cells. **B.** The figure depicts the induction of Dll1-mCherry in signal-sending cells through the T-Rex system, in which the expression of Dll1-mCherry is under the control of the strong human CMV (cytomegalovirus) immediate-early promoter and two copies of TetO2 (tetracycline operator 2). In the absence of antibiotics of tetracycline class, TetR (tetracycline repressor) binds to TetO2, thus inhibiting the expression of Dll1-mCherry. When an antibiotic of the tetracycline class, such as doxycycline, is added, it binds to TetR and causes a conformational change in the repressor, which can no longer to bind to TetO2, thus allowing induction of Dll1-mCherry.

These proteolytic cleavages result in the release of Gal4 in the cytoplasm, which translocates to the nucleus and bind to the UAS region (upstream activating sequence), leading to the expression of the histone H2B protein fused to citrine, otherwise called YFP (yellow fluorescent protein). YFP expression detected by cytofluorimetry is a direct measurement of receptor activation.

1.2. Set-up of the FACS-based co-culture assay

We analysed the expression of Dll1-mCherry in WT MEF-Dll1 cells by FACS. First, we defined the optimal concentration of doxycycline required to induce Dll1-mCherry in these cells. At the same time, by surface staining with an anti-mouse Dll1 antibody conjugated to Alexa Fluor 647 dye, we measured, among Dll1-mCherry positive cells, the percentage of cells in which Dll1-mCherry was exposed on the PM. We detected a leaky induction of Dll1-mCherry when cells were cultivated in the absence of doxycycline (~20%). However, about 90% of the cells expressed Dll1-mCherry when treated for 24 hours with 50 ng/ml doxycycline.

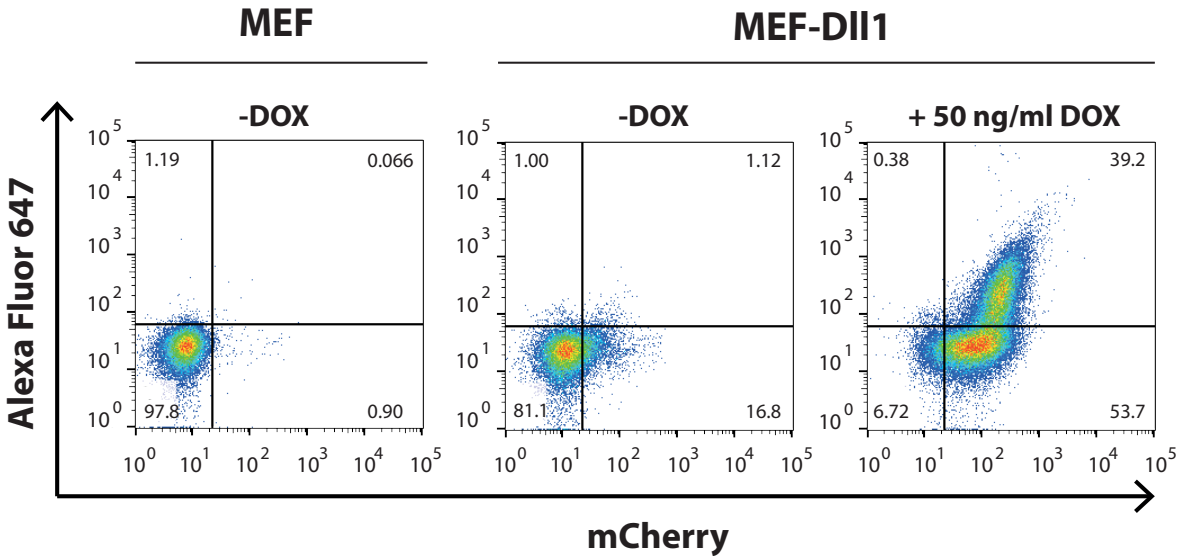

Figure 15. FACS analysis of MEF-Dll1 cells.

MEF and MEF-Dll1 cells were analysed by FACS for the expression of mCherry and Alexa Fluor 647. Cells were cultured for 24 hours in the absence (-DOX) or in the presence of 50 ng/ml doxycycline (+50 ng/ml DOX) and, then, surface stained with an Alexa Fluor 647 anti-mouse Dll1 antibody. MEFs were used to define background fluorescence intensities for mCherry and Alexa Fluor 647 and to gate the following subpopulations: double negative cells for mCherry and Alexa Fluor 647, single positive cells for mCherry, double positive cells for mCherry and Alexa Fluor 647 and single positive cells for Alexa Fluor 647. Numbers refer to the percentage of gated cells.

Of these, ~40% of the cells expressed Dll1-mCherry on the surface (Figure 15). Increased amounts of doxycycline (100 and 150 ng/ml) did not increase the percentage of Dll1-mCherry expressing cells or the protein expression levels, as assessed by mean fluorescence intensity (data not shown). The same Dll1-mCherry induction was observed also when cells were cultivated in the presence of different doses of doxycycline (tested: 50-100-150 ng/ml) for 48 and 72 hours (data not shown). In subsequent experiments, Dll1-mCherry was induced by the addiction of 50 ng/ml doxycycline at the beginning of co-culture. The antibiotic was maintained in the co-culture medium until the end of the experiment (48 hours).

Next, we analysed the expression of YFP in CHO-hN1Gal4 cells when cultured alone. We observed that, at steady state, almost all cells expressed YFP (all positive cells for YFP are indicated as YFP+). Among the YFP-positive cells, about 20% expressed high levels of YFP (cells expressing high levels of YFP are indicated as YFP++, while the YFP++/YFP+ ratio refers to the percentage of cells expressing high levels of YFP relative to total positive YFP cells). As a control, we tested whether YFP basal expression was perturbed by doxycycline. We observed that neither the percentage of YFP-positive cells, nor the protein expression levels, assessed by mean fluorescence intensity, were perturbed when cells were cultured in the presence of the antibiotic (Figure 16).

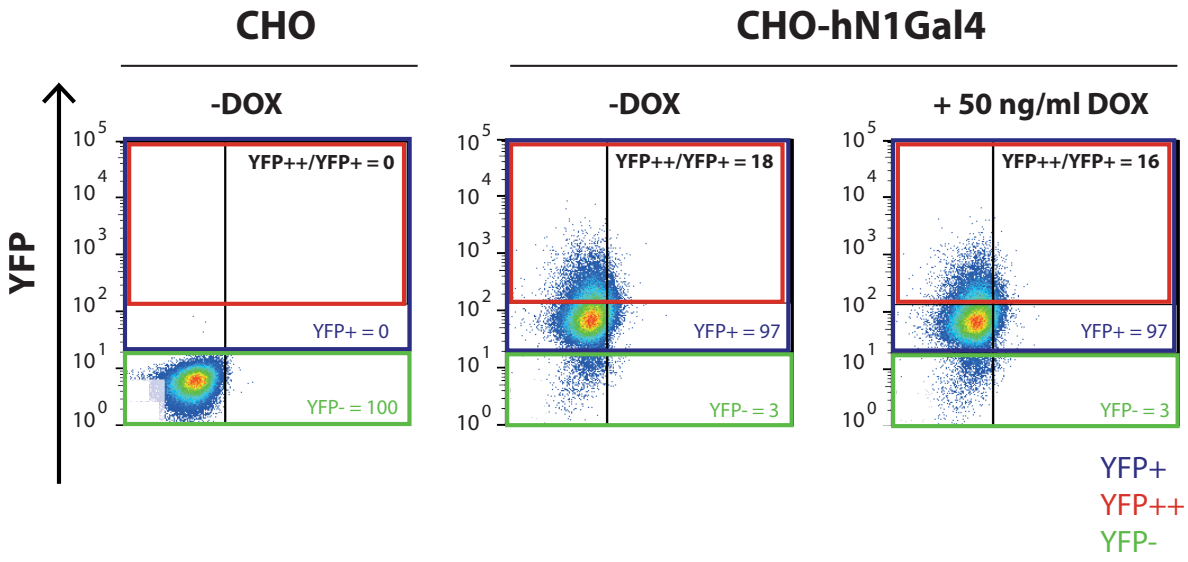

Figure 16. FACS analysis of CHO-hN1Gal4 cells.

CHO and CHO-hN1Gal4 cells were analysed by FACS for the expression of YFP when cultured at steady state in the absence (-DOX) or in the presence of 50 ng/ml doxycycline (+ 50 ng/ml DOX), administered for 48 hours. CHO cells were used to define background fluorescence intensities for basal YFP and to gate the following subpopulations: YFP-negative cells (YFP-, green gate) and YFP-positive cells (YFP+, blue gate). Among YFP-positive cells, a subpopulation of cells expressing higher levels of YPF was gated (YFP++, red gate). Numbers refer to the percentage of YFP-negative cells, YFP-positive cells and cells expressing higher levels of YFP, relative to total YFP-positive cells (YFP++/YFP+).

After the analysis of the single populations of signal-sending and signal-receiving cells, we defined the optimal time and modality of doxycycline administration during co-culture of MEF-Dll1 with CHO-hN1Gal4 cells. To this end, we tested the following conditions: i) co-culture for 24 hours and administration of 50 ng/ml doxycycline for the total co-culture time, e. g. 24 hours; ii) co-culture for 48 hours and administration of 50 ng/ml doxycycline for the first 24 hours; iii) co-culture for 48 hours and administration of 50 ng/ml doxycycline for the total co-culture time, e. g., 48 hours.

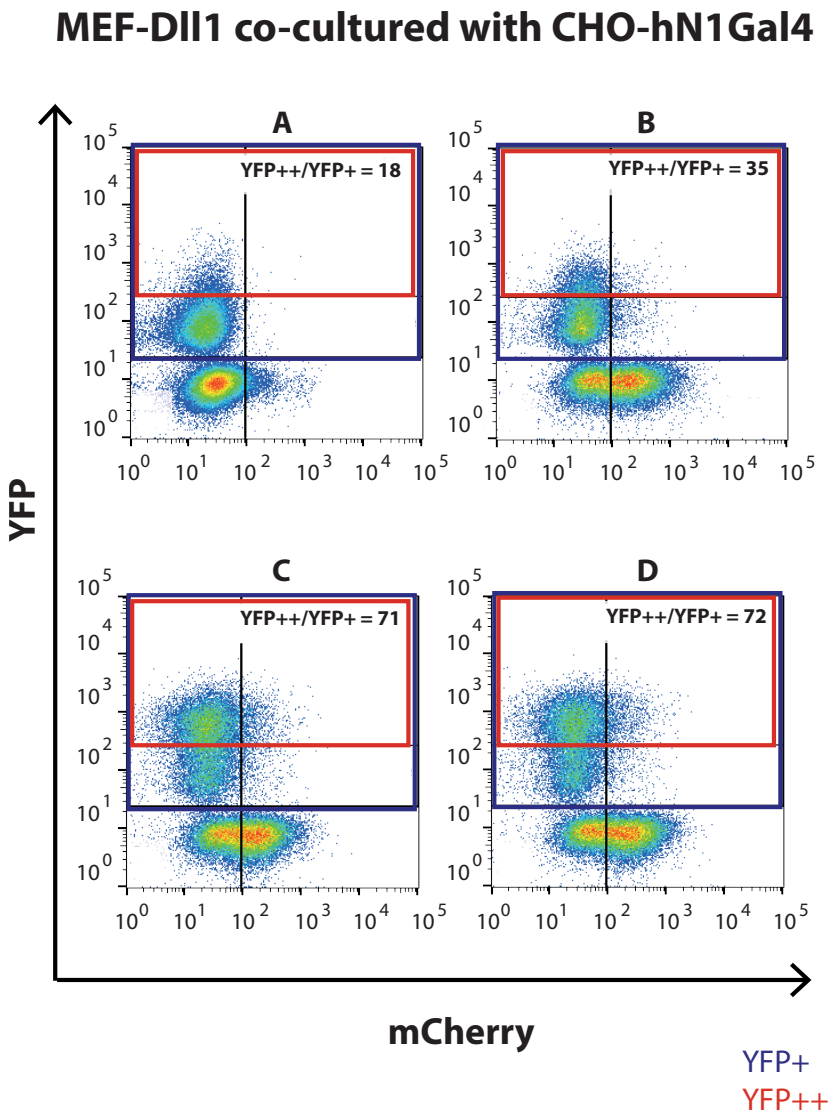

Figure 17. Optimal time and modality of doxycycline administration during co-culture.

CHO-hN1Gal4 cells were analysed by FACS for the expression of YFP after co-culture with MEF-Dll1 cells. **A.** Cells were co-cultured for 48 hours in the absence of doxycycline. **B.** Cells were co-cultured for 24 hours in the presence of doxycycline. **C.** Cells were co-cultured for 48 hours in the presence of doxycycline, administered for the first 24 hours. **D.** Cells were co-cultured for 48 hours in the presence of doxycycline, administered for the total co-culture time. Cells expressing higher levels of YPF (YFP++, red gate), among YFP-positive cells (YFP+, blue gate), were gated. Notch induction was measured as the percentage of cells expressing higher levels of YFP, relative to total YFP-positive cells (YFP++/YFP+).

We found that Notch induction, measured as percentage of cells expressing higher levels of YFP relative to total YFP-positive cells, was higher when cells were co-cultivated for 48 hours in the presence of doxycycline, both when it was administered for the first 24 hours and for the total co-culture time (Figure 17). Thus, in the following experiments, we co-cultured cells for 48 hours in the presence of 50 ng/ml doxycycline, administered for the total co-culture time.

We then defined the optimal percentage ratio of MEF-Dll1 and CHO-hN1Gal4 cells to be co-cultured. We observed an efficient Notch induction, measured as percentage of cells expressing higher levels of YFP relative to total YFP-positive cells, when signal-sending and signal-receiving cells were co-cultured at a percentage ratio of 60/40 (Figure 18).

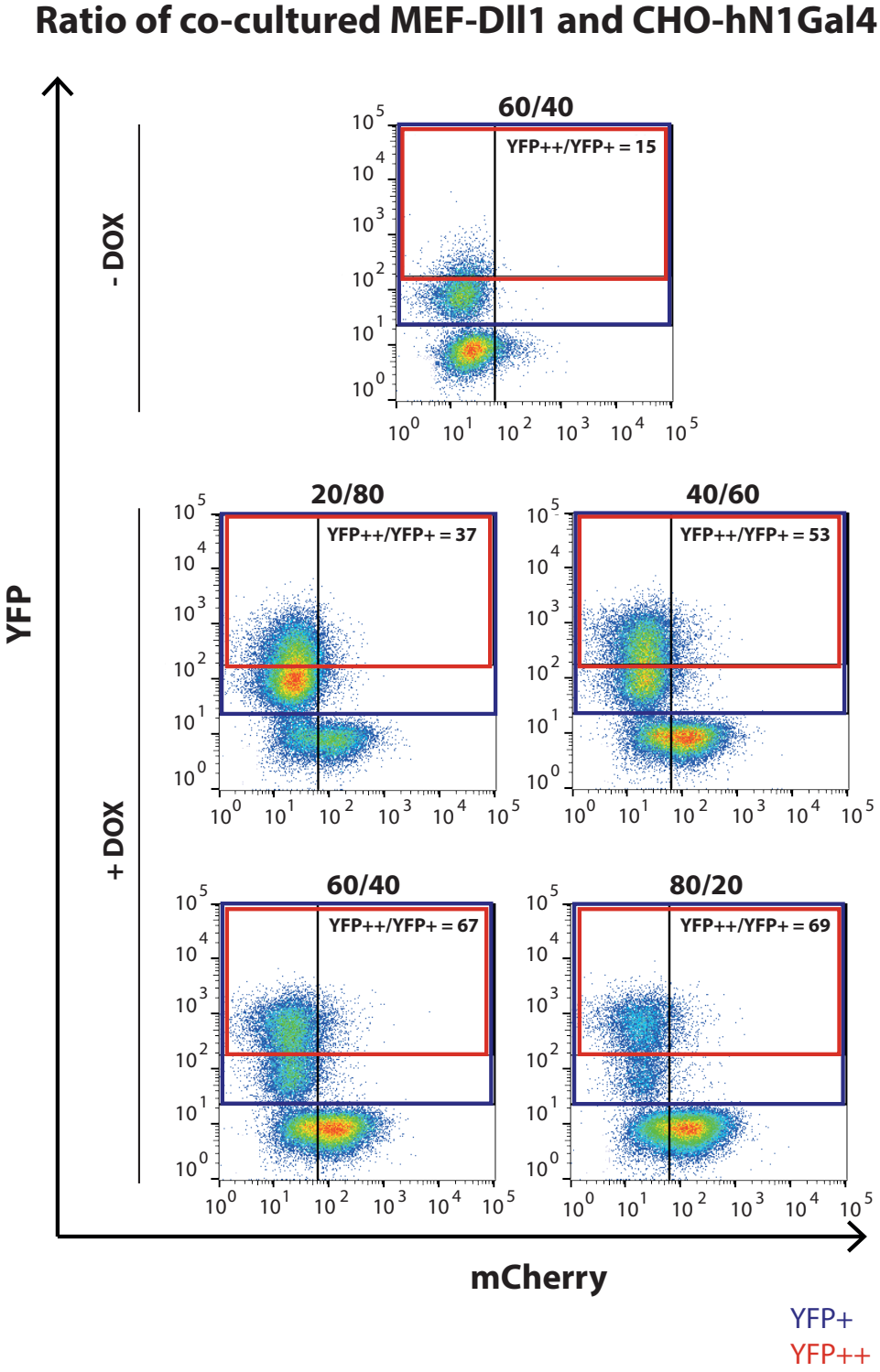

Figure 18. The optimal ratio of MEF-Dll1 and CHO-hN1Gal4 cells in a co-culture.

CHO-hN1Gal4 cells were analysed by FACS for the expression of YFP after co-culture with MEF-Dll1 cells. Co-culture was performed for 48 hours, in the absence (-DOX) or in the presence (+DOX) of 50 ng/ml doxycycline. Doxycycline was administered for the total co-culture time. Different ratios of MEF-Dll1 and CHO-hN1Gal4 cells were tested, both in absence and in the presence of doxycycline: 20/80; 40/60; 60/40; 80/20. For simplicity, only the 60/40 ratio condition

is reported as a control of co-cultures performed in the absence of doxycycline (similar at all ratios). In CHO-hN1Gal4 cells, high levels of YPF (YFP++, red gate), among YFP-positive cells (YFP+, blue gate), were gated. Notch induction was measured as the percentage of cells expressing higher levels of YFP relative to total YFP-positive cells (YFP++/YFP+).

After having set-up the experimental conditions for co-culture (time: 48 hours; modality of doxycycline administration: 50 ng/ml doxycycline, administered for the total co-culture time; ratio among signal-sending and signal-receiving cells: 60/40), we validated the co-culture system. We observed that the increased percentage of cells expressing higher levels of YFP, among all YFP-positive cells, in the chosen experimental conditions, was Notch-dependent, since it was not observable when cells were co-cultivated in the presence of DAPT, a Notch signalling inhibitor that acts by inhibiting the proteolytic cleavage of Notch receptor by γ–secretase (Figure 19).

As a further control, we tested YFP induction in CHO-hN1Gal4 cells after co-culture with MEF-Dll1 cells knocked-down for Mib1. Mib1 is an E3 ubiquitin ligase that is required for the activation of the Notch signalling in the signal-sending cell (Le Borgne 2006). As expected, KD of Mib1 in MEF-Dll1 cells reduced Notch activation almost to basal levels (Figure 20A). Efficient downregulation of Mib1 protein levels after KD was confirmed by WB analysis (Figure 20B).

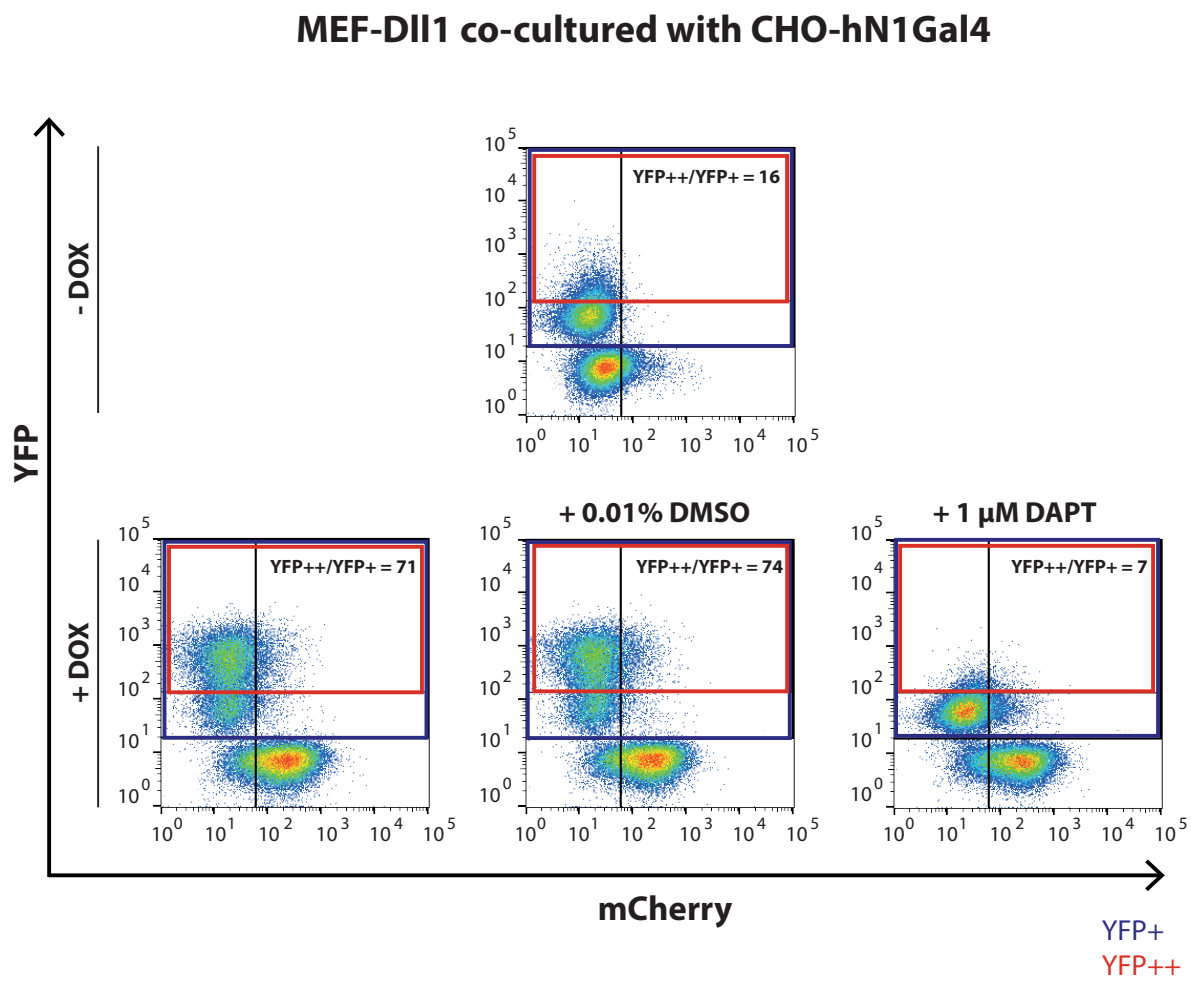

Figure 19. Increased YFP expression in CHO-hN1Gal4 cells upon co-culture with MEF-Dll1 cells is Notch-dependent.

CHO-hN1Gal4 cells were analysed by FACS for the expression of YFP after co-culture with MEF-Dll1 cells. MEF-Dll1 and CHO-hN1Gal4 cells were co-cultured at percentage ratio of 60/40 for 48 hours, in the absence (-DOX) or the presence (+DOX) of 50 ng/ml doxycycline. Co-cultures were performed in the absence or in the presence of the Notch signalling inhibitor DAPT or DMSO as vehicle. Drugs (doxycycline and DAPT) and DMSO, when added, were administered for the total co-culture time. In CHO-hN1Gal4 cells, cells with high levels of YPF (YFP++, red gate), among YFP-positive cells (YFP+, blue gate), were gated. Notch induction was measured as the percentage of cells expressing higher levels of YFP relative to total YFP-positive cells (YFP++/YFP+).

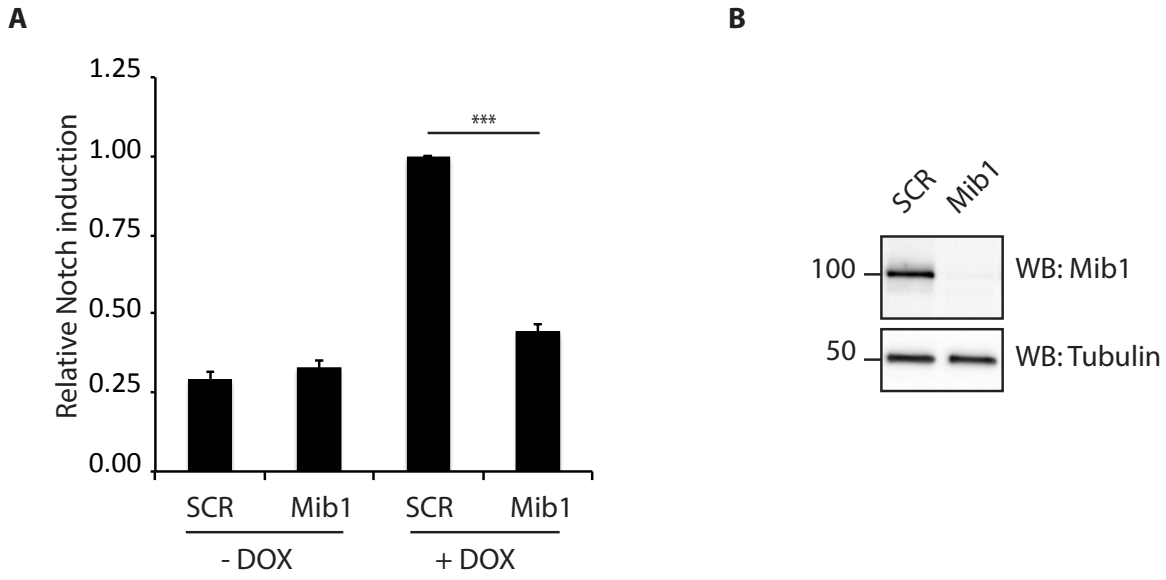

Figure 20. KD of Mib1 in MEF-Dll1 cells reduces Notch signalling activation.

A. The bar graph depicts Notch induction in CHO-hN1Gal4 cells when co-cultured with MEF-Dll1 cells. MEF-Dll1 cells were transfected with a siRNA oligo targeting Mib1 RNA (Mib1) or a scrambled siRNA oligo (SCR) as a control. Co-cultures were performed both in the absence (-DOX) and in the presence (+DOX) of 50 ng/ml doxycycline. When added, doxycycline was administered for the total co-culture time. Notch induction, measured as the percentage of CHO-hN1Gal4 cells expressing higher levels of YFP relative to total YFP-positive cells (YFP++/YFP+), is relative to the induction observed when CHO-hN1Gal4 cells were co-cultured, in the presence of doxycycline, with MEF-Dll1 cells previously transfected with a scrambled oligo. Data are presented as an average of two independent experiments; error bars represent standard error deviation. Statistical significance was assessed using 2-tailed student's t-test (***=$p<0.005$). **B.** WB of Mib1 protein levels in MEF-Dll1 cells transfected with a scrambled oligo (SCR) or a siRNA oligo targeting Mib1 RNA (Mib1). 20 µg of each cell lysate were separated on SDS-PAGE, transferred on a nitrocellulose filter and probed with antibodies for Mib1 and tubulin, as indicated. MWs (kDa) are indicated on the left.

1.3. Dll1 induction in WT, single and double Eps15 and Eps15L1 KO MEF-Dll1 cells

Before testing the role of Eps15 and Eps15L1 in the regulation of Dll1 biology (using single and double Eps15 and Eps15L1 KO MEF-Dll1 cells as signal-sending cells), we compared the expression of doxycycline-inducible Dll1-mCherry in WT, single and double Eps15 and Eps15L1 KO MEF-Dll1 cells by FACS. At the same time, the cells were surface stained with an anti-mouse Dll1 antibody conjugated to an Alexa Fluor 647 dye in order to measure the percentage of cells in which the ligand was exposed on the PM and, therefore, available to absolve its biological function. We found that the percentage of Dll1-mCherry expressing cells was similar in WT, single and double Eps15 and Eps15L1 KO MEF-Dll1 cells upon treatment with 50 ng/ml doxycycline for 48 hours (Figure 21A). Nevertheless, analysis of Dll1-mCherry mean fluorescence showed that, while Eps15/Eps15L1-DKO cells expressed similar levels of Dll1-mCherry compared to WT, the protein was differently expressed in single KO cells: Eps15L1-KO cells expressed lower levels of Dll1-mCherry compared to WT, while Eps15-KO cells tended to express higher levels of the protein (Figure 21B). These results might suggest that Eps15 could have a role in the degradation of Dll1-mCherry.

Then, we analysed the percentage of cells that exposed Dll1 on the PM, e.g., the percentage of cells that were double positive for both mCherry and Alexa Fluor 647. We found that the percentage of cells exposing Dll1 on the PM was reduced in Eps15L1-KO and Eps15/Eps15L1-DKO cells, compared to WT cells, suggesting that Eps15L1 might have a role in the trafficking of the protein towards the cell surface (Figure 21C).

When we analysed the levels of Dll1 on the cell surface by mean fluorescence analysis of Alexa Fluor 647, we found that both single and double Eps15 and Eps15L1 KO cells expressed high levels of Dll1. This result might suggest that Eps15 and Eps15L1 have a role in the internalization of Dll1 (Figure 21D).

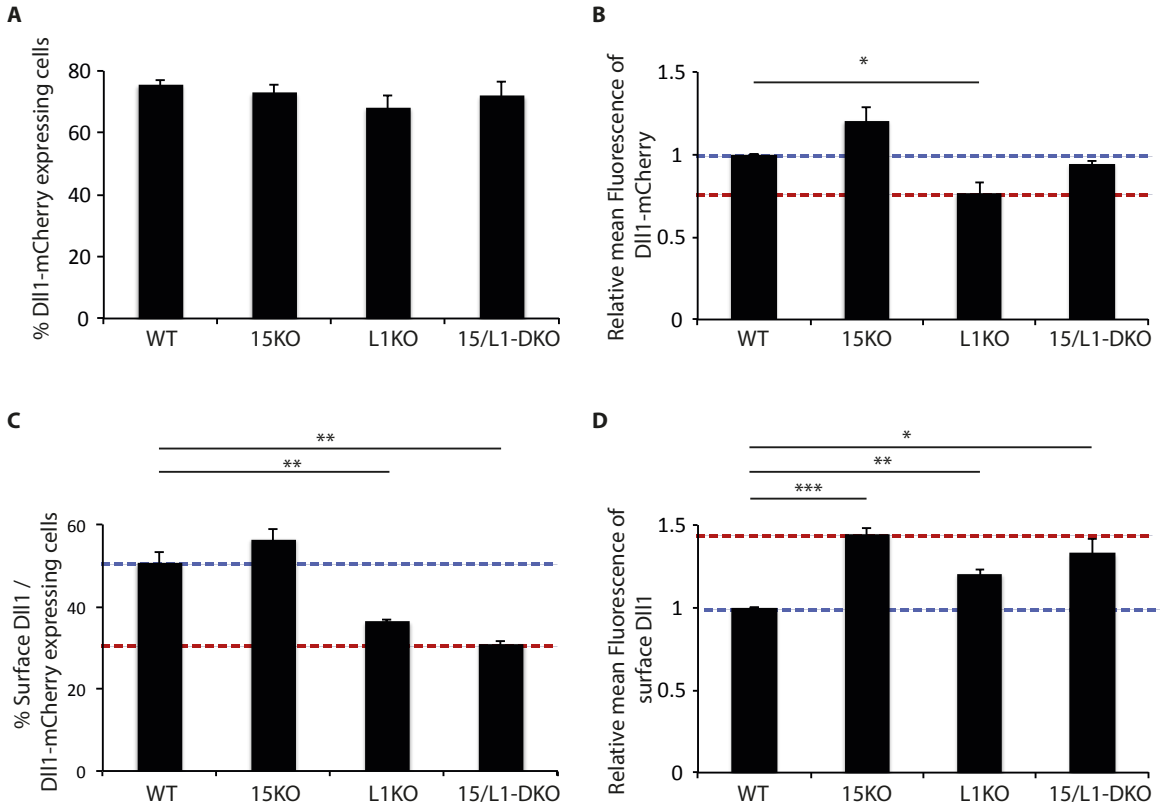

Figure 21. Expression of Dll1 in WT, single and double Eps15 and Eps15L1 KO MEF-Dll1 cells.

The bar graphs depict the percentage of cells expressing Dll1 and the levels of Dll1 in wild type (WT), Eps15-KO (15KO), Eps15L1-KO (L1KO) and Eps15/Eps15L1-DKO (15/L1-DKO) MEF-Dll1 cells. **A**. Percentage of cells expressing Dll1-mCherry. **B.** Mean fluorescence intensity of Dll1-mCherry in the different cell populations relative to WT cells. **C**. Percentage of cells expressing Dll1 on the cell surface among Dll1-mCherry-positive cells. **D.** Mean fluorescence intensity of surface Dll1 relative to WT cells. All the measurements were obtained by FACS analysis of mCherry and Alexa Fluor 647 in the different populations of MEF-Dll1 cells, as indicated, after treatment with 50 ng/ml doxycycline, administered for 48 hours, and surface staining with an Alexa Fluor 647 anti-mouse Dll1 antibody. Data are presented as an average of three independent experiments; error bars represent standard error deviation. Statistical significance was assessed using 2-tailed student's t-test (*=$p<0.05$; **=$p<0.01$; ***=$p<0.005$).

1.4. Eps15L1 is required in MEF-Dll1 cells for activation of the Notch signalling pathway

To test whether Eps15 and Eps15L1 impact on the Notch signalling through the regulation of Dll1 biology in MEF-Dll1 cells, single and double Eps15 and Eps15L1 KO MEF-Dll1 cells were co-cultured with CHO-hN1Gal4 cells. A representative FACS-based co-culture experiment is shown in Figure 22. Our first observation was that deletion of Eps15 alone in MEF-Dll1 cells did not affect Notch activation (Figure 22; 23A), in contrast to what has been previously observed in OP9-Dll1 cells, in which KD of Eps15 by RNA interference reduced Notch activation to ~50% (Lucano et al., unpublished results). Secondly, Eps15L1-KO MEF-Dll1 cells had a reduced ability to induce Notch activation (Figure 22; 23A), as previously observed in OP9-Dll1 cells, in which a reduction (to ~50%) of Notch signalling activation following KD of Eps15L1 was shown (Lucano et al., unpublished results). Thirdly, we observed that the combined loss of Eps15 and Eps15L1 in MEF-Dll1 cells did not further affect Notch activation compared to the KO of Eps15L1 alone (Figure 22; 23A). Similarly, no further reduction of Notch signalling had been observed in OP9-Dll1 cells knocked-down for both Eps15 and Eps15L1 (Lucano et al., unpublished results). These results indicate that, in MEF-Dll1 cells, Eps15L1, but not Eps15, is required for proper activation of Notch signalling. Efficient downregulation of Eps15 protein levels after (Z)-4-hydroxytamoxifen treatment of MEF-Dll1 cells was confirmed by WB analysis (Figure 23B).

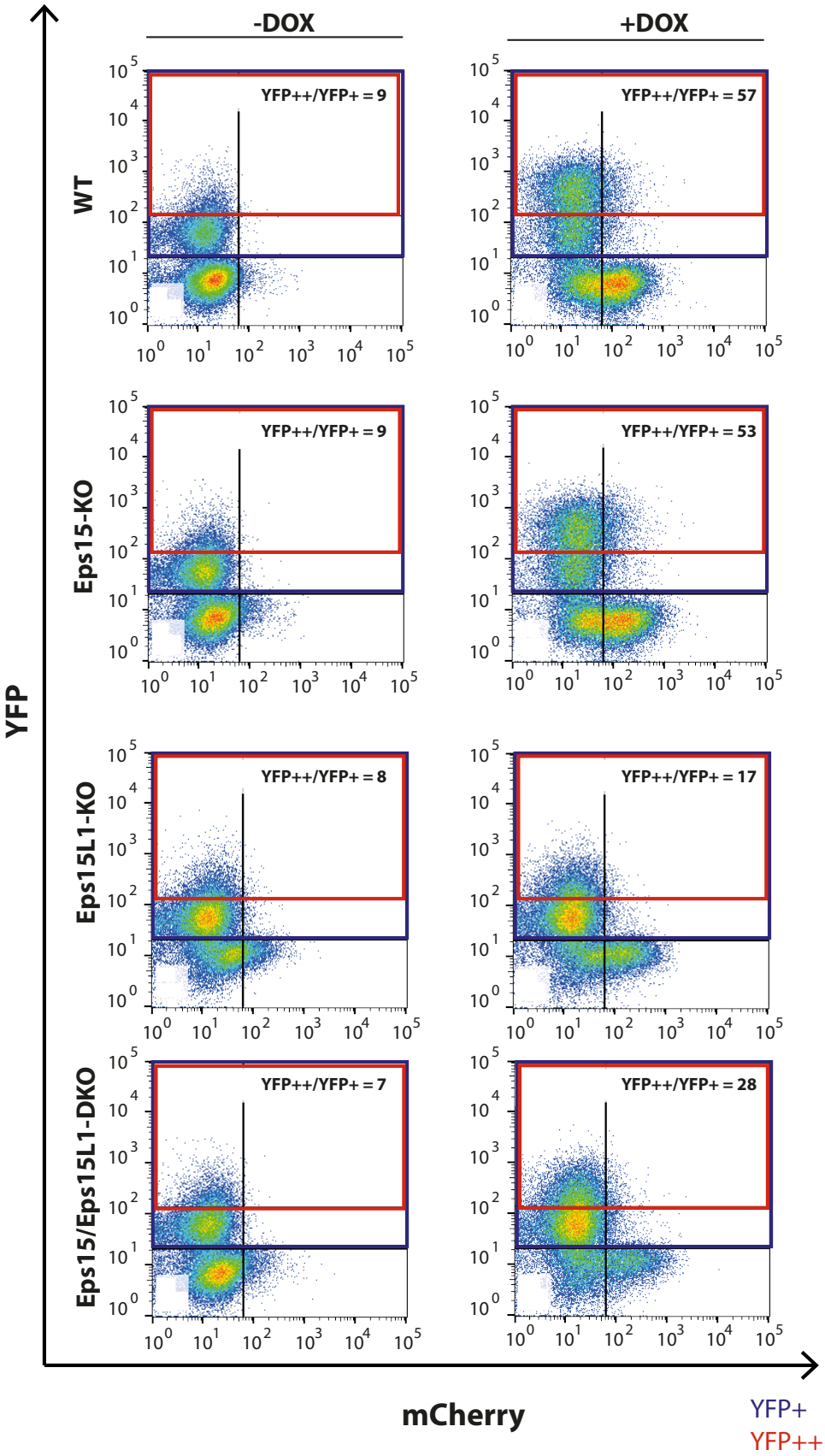

Figure 22. Representative FACS-based co-culture experiment.

CHO-hN1Gal4 cells were analysed by FACS for the expression of YFP after co-culture with wild type (WT), Eps15-KO, Eps15L1-KO and Eps15/Eps15L1-DKO MEF-Dll1 cells. MEF-Dll1 and

CHO-hN1Gal4 cells were co-cultured at a percentage ratio of 60/40 for 48 hours, in the absence (-DOX) or the presence (+DOX) of 50 ng/ml doxycycline. When added, doxycycline was administered for the total co-culture time. In CHO-hN1Gal4 cells, cells expressing higher levels of YPF (YFP++, red gate), among YFP-positive cells (YFP+, blue gate), were gated. Notch induction was measured as the percentage of cells expressing higher levels of YFP relative to total YFP-positive cells (YFP++/YFP+).

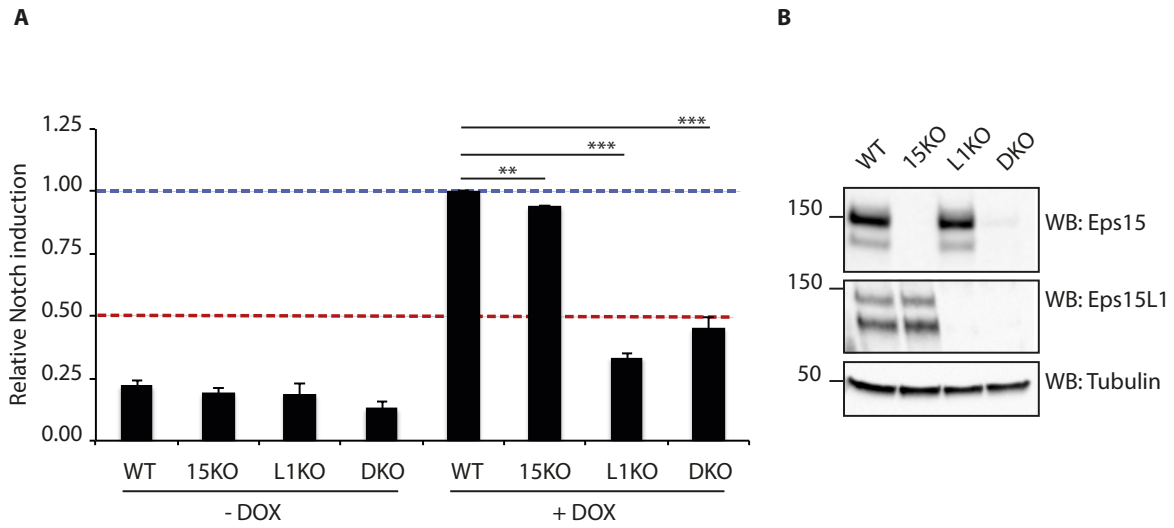

Figure 23. Eps15L1 is required for the activation of Notch signalling in MEF-Dll1 cells

A. The bar graph depicts Notch induction in CHO-hN1Gal4 cells when co-cultured with wild type (WT), Eps15-KO (15KO), Eps15L1-KO (L1KO) and Eps15/Eps15L1-DKO (DKO) MEF-Dll1 cells. MEF-Dll1 and CHO-hN1Gal4 cells were plated at a percentage ratio of 60/40 ratio and co-cultured for 48 hours. The co-cultures were performed both in the absence (-DOX) and in the presence (+DOX) of 50 ng/ml doxycycline. When added, doxycycline was administered for the total co-culture time. Notch activation, measured as the percentage of CHO-hN1Gal4 cells expressing higher levels of YFP, relative to total YFP-positive cells (YFP++/YFP+), is relative to the activation observed when CHO-hN1Gal4 cells were co-cultured with WT MEF-Dll1 cells in the presence of doxycycline. Data are presented as an average of three independent experiments; error bars represent standard error deviation. Statistical significance was assessed using 2-tailed student's t-test (**=$p<0.01$; ***=$p<0.005$). **B.** WB of Eps15 and Eps15L1 protein levels in wild type (WT), Eps15-KO (15KO), Eps15L1-KO (L1KO) and Eps15/Eps15L1-DKO (DKO) MEF-Dll1 cells. Eps15-KO and Eps15/Eps15L1-DKO cells were generated through (Z)- 4-hydroxytamoxifen treatment of WT and Eps15L1-KO cells, respectively. 20 µg of each cell lysate were separated on SDS-PAGE, transferred on a nitrocellulose filter and probed with antibodies for Eps15, Eps15L1 and tubulin, as indicated. MWs (kDa) are indicated on the left.

To confirm these observations and to exclude cell line-specific effects, we will investigate the role of Eps15 and Eps15L1 in isogenic cellular systems, in which single and double Eps15 and Eps15L1 KO cells will be directly compared with the parental WT cell line. In detail, we will use MEF-Dll1 cells transgenic for CreERT2 and floxed for both Eps15 and Eps15L1, e.g. $Eps15^{flp/flp}/Eps15L1^{flp/flp}/tg^{CreERT2}$ (these cells are WT when not treated with (Z)-4-hydroxytamoxifen), in order to generate DKO cells upon (Z)-4-hydroxytamoxifen treatment. As control we will also use MEF-Dll1 cells transgenic for CreERT2 and floxed for only Eps15 or Eps15L1, e.g. $Eps15^{flp/flp}/Eps15L1^{+/+}/tg^{CreERT2}$ and $Eps15^{+/+}/Eps15L1^{flp/flp}/tg^{CreERT2}$ cell lines (these cells are WT when not treated with (Z)-4-hydroxytamoxifen), in order to generate Eps15-KO or Eps15L1-KO cells upon (Z)-4-hydroxytamoxifen treatment, respectively (Table 6).

Cell line	- TMX	+ TMX
$Eps15^{flp/flp}/Eps15L1^{flp/flp}/tg^{CreERT2}$	WT	DKO
$Eps15^{flp/flp}/Eps15L1^{+/+}/tg^{CreERT2}$	WT	Eps15-KO
$Eps15^{+/+}/Eps15L1^{flp/flp}/tg^{CreERT2}$	WT	Eps15L1-KO

Table 6. Generation of single and double Eps15 and Eps15L1 KO MEF-Dll1 cells from the parental WT cell line.

$Eps15^{flp/flp}/Eps15L1^{flp/flp}/tg^{CreERT2}$, $Eps15^{flp/flp}/Eps15L1^{+/+}/tg^{CreERT2}$ and $Eps15^{+/+}/Eps15L1^{flp/flp}/tg^{CreERT2}$ untreated with (Z)-4-hydroxytamoxifen (-TMX) are used as WT. Treatment of these cells with (Z)-4-hydroxytamoxifen (+TMX) leads to the formation of DKO, Eps15-KO and Eps15L1-KO cells.

2. Eps15 and Eps15L1 redundantly regulate VEGFR-2 turnover, but vascular defects are not the main cause of lethality in Eps15/Eps15L1-DKO embryos

2.1. Total expression levels of VEGFR-2 are reduced in DKO endothelial cells, but VEGFR-2 and Notch downstream signalling are not altered in these cells.

Eps15/Eps15L1-DKO embryos show serious vascular defects (see section "5.1. Eps15, Eps15L1 and Eps15/Eps15L1 KO mice" in Chapter 1). We asked whether vascular defects were due to a cell–autonomous function of Eps15 and Eps15L1 in the vascular system and whether they were responsible for midgestation lethality of Eps15/Eps15L1-DKO mice. To address these questions, we exploited both an *in vitro* and an *in vivo* strategy. As an *in vitro* model system, we used murine endothelial cells to investigate whether the major signalling pathways regulating vascular development, e.g., the VEGFR-2 (vascular endothelial growth factor receptor 2) and the Notch signalling pathways, were altered upon Eps15/Eps15L1 impairment. We tested whether Eps15 and Eps15L1 had a cell-autonomous function in endothelial cells. As an *in vivo* model system, we generated cDKO mice through the Tie2-Cre strategy, to see whether vascular defects were present also in these mice and whether they caused embryo lethality.

In detail, as an *in vitro* model system, we generated isogenic endothelial cells to avoid cell line-specific effects. To this end, we established an immortalized endothelial cell line from $Eps15^{flp/flp}/Eps15L1^{-/-}$ mice. These cells were floxed for Eps15 and KO for Eps15L1. We confirmed the endothelial origin of this cell line by IF staining of the main endothelial markers PECAM-1 and VE-cadherin (Figure 24).

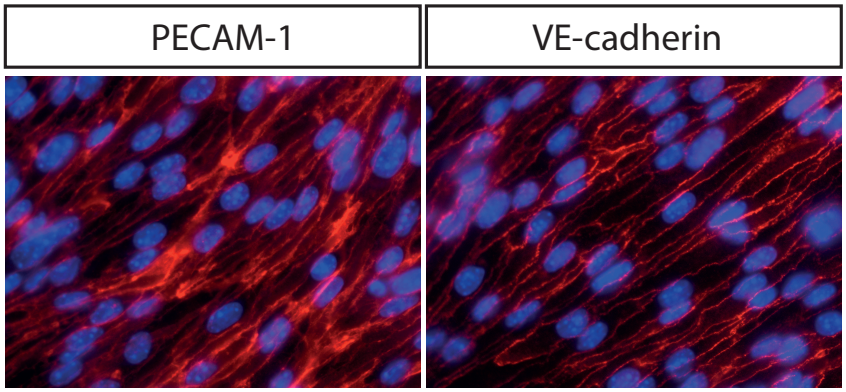

Figure 24. Expression of the endothelial markers PECAM-1 and VE-cadherin in immortalized endothelial Eps15$^{flp/flp}$/Eps15L1$^{-/-}$ cells.

Endothelial Eps15$^{flp/flp}$/Eps15L1$^{-/-}$ cells were stained with anti-PECAM-1 or anti-VE-Cadherin antibodies (red) to confirm their endothelial origin. Nuclei were identified through DAPI staining (blue). Images were acquired with a wide-field microscope.

Next, we performed retroviral transduction of murine Eps15L1 to generate WT endothelial cells from Eps15L1-KO cells. Following deletion of the floxed Eps15 locus by *in vitro* treatment with Tat-Cre Recombinase, we generated Eps15-KO and Eps15/Eps15L1-DKO cells from WT and Eps15L1-KO cells, respectively (Figure 25). In these cells, we investigated whether Eps15 and Eps15L1 regulate the VEGFR-2 signalling pathway. VEGFR-2 triggers two different downstream signalling pathways that mediate cell proliferation or survival. In detail, activation of PLCγ induces the activation of a MAP kinase cascade, which leads to cell division (Takahashi, Yamaguchi et al. 2001). Instead, PI3K activation and Akt phosphorylation promote cell survival (Gerber, McMurtrey et al. 1998). Reports in the literature claim that confluent endothelial cells are contact inhibited and respond poorly to VEGF-induced proliferation: in this condition, indeed, VEGFR-2 is clustered, together with VE-cadherin, in cell-cell contact sites, where it signals preferentially through PI3K and Akt for survival (Lampugnani, Zanetti et al. 2003).

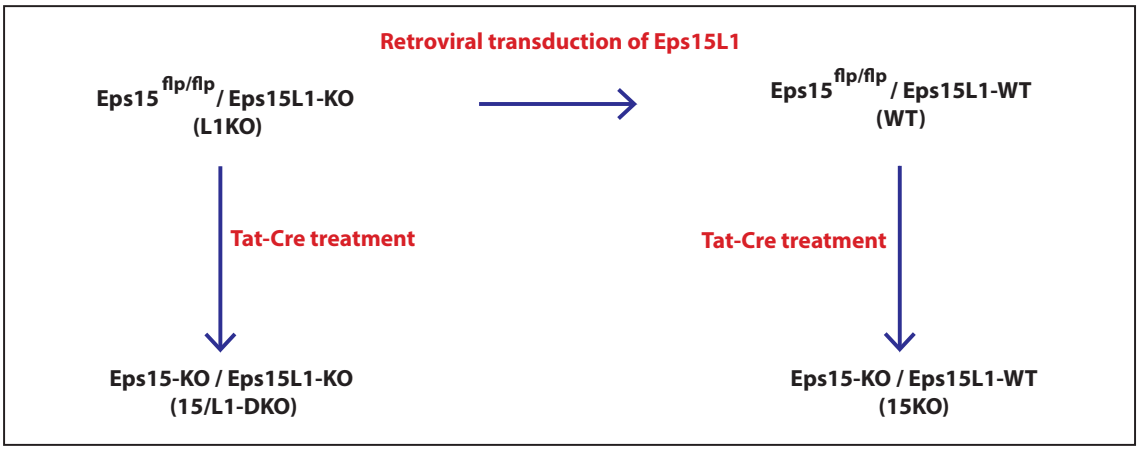

Figure 25. Generation of WT, single and double Eps15 and Eps15L1 KO endothelial cells.

The figure depicts the generation of WT, single and double Eps15 and Eps15L1 KO endothelial cells from the parental $Eps15^{flp/flp}/Eps15L1^{-/-}$ cell line (L1KO). WT cells were generated through retroviral transduction of Eps15L1 into $Eps15^{flp/flp}/Eps15L1^{-/-}$ cells. Eps15-KO (15KO) and Eps15/Eps15L1-DKO (15/L1-DKO) cells were generated through *in vitro* Tat-Cre treatment of Eps15L1-KO and WT cells, respectively.

Instead, in sub-confluent endothelial cells, VEGF stimulation induces the CDE of VEGR-2 in the endosomal compartment, where it activates the PLCγ and the p44/p42 MAP kinase cascade, thus promoting cellular proliferation (Lampugnani, Orsenigo et al. 2006).

To study the possible role, if any, of Eps15 and Eps15L1 in VEGFR-2 signalling, we stimulated sub-confluent endothelial cells with VEGF and we analyzed, by WB analysis, receptor levels, receptor phosphorylation and activation of the MAP kinase cascade. We observed reduced receptor phosphorylation in Eps15/Eps15L1-DKO cells (Figure 26A, B), possibly due to decreased total VEGFR-2 levels (Figure 26A, C). Indeed, receptor phosphorylation relative to total VEGFR-2 levels was similar as in WT cells (Figure 26A, D). Nevertheless, even if total VEGFR-2 levels were decreased, we found that the activation of the p44/p42 MAP kinase cascade was not affected in Eps15/Eps15L1-DKO cells (Figure 26A, E), thus indicating that the available amount of VEGFR-2 was sufficient to sustain appropriate MAP kinase signalling. AKT signalling, instead, was activated at

similar basal levels in all genotypes (Figure 26A, F). These data indicate that no major impact by Eps15 and Eps15L1 is visible on canonical VEGFR-2 downstream signalling. However, since VEGFR-2 levels were reduced in Eps15/Eps15L1-DKO cells, thus indicating a defect in VEGFR-2 turnover, there might be spatio-temporal differences of downstream signalling difficult to access by WB analysis.

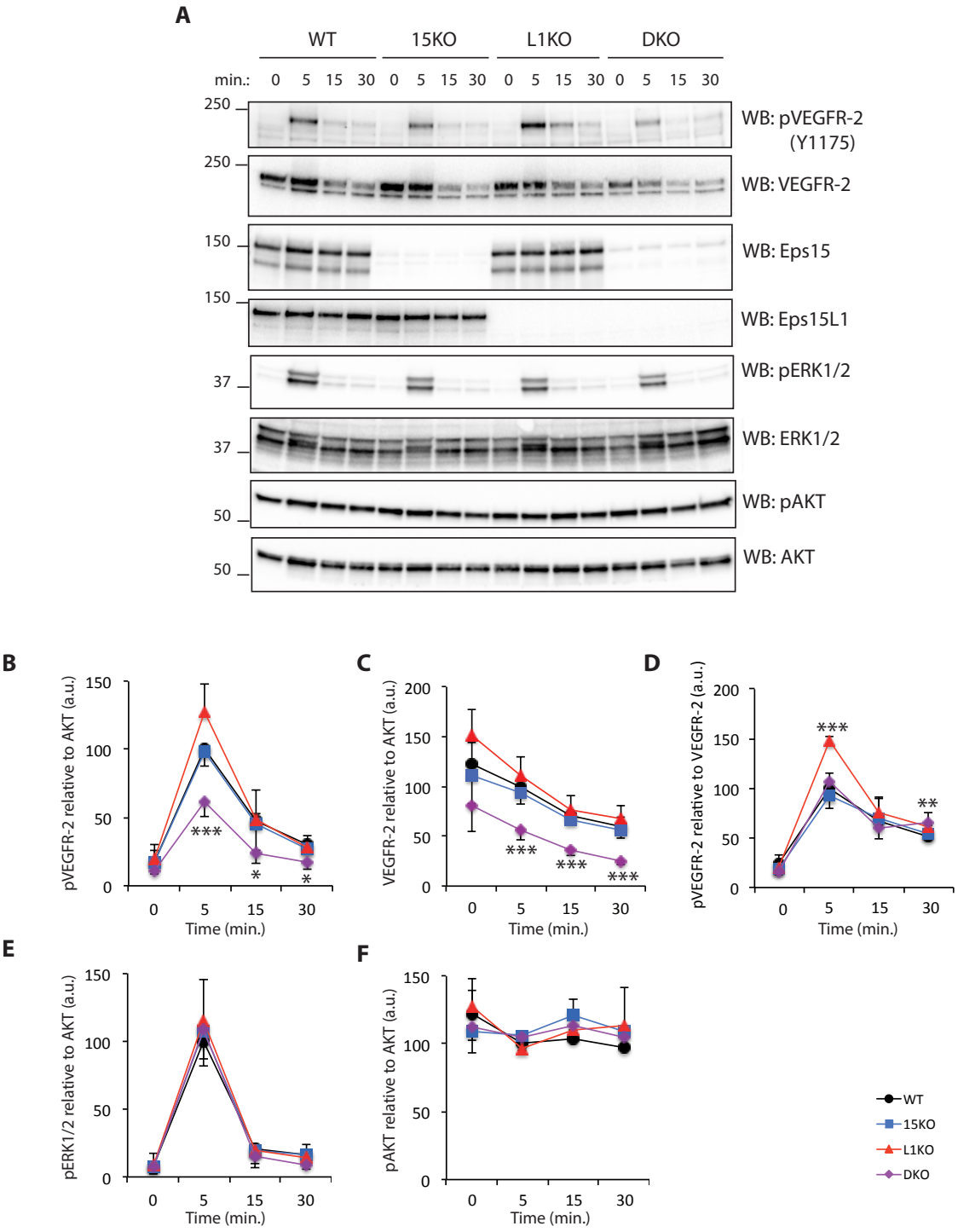

Figure 26. VEGFR-2 downstream signalling is unaltered in DKO endothelial cells.

A. Representative WB of VEGF stimulation on wild type (WT), Eps15-KO (15KO), Eps15L1-KO (L1KO) and Eps15/Eps15L1-DKO (DKO) endothelial cells (n=3). Sub-confluent endothelial cells were stimulated with 80 ng/ml VEGF for 0, 5, 15 and 30 minutes and then lysed. 20 µg of each cell lysate were separated on SDS-PAGE, transferred on a nitrocellulose filter and probed with antibodies for pVEGFR-2 (Y1175), total VEGFR-2, Eps15, Eps15L1, pAKT, total AKT, pERK1/2 and total ERK1/2, as indicated. MWs (kDa) are indicated on the left. **B.** Quantification in arbitrary units (a.u.) of pVEGFR-2 (Y1175) relative to total AKT at 0, 5, 15 and 30 minutes after stimulation. **C.** Quantification in arbitrary units (a.u.) of total VEGFR-2 relative to total AKT at 0, 5, 15 and 30 minutes after stimulation. **D.** Quantification in arbitrary units (a.u.) of pVEGFR-2 (Y1175) relative to total VEGFR-2 at 0, 5, 15 and 30 minutes after stimulation. **E.** Quantification in arbitrary units (a.u.) of pERK1/2 relative to total AKT at 0, 5, 15 and 30 minutes after stimulation. **F.** Quantification in arbitrary units (a.u.) of pAKT relative to total AKT at 0, 5, 15 and 30 minutes after stimulation. WB bands for pVEGFR-2 (Y1175) (B and D), total VEGFR-2 (C), pERK1/2 (E) and pAKT (F) were quantified by Image Lab Software and each value was normalized to the corresponding total AKT value (B, C, E, F) or total VEGFR-2 value (D). Normalized values are represented as a ratio on the WT. Data are presented as an average of three independent experiments; error bars represent standard error deviation. Statistical significance was assessed using 2-tailed student's t-test (*=$p<0.05$; **=$p<0.01$).

To analyze alterations in the Notch signalling pathway, we cultured endothelial cells of the four genotypes to confluency, in order to allow cell-cell contact, a prerequisite for Notch signalling activation. We, then, assessed the activation of Notch signalling by WB analysis with an antibody detecting the cleaved-Notch1^{Val1744} (NICD). In lysates from WT cells, we detected the presence of the NICD, thus indicating that Notch signalling was activated in these cells. As expected, the NICD protein was not detectable in lysates from cells that had been cultured in the presence of the Notch signalling inhibitor DAPT. When we assessed the activation of Notch signalling in endothelial cells knocked-out for Eps15, Eps15L1 or both, we found no differences compared to WT cells (Figure 27).

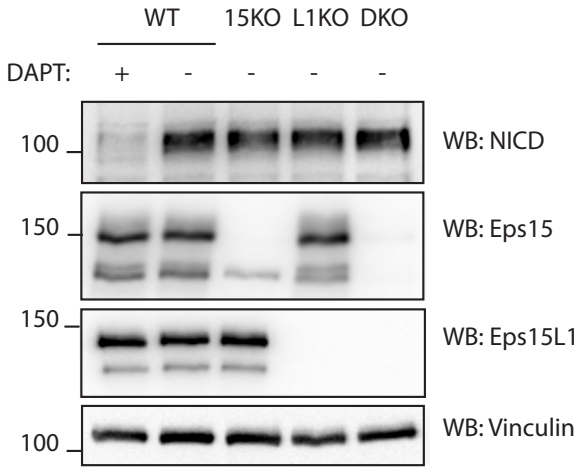

Figure 27. Notch signalling is unaltered in DKO endothelial cells.

WB analysis showing the levels of Cleaved-Notch1^{Val1744} (NICD) protein in wild type (WT), Eps15-KO (15KO), Eps15L1-KO (L1KO) and Eps15/Eps15L1-DKO (DKO) endothelial cells, cultured to confluency in the presence of the Notch signalling inhibitor DAPT (+) or DMSO as vehicle (-). 20 µg of each cell lysate were separated on SDS-PAGE, transferred on a nitrocellulose filter and probed with antibodies for Cleaved-Notch1^{Val1744} (NICD), Eps15, Eps15L1 and vinculin, as indicated. MWs (kDa) are indicated on the left.

2.2. cDKO mice do not recapitulate embryo lethality of constitutive Eps15/Eps15L1-DKO mice

In endothelial cells, we found that Eps15 and Eps15L1 regulate VEGFR-2 turnover, thus indicating that they play a cell-autonomous function in the vascular system by regulating VEGFR-2 and, possibly, other unexplored receptors.

Through the Tie2-Cre strategy, we generated cDKO mice to see whether the lack of Eps15 and Eps15L1 in the vascular system was sufficient to cause midgestation lethality, as occurs in constitutive Eps15/Eps15L1-DKO mice. To this end we crossed Eps15$^{flp/flp}$/Eps15L1$^{+/-}$ females with Eps15$^{flp/flp}$/Eps15L1$^{+/-}$/tg$^{Tie2\text{-}Cre}$ males and we generated Eps15$^{flp/flp}$/Eps15L1$^{-/-}$/tg$^{Tie2\text{-}Cre}$ mice. In Eps15$^{flp/flp}$/Eps15L1$^{-/-}$/tg$^{Tie2\text{-}Cre}$ mice, Eps15L1 is constitutively deleted in all tissues, while Cre expression, driven by the Tie2

promoter, leads to the deletion of the floxed Eps15 specifically in hematopoietic and endothelial cells. In this thesis project, these mice ($Eps15^{flp/flp}/Eps15L1^{-/-}/tg^{Tie2\text{-}Cre}$) are referred to as cDKO mice.

PECAM-1 staining of 9.5 dpc embryos showed that cDKO mice present an altered angiogenesis, with enlarged vessels and reduced and disorganized branching in the head (Figure 28). Vascular defects due to the lack of Eps15 and Eps15L1 might contribute to the severe phenotype of constitutive Eps15/Eps15L1-DKO mice, together with other perturbed developmental processes.

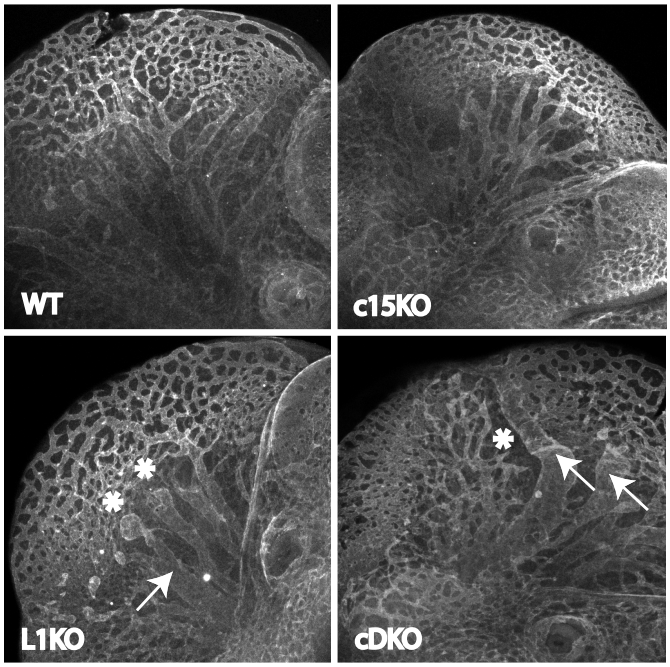

Figure 28. cDKO mice have vascular defects but do not recapitulate embryo lethality of constitutive Eps15/Eps15L1-DKO mice.

IF PECAM-1 staining of the head vasculature of 9.5 dpc wild type (WT), conditional-Eps15KO ($Eps15^{flp/flp}/Eps15L1^{+/+}/tg^{Tie2\text{-}Cre}$, indicated as c15KO), constitutive Eps15L1-KO (indicated as L1KO) and conditional-DKO mice ($Eps15^{flp/flp}/Eps15L1^{-/-}/tg^{Tie2\text{-}Cre}$, indicated as cDKO). White arrows and white asterisks indicate enlarged vessels and blind vessels, respectively.

Based on our *in vitro* data, vascular defects in cDKO mice might be linked to altered VEGFR-2 turnover. Nevertheless, these vascular defects were not sufficient to cause embryo lethality, indeed, in contrast to constitutive Eps15/Eps15L1-DKO mice, cDKO mice survived to birth. These results indicate that, even if Eps15 and Eps15L1 regulate cell-autonomously vascular development through the regulation of VEGFR-2 turnover and, eventually, of other receptors, vascular defects do not cause embryo lethality in cDKO mice.

3. Eps15 and Eps15L1 regulate TfR internalization in a redundant-manner and are required for proper development of RBCs

3.1. MEFs as a model system to study the role of Eps15 and Eps15L1 in the internalization of EGFR and TfR

Previous *in vitro* studies demonstrated that Eps15 and Eps15L1 proteins regulate the internalization of EGFR and TfR. These results were derived through the use of specific antibodies blocking Eps15 and Eps15L1 (Carbone, Fre et al. 1997) or through siRNA interference of the proteins (Huang, Khvorova et al. 2004). To confirm the function of Eps15 and Eps15L1 in these pathways in a cleaner and in a physiological setting, we generated MEFs from KO mice for Eps15 and Eps15L1. In detail, to study the role of Eps15 and Eps15L1 in the internalization of EGFR and TfR, we used two different cell lines of MEFs: $Eps15^{flp/flp}/Eps15L1^{+/+}/tg^{CreERT2}$ and $Eps15^{flp/flp}/Eps15L1^{-/-}/tg^{CreERT2}$. In the absence of (Z)-4-hydroxytamoxifen treatment, these cell lines were used as WT and

Eps15L1-KO, respectively. When treated with (Z)-4-hydroxytamoxifen, deletion of Eps15 in WT cells leads to the generation Eps15-KO cells, while deletion of Eps15 in Eps15L1-KO cells leads to the generation of Eps15/Eps15L1-DKO cells.

As better described in the next sections, in these cellular model systems, we performed radioactive assays with ^{125}I-EGF and ^{125}I-Tf to follow the internalization of EGFR and TfR, respectively.

3.2. Eps15 and Eps15L1 have a minor impact on EGFR internalization

To test whether Eps15 and Eps15L1 regulated EGFR internalization in MEFs, we performed radioactive internalization assays with ^{125}I-EGF, at low (when only CDE is active) and high doses (when both CDE and CIE are active) of EGF. We observed that the K_e was slightly but significantly reduced (~20%) in Eps15-KO, Eps15L1-KO and Eps15/Eps15L1-DKO cells both at low and high concentrations of EGF (Figure 29A), suggesting that there might be an effect on both CDE and CIE of EGFR.

By saturation binding with ^{125}I-EGF, we measured the total number of EGFR at the cell surface. We found that surface levels of EGFR were altered only in Eps15L1-KO: in these cells, surface EGFR was reduced by ~15% (Figure 29B). Reduced surface levels of EGFR in Eps15L1-KO cells might indicate some alterations in the constitutive EGFR turnover, e.g. increased degradation and/or reduced biosynthesis of the receptor.

These data indicated that Eps15 and Eps15L1 have a minor impact on EGFR endocytosis and that they act in a non-redundant manner, since no worsening of the phenotype was observed in DKO cells.

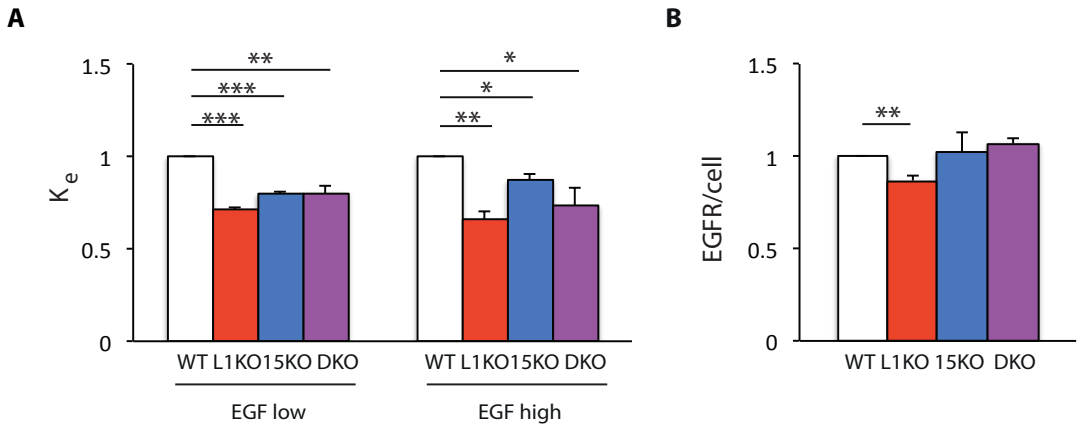

Figure 29. EGFR internalization is partially reduced in single and double Eps15 and Eps15L1 KO MEFs.

A. The bar graph represents the endocytic rate constant (K_e) for EGFR in wild type (WT), Eps15L1-KO (L1KO), Eps15-KO (15KO) and Eps15/Eps15L1-DKO (DKO) MEFs, when stimulated with low (1.5 ng/ml) and high (30 ng/ml) doses of EGF. The K_e value was normalized as a ratio to WT. Data are presented as an average of three (EGF low) or four (EGF high) different independent experiments; error bars represent the standard error mean. Statistical significance was assessed using 2-tailed student's t-test (*=p<0.05; **=p<0.01; ***p=<0.005). **B.** The bar graph represents steady state surface levels of EGFR in wild type (WT), Eps15L1-KO (L1KO), Eps15-KO (15KO) and Eps15/Eps15L1-DKO (DKO) MEFs. The numbers of surface receptors/cell were normalized to WT. Data are presented as an average of four different independent experiments; error bars represent the standard error mean. Statistical significance was assessed using 2-tailed student's t-test (**=p<0.01).

3.3. Internalization of TfR is impaired in Eps15/Eps15L1-DKO MEFs

To test whether Eps15 and Eps15L1 regulated TfR internalization in MEFs, we performed radioactive internalization assays with ^{125}I-Tf, to follow CDE of the receptor.

We found that the K_e of the TfR was strongly reduced in Eps15/Eps15L1-DKO cells (~50%), but only a minor effect in single Eps15 or Eps15L1 KO MEFs was detected, even if statistically significant in Eps15L1-KO cells (Figure 30A).

When we analyzed the total number of TfR at the cell surface by saturation binding with ^{125}I-Tf, we found that in DKO cells steady state surface levels of the TfR were increased with respect to WT or single KO cells, consistent with its reduced internalization (Figure 30B). This result suggests a critical redundant role of Eps15 and Eps15L1 in the internalization of TfR.

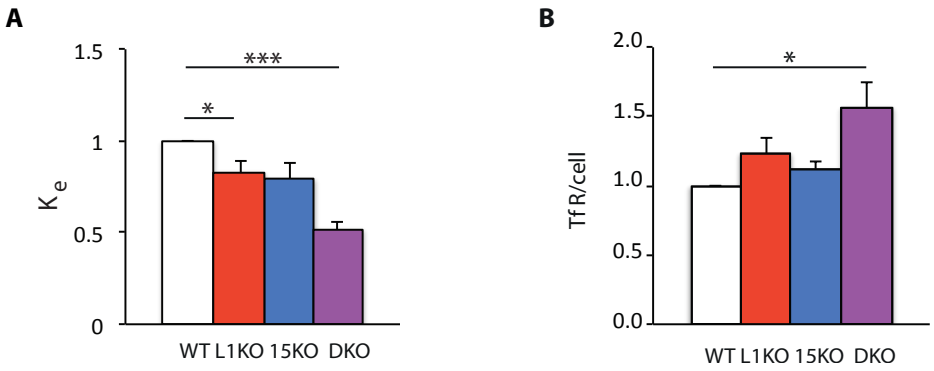

Figure 30. Internalization of TfR is strongly reduced in DKO MEFs.

A. The bar graph represents the endocytic rate constant (K_e) for TfR in wild type (WT), Eps15L1-KO (L1KO), Eps15-KO (15KO) and Eps15/Eps15L1-DKO (DKO) MEFs, when stimulated with ^{125}I-Tf. The K_e value was normalized as a ratio to WT. Data are presented as an average of three different independent experiments; error bars represent the standard error mean. Statistical significance was assessed using 2-tailed student's t-test (*=p<0.05; ***p=<0.005). **B.** The bar graph represents steady state surface levels of TfR in wild type (WT), Eps15L1-KO (L1KO), Eps15-KO (15KO) and Eps15/Eps15L1-DKO (DKO) MEFs. The numbers of surface receptors/cell were normalized to WT. Data are presented as an average of four different independent experiments; error bars represent the standard error mean. Statistical significance was assessed using 2-tailed student's t-test (*=p<0.05).

3.4. cDKO mice suffer from microcytic hypochromic anemia

We demonstrated that TfR internalization was impaired in Eps15/Eps15L1-DKO MEFs. Since TfR mediates the internalization of iron (Ponka and Lok 1999), impaired TfR internalization is generally correlated with reduced iron uptake. In the organism, immature RBCs are the most avid consumers of iron as this mineral is fundamental in these cells for hemoglobin production (Ponka and Lok 1999). As a consequence, studies in genetically engineered mice indicate that perturbations in proteins involved in iron uptake, linked to TfR signalling, greatly impact on the development of RBCs (Levy, Jin et al. 1999, Zhu, McLaughlin et al. 2008, Ishikawa, Maeda et al. 2015).

To assess whether defective internalization of TfR, due to the lack of Eps15 and Eps15L1, impacted on the development of RBCs, we analyzed the blood of cDKO mice, generated through the Tie2-Cre strategy, as reported in section "2.2. cDKO mice do not recapitulate embryo lethality of constitutive Eps15/Eps15L1-DKO mice". In these mice, which have genotype $Eps15^{flp/flp}/Eps15L1^{-/-}/tg^{Tie2\text{-}Cre}$, Eps15L1 was constitutively deleted in all tissues, while floxed Esp15 was specifically deleted in hematopoietic and endothelial cells through Cre expression driven by the Tie2 promoter.

Analysis of hematic parameters showed that, in cDKO mice, the MCV of RBCs was strongly reduced compared to WT mice. Of note, also in cEps15-KO mice, the MCV was significantly reduced, even if to a lesser extent compared to cDKO mice. Since MCV reduction had already been observed in constitutive Eps15-KO mice, this result confirmed and extended previous findings in the laboratory (Pozzi et al., unpublished results). A second observation was that the RDW, index of anisocytosis, was increased in cDKO, indicating a high degree of variation in the size of RBCs. The number of RBCs, instead, was unchanged in cDKO (Table 7).

Genotype	MCV (fl)	RBCs (10^6/µl)	RDW (%)	Total
WT	90 ± 1.0	2.5 ± 0.3	15 ± 0.4	17
L1KO	94 ± 2.2	2.6 ± 0.5	16 ± 0.5	3
c15KO	87 ± 0.7**	2.6 ± 0.3	16 ± 0.4	21
cDKO	83 ± 1.4 ***	2.2 ± 0.4	20 ± 1.6 ***	6

Table 7. Hematic parameters of cDKO newborn mice.

The table reports, in wild type (WT), constitutive Eps15L1-KO (L1KO), conditional Eps15-KO (c15KO) and conditional Eps15/Eps15L1-DKO (cDKO) newborn mice, the mean ± the standard error mean of the following hematic parameters: the MCV of RBCs, expressed in femtoliters (fl); the number of RBCs in 1 microliter of blood (10^6/µl); the RDW expressed in percentage (%). The total number of mice analysed for each genotype is indicated. Statistical significance was assessed using 2-tailed student's t-test (**=$p<0.01$; ***=$p<0.005$).

To directly visualize the morphology, the size and the maturation state of RBCs, we performed a May-Grünwald Giemsa staining on blood smears. We observed that the morphology and the size of RBCs were altered in cDKO mice. Moreover, in these mice, RBCs were paler, indicating a reduced content of hemoglobin.

When we counted the number of immature RBCs, represented by blue colored cells and cells containing blue granules, we found an increase in the number of these cells in cDKO mice (Figure 31).

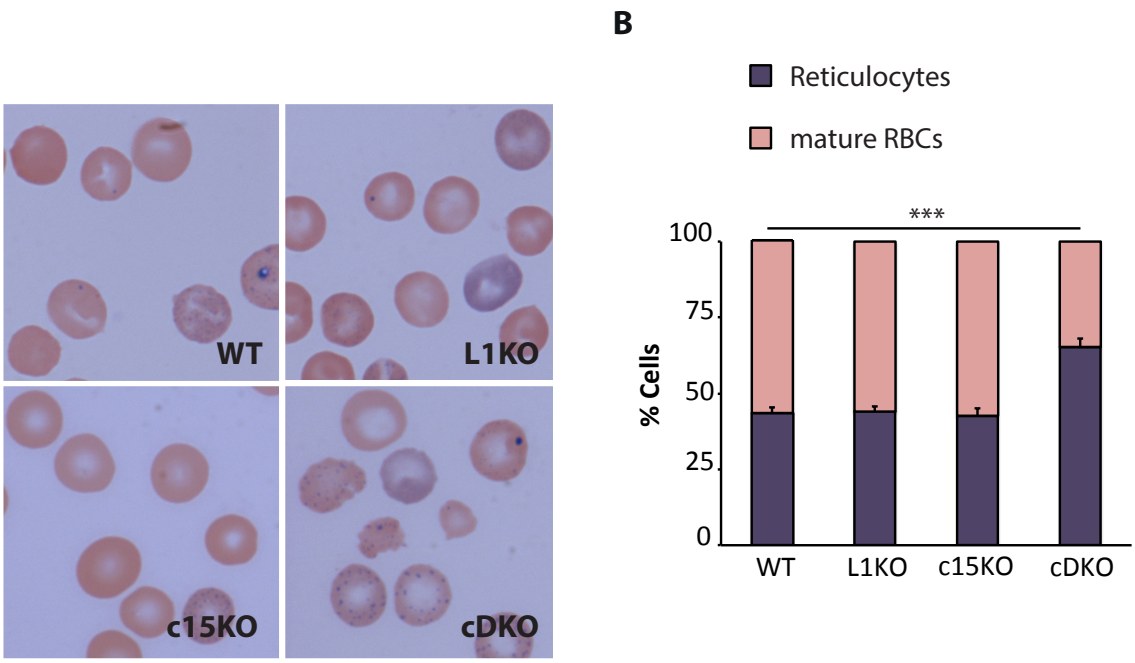

Figure 31. cDKO mice have an increased number of immature RBCs.

A. Representative images of May-Grünwald Giemsa stainings of blood smears from wild type (WT), constitutive Eps15L1-KO (L1KO), conditional Eps15-KO ($Eps15^{flp/flp}/Eps15L1^{+/+}/tg^{Tie2\text{-}Cre}$, c15KO) and conditional Eps15/Eps15L1-DKO ($Eps15^{flp/flp}/Eps15L1^{-/-}/tg^{Tie2\text{-}Cre}$, cDKO) newborn mice. Images were acquired with a stereomicroscope. **B.** The bar graph represents the percentage of reticulocytes (immature RBCs) and mature RBCs, detected by May-Grünwald Giemsa staining of blood smears from wild type (WT, n=7), constitutive Eps15L1-KO (L1KO, n=6), conditional Eps15-KO (c15KO, n=6) and conditional Eps15/Eps15L1-DKO (cDKO, n=5) newborn mice. Error bars represent the standard error mean. Statistical significance was assessed using 2-tailed student's t-test (***=$p<0.005$).

All these observations suggest that cDKO mice suffer from microcytic hypochromic anemia. Altered development of RBCs might be caused by defective TfR internalization.

4. Defective internalization of TfR in Eps15/Eps15L1-DKO MEFs is paralleled by defective formation of clathrin endocytic structures

4.1. Eps15 and Eps15L1 differentially interact with proteins participating in CDE

Since we observed that TfR internalization was impaired in Eps15/Eps15L1-DKO MEFs, we wanted to elucidate the molecular mechanism by which Eps15 and Eps15L1 regulate this process. Since TfR is internalized via CDE, we initially investigated, by Co-IP experiments, in single and double KO MEFs the interaction of Eps15 and Eps15L1 with proteins of the clathrin endocytic machinery, AP-2 and Itsn1, previously characterized as major binding partners of Eps15 (Benmerah, Gagnon et al. 1995, Sengar, Wang et al. 1999). In whole cell lysates, we found that, in WT MEFs, Eps15 and Eps15L1 differentially bind to these two CDE components: AP-2 preferentially interacted with Eps15 (Figure 32A, B, C-a, b, c), while Itsn1 mainly associated with Eps15L1 (Figure 32A, B, C-d, e, f). Of note, the interaction between Itsn1 and Eps15 increased in Eps15L1-KO cells (Figure 32B, D-e, f). This result may suggest that at steady state Eps15L1 competes with Eps15 for the binding to Itsn1 and, when Eps15L1 is absent, Itsn1 becomes available for the binding with Eps15. In Eps15L1-KO cells we also observed an increased interaction between AP-2 and Itsn1 (Figure 32B), which could simply be the consequence of the increased association between Itsn1 and Eps15 that in turn brings down more AP-2 to the complex. These data suggest that there is specificity embedded in Eps15 versus Eps15L1 interactions with the endocytic machinery and shows rearrangements of the interactions upon KO of Eps15L1.

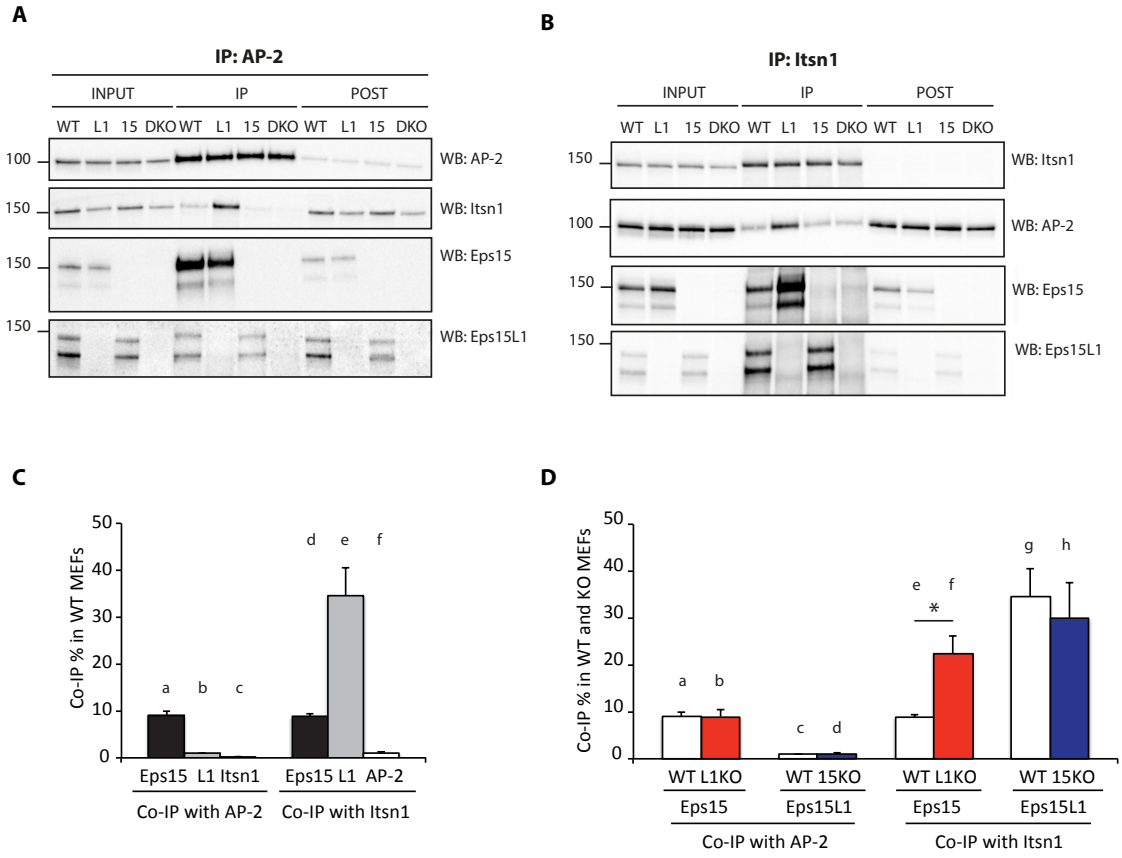

Figure 32. Eps15 and Eps15L1 bind to different components of the clathrin endocytic machinery.

A. Representative WB showing the Co-IP of intersectin1 (Itsn1), Eps15 and Eps15L1 proteins with anti-alpha Adaptin antibody. **B.** Representative WB showing the Co-IP of AP-2, Eps15 and Eps15L1 proteins with anti-Itsn1 antibody. In panels A and B, proteins were co-immunoprecipitated from fresh lysates of primary wild type (WT), Eps15L1-KO (L1), Eps15-KO (15) and Eps15/Eps15L1-DKO MEFs (n=4). Immunoprecipitated lysates (IP), total lysates (INPUT) and post-immunoprecipitated lysates (POST) were separated on SDS-PAGE, transferred on a nitrocellulose filter and probed with antibodies for AP-2, Itsn1, Eps15 and Eps15L1, as indicated. In panel A, in the control of IP efficiency (filter probed with AP-2), INPUT and POST were 25% of the IP (20 µg of IP were loaded), while in the control of Co-IP efficiency of Itsn1, Eps15 and Eps15L1 (filters probed with Itsn1, Eps15 and Eps15L1), INPUT and POST were 1% of the IP (200 µg of IP were loaded). In panel B, in the control of IP efficiency (filter probed with Itsn1), INPUT and POST were 20% of the IP (20 µg of IP were loaded), while in the control of Co-IP efficiency of AP-2, Eps15 and Eps15L1 (filters probed with AP-2, Eps15 and Eps15L1), INPUT and POST were 5% of the IP (200 µg of IP were loaded). MWs are indicated on the left (kDa). **C.**

The bar graph depicts, in WT MEFs, the percentage of Co-IP of Eps15, Eps15L1 and Itsn1 proteins with anti-alpha Adaptin antibody (a, b, c) and the percentage of Co-IP of Eps15, Eps15L1 and AP-2 proteins with anti-Itsn1 antibody (d, e, f). Data are presented as an average of four independent experiments; error bars represent the standard error mean. **D.** The bar graph compares: in wild type (WT) and Eps15L1-KO (L1KO) MEFs, the percentage of Co-IP of Eps15 with anti-alpha Adaptin antibody (a, b) or anti-Itsn1 antibody (e, f); in wild type (WT) and Eps15-KO (15KO) MEFs, the percentage of Co-IP of Eps15L1 with anti-alpha Adaptin antibody (c, d) or anti-Itsn1 antibody (g, h). Data are presented as an average of four independent experiments; error bars represent the standard error mean. Statistical significance was assessed using 2-tailed student's t-test (*=$p<0.05$).

4.2. Impairment of Eps15 and Eps15L1 alters the number of AP-2-positive structures

To further study the relation between these proteins, we performed preliminary co-localization studies of Eps15, Eps15L1 and Itsn1 in clathrin-structures, using AP-2 as a marker. In WT MEFs, we observed that Eps15, Eps15L1 and Itsn1 proteins co-localized with AP-2-positive dots. Co-localization was observed predominantly with bigger AP-2-positive structures but not with the smaller structures (Figure 33A). When Eps15 or Eps15L1 were individually knocked-out, we observed a reduction in the number of smaller AP-2-positive structures, while the bigger ones were unchanged (Figure 33A, B). Concomitantly, an increased percentage of co-localization of AP-2 with Eps15 and Itsn1 (in Eps15L1-KO cells), or with Eps15L1 and Itsn1 (in Eps15-KO cells) was observed (Figure 33A, C). This apparent increase may be the result of the reduction in single KO cells of smaller AP-2-positive dots. This phenotype was completely reverted in DKO cells, which showed an increment of smaller structures, even compared to WT cells (Figure 33A, B). Moreover, in DKO cells the percentage of co-localization between AP-2 and Itsn1 was decreased (Figure 33A, D). This decrease may be the result of the increased number of smaller AP-2-positive dots in single KO cells. Since we observed only a minor defect in

the internalization of TfR in single KO MEFs, we may speculate that endocytic structures lacking Eps15 or Eps15L1 are still efficiently assembled, probably by rearrangement of interactions among CDE proteins, as observed in Eps15L1-KO through Co-IP analysis. On the contrary, in DKO cells, defective internalization of TfR might be linked to a defect in the maturation of endocytic structures, due to the lack of both Eps15 and Eps15L1 and reduced co-localization of Itsn1 with AP-2-positive structures. This hypothesis will require high resolution and live imaging studies to be addressed.

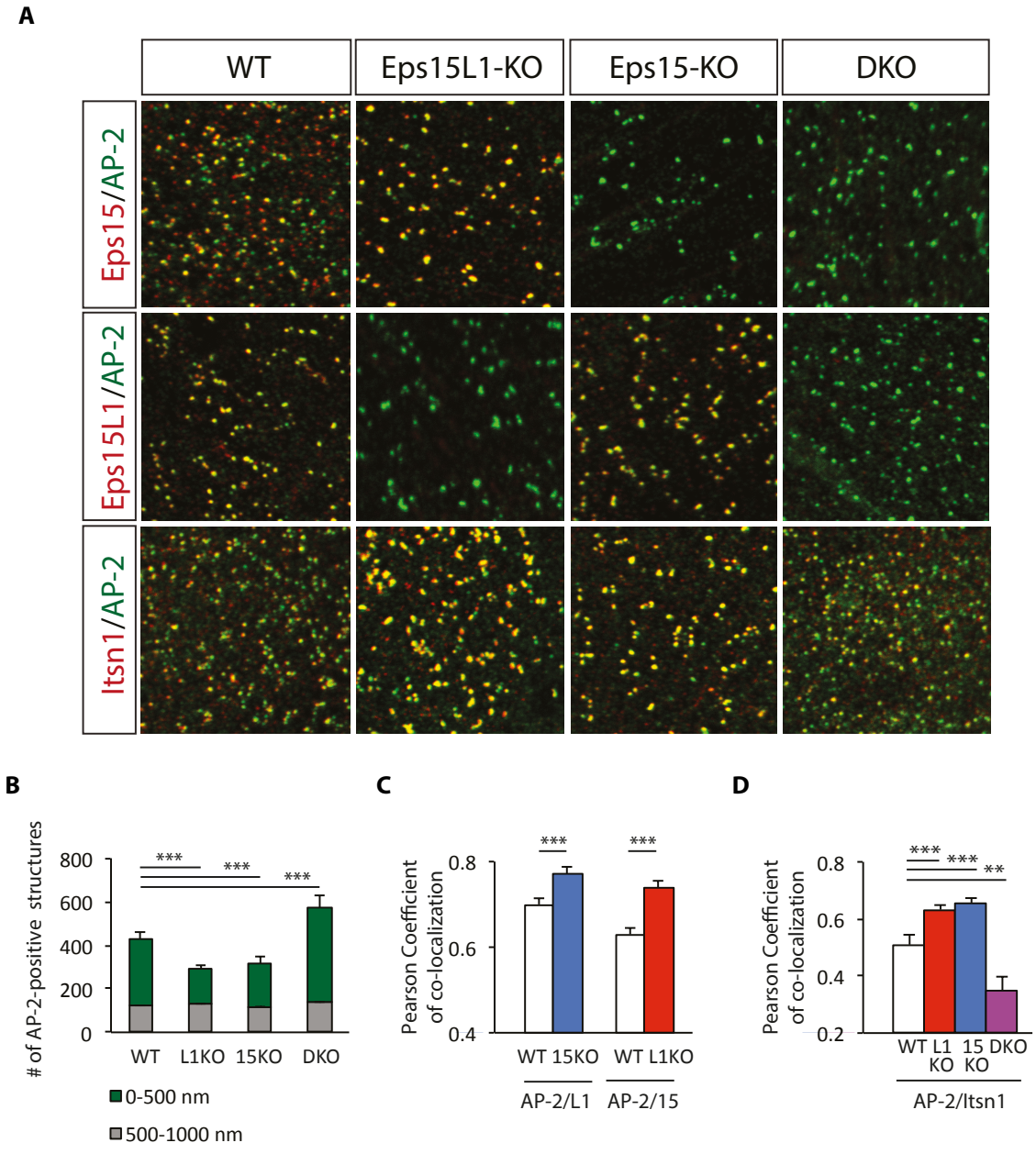

Figure 33. The number of AP-2-positive structures is altered following impairment of Eps15 and Eps15L1.

A. The IF images depict the co-localization of AP-2 (green) with Eps15, Eps15L1 and Itsn1 (red) in primary wild type (WT), Eps15L1-KO, Eps15-KO and Eps15/Eps15L1-DKO (DKO) MEFs. Images were acquired with a SP5 inverted confocal microscope. **B.** The bar graph depicts the number of AP-2-positive structures of 0-500 nm diameter (green) and 500-1000 nm diameter (gray) in primary wild type (WT), Eps15L1-KO (L1KO), Eps15-KO (15KO) and Eps15/Eps15L1-DKO (DKO) MEFs. Error bars represent the standard error mean. Statistical significance was assessed using 2-tailed student's t-test (***=$p<0.005$). **C.** The bar graph depicts the Pearson Coefficient of co-localization of a) AP-2 with Eps15L1 (AP-2/L1) in primary wild type (WT) and Eps15-KO (15KO) MEFs and of b) AP-2 with Eps15 (AP-2/15) in primary wild type (WT) and Eps15L1-KO (L1KO) MEFs. Error bars represent the standard error mean. Statistical significance was assessed using 2-tailed student's t-test (***=$p<0.005$). **D.** The bar graph depicts the Pearson Coefficient of co-localization of AP-2 with Itsn1 (AP-2/Itsn1) in primary wild type (WT), Eps15L1-KO (L1KO), Eps15-KO (15KO) and Eps15/Eps15L1-DKO (DKO) MEFs. Error bars represent the standard error mean. Statistical significance was assessed using 2-tailed student's t-test (**=$p<0.01$; ***=$p<0.005$).

Chapter 4

DISCUSSION

The Eps15 protein family is composed of two members, Eps15 and Eps15L1, which share high co-linearity and homology. Since their discovery in 1993 as substrates of the tyrosine kinase activity of the EGFR, several studies delineating the cellular function(s) of these proteins have arisen. From these studies, it emerged that Eps15 and Eps15L1 are two scaffolding proteins, which serve pleiotropic functions in endocytosis: they regulate the early events of CDE and CIE of several cargoes, their sorting in the EEs and protein trafficking from the TGN. However, to our knowledge, most of the *in vitro* studies have been focused on Eps15, while fewer have addressed the functions of Eps15L1. The reason resides in the fact that Eps15 and Eps15L1 have always been thought to have a redundant role in several cellular processes due to their homology, their common binding partners and their similar cellular localization. Moreover, both Eps15 and Eps15L1 have been found to regulate the CDE of EGFR and TfR. Nevertheless, these findings were derived from *in vitro* studies dissecting the effects on EGFR and TfR internalization upon injection of antibodies blocking Eps15 or Eps15L1 (Carbone, Fre et al. 1997) or upon siRNA interference of the proteins (Huang, Khvorova et al. 2004). Therefore, their role in EGFR and TfR internalization has never been demonstrated in a clean and more physiological setting. Furthermore, no studies have been performed to investigate their role *in vivo*.

Our laboratory addresses whether Eps15 and Eps15L1 exert redundant and/or non-redundant roles in mammals, using genetically engineered mice as a model system. In these organisms, the genetical removal of the components of the endocytic machinery rarely impinge on viability, likely because functionally redundant proteins or pathways are capable to compensate for their loss. This is the case for Eps15, whose removal in the

organism has no evident effects, apart from a defect in the development of marginal zone B cells (Pozzi, Amodio et al. 2012) and mild microcytosis (Pozzi et al., unpublished results). In contrast to Eps15-KO mice, which are viable and fertile, Eps15L1-KO mice die at birth (Alberici et al., unpublished results). Moreover, deeper investigations showed that that Eps15L1 plays a non-redundant role in the regulation of SVR (Alberici et al., unpublished results), which is reminiscent of the role played by its orthologous in lower organisms (Salcini, Hilliard et al. 2001, Koh, Korolchuk et al. 2007, Rose, Malabarba et al. 2007, Wang, Bouhours et al. 2008). Eps15/Eps15L1-DKO mice have a more severe phenotype and die at midgestation. The phenotype of Eps15/Eps15L1-DKO mice, together with the one of the single KO mice, suggests that Eps15 and Eps15L1 have both redundant and non-redundant functions. Thus, the severe phenotype of Eps15/Eps15L1-DKO might result from the impairment of a redundant function essential for embryo development or from the combined impairment of redundant and non-redundant functions, which, even if not essential, might addictively contribute to embryo lethality.

The aim of this project was to investigate redundant and non-redundant functions of Eps15 and Eps15L1 in order to unmask the underlying causes of embryo lethality in Eps15/Eps15L1-DKO mice.

1. The non-redundant role of Eps15 and Eps15L1 in the regulation of the Notch signalling pathway

Our initial hypothesis was that Eps15 and Eps15L1 are redundantly required in the regulation of Notch signalling. Indeed, morphological alterations of Eps15/Eps15L1-DKO mice phenocopied Notch loss-of-function mutants and the Notch target genes HES1, HES5 and NRARP were found to be downregulated in Eps15/Eps15L1-DKO mice, similar to epsin1/2-DKO mice. Other considerations sustained this hypothesis: i) Eps15 and Eps15L1 physically interact with Numb and epsin (Chen, Fre et al. 1998, Saffarian, Cocucci et al.

2009), key regulators of Notch receptor and ligand activity, respectively; ii) Eps15 and Eps15L1 act in complex with epsin1 to modulate EGFR endocytosis (Chen, Fre et al. 1998, Sigismund, Woelk et al. 2005); iii) Eps15 and Eps15L1 possess two UIM domains, one of two essential domains needed for epsin-dependent activation of Notch ligands (Xie, Cho et al. 2012). Previous *in vitro* work in the laboratory confirmed that Eps15 and Eps15L1 are effectively involved in the regulation of Notch signalling in signal-sending cells. Indeed, by a luciferase-based co-culture assay, in which OP9 cells overexpressing the Notch ligand Dll1 (OP9-Dll1 cells) (Schmitt and Zuniga-Pflucker 2002) were used as signal-sending cells, and C2C12 cells overexpressing human Notch-1 receptor (C2C12-Notch1 cells) were used as signal-receiving cells, it was found that transient KD of Eps15 or Eps15L1 in OP9-Dll1 cells lead to a ~50% reduction of Notch activation. Of note, no further reduction of Notch signalling was observed when both Eps15 and Eps15L1 were knocked-down in OP9-Dll1 cells (Lucano et al., unpublished results).

To confirm this finding in a physiological setting, we investigated whether Eps15 and Eps15L1 played a role in the regulation of Notch signalling, using MEFs derived from KO mice for Eps15 and Eps15L1 as a model for the signal-sending cell (MEF-Dll1 cells). While in OP9-Dll1 cells transient KD of Eps15 or Eps15L1 reduced Notch activation, in MEF-Dll1 cells only deletion of Eps15L1 impaired Notch signalling. No further reduction of Notch signalling was observed when both Eps15 and Eps15L1 were deleted. Therefore, in MEF-Dll1 cells, Eps15L1 is required in a non-redundant manner for proper activation of Notch signalling. Of note, a partial downregulation of the Notch target genes had been observed also in Eps15L1-KO embryos.

To reinforce our results in MEF-Dll1 cells, we will investigate the role of Eps15 and Eps15L1 in Notch signalling in an isogenic cellular system, in which parental WT cell lines, transgenic for CreERT2 and floxed for Eps15 and/or Eps15L1, will be directly compared with the single or double KO cell line generated by (Z)-4-hydroxytamoxifen treatment.

There are several possibilities that might explain the reason for which Eps15 seems to regulate ligand biology in OP9-Dll1 cells but not in MEF-Dll1 cells. One of these possibilities is that the role of Eps15 in this pathway is cell-context dependent. If so, Eps15 and Eps15L1 may be differently expressed in OP9-Dll1 and in MEF-Dll1 cells. Expression levels of Eps15 and Eps15L1 in these model systems will be evaluated. Another observation is that deletion of Eps15 in OP9-Dll1 and MEF-Dll1 cells was obtained in two different ways, by siRNA interference in the first cell line and gene KO in the second one. Therefore, one risk is that reduced Notch activity upon KD of Eps15 in OP9-Dll1 cells is an off-target effect, even if this reduction was observed with three different siRNA oligos targeting Eps15. Another possibility, instead, is that the acute downregulation of Eps15, obtained by siRNA interference, may impact on Notch activity, while when chronically deleted, as occurs in MEF-Dll1 cells, other pathways compensate for the lack of Eps15.

As mentioned before, luciferase-based co-culture assays showed that Eps15 and Eps15L1 regulate Notch signalling in the signal-sending cell but not in the signal-receiving cell. Indeed, when Eps15 and Eps15L1 where knocked-down, alone or in combination, in C2C12-Notch1 cells, no reduction of Notch activity was observed. Moreover, no further reduction of Notch activity was observed when Eps15 and Eps15L1 were knocked-down both in the signal-sending and in the signal-receiving cell. To confirm this finding, we will test the role of Eps15 and Eps15L1 in signal-receiving cells using MEFs as a model system.

Up to now, our *in vitro* studies of OP9-Dll1 and MEF-Dll1 cells indicate that Eps15 and Eps15L1 are required for the regulation of Notch signalling in a non-redundant manner. Since Eps15/Eps15L1-DKO mice, but not single KO mice, were found to be severely affected, similar to Notch-loss-of-function mutants, their non-redundancy was unexpected. Based on this, we can conclude that the severe phenotype of Eps15/Eps15L1-DKO mice cannot be exclusively assessed as a defect in the Notch pathway. Alternatively, we can speculate that, by acting in different cellular contexts, Eps15 and Eps15L1 additively contribute to this phenotype.

2. The redundant role of Eps15 and Eps15L1 in the regulation of VEGFR-2 turnover

PECAM-1 staining of 9.5 dpc Eps15/Eps15L1-DKO mice revealed reduced vascularization in different anatomical districts (head, somites, yolk sac), due to a defect in angiogenesis. We hypothesized that impaired vascular development might be the major cause of midgestation lethality of these mice (Rossant and Howard 2002). To directly test this hypothesis, we generated cDKO mice (in detail, we generated $Eps15^{flp/flp}/Eps15L1^{-/-}/tg^{Tie2Cre}$ mice, in which Eps15L1 is ubiquitously deleted, while Eps15 is specifically deleted in endothelial and hematopoietic cells), to see whether they recapitulated the severe phenotype of constitutive Eps15/Eps15L1-DKO mice. Angiogenesis was impaired also in these mice. Nevertheless, the morphology of cDKO mice was not as seriously compromised as constitutive DKO mice and arrived at birth. This observation indicated that impaired angiogenesis was not the primary lethality cause of Eps15/Eps15L1-DKO mice.

Our *in vitro* studies on endothelial cells indicate that Eps15 and Eps15L1 have a redundant role in VEGFR-2 turnover, one of the major signalling pathways regulating vascular development: indeed, total receptor levels were reduced in Eps15/Eps15L1-DKO endothelial cells. Decreased receptor levels did not impact on the downstream signalling response, at least under the *in vitro* conditions tested. However, we cannot exclude that in the organism there are spatial and temporal defects in VEGFR-2 turnover that may addictively contribute to the *in vivo* phenotype of Eps15/Eps15L1-DKO mice.

3. The redundant role of Eps15 and Eps15L1 in TfR internalization

Previous *in vitro* studies showed that Eps15 and Eps15L1 regulate the internalization of

EGFR and TfR (Carbone, Fre et al. 1997, Benmerah, Lamaze et al. 1998, Huang, Khvorova et al. 2004). Mutant mice for EGFR are growth-retarded and die at different stages of development depending on their genetic background. Loss of EGFR in the CF-1 background leads to peri-implantation lethality; in the 129/Sv genetic background, EGFR-null embryos die around day 11.5 of gestation, whereas in other backgrounds mutant mice survive until birth (C57BL/6) or to postnatal day 20 (MF1 or C3H). Of note, all surviving mutant mice show abnormalities in various epithelia, including placenta, skin, lung and gastrointestinal tract (Miettinen, Berger et al. 1995, Sibilia and Wagner 1995, Threadgill, Dlugosz et al. 1995), and develop a progressive neurodegeneration, thus indicating an essential function for EGFR in epithelial and neuronal development. TfR-null mice die before embryonic day 12.5 (Levy, Jin et al. 1999) and have growth retardation, severe pallor and pericardial effusions and present both erythropoiesis and neural defects. Also Eps15/Eps15L1-DKO mice dye at midgestation and present morphological alterations that might be linked to impaired EGFR and/or TfR signalling, such as growth retardation, neural defects, pallor (indicative of defective vascular development) and pericardial effusions.

We used MEFs, derived from KO mice for Eps15 and Eps15L1, to confirm whether the internalization of EGFR and/or TfR was impaired upon KO of Eps15 and Eps15L1. We found that the K_e of EGFR was slightly but significantly reduced (~20%) in Eps15-KO, Eps15L1-KO and DKO cells to a similar extent. Instead, the K_e of the TfR was strongly reduced in DKO (~50%), with only a minor effect in single KO MEFs. Moreover, while surface levels of EGFR were not altered in single and double KO cells, surface levels of TfR were increased in DKO cells.

These results suggest that Eps15 and Eps15L1 have a major impact on the internalization of TfR and regulate it in a redundant manner. The function of Eps15 and Eps15L1 in this pathway may partially contribute to the *in vivo* phenotype of DKO mice.

4. The redundant role of Eps15 and Eps15L1 in the formation of clathrin-structures

In vitro studies in HeLa cells demonstrated that Eps15 and Itsn proteins redundantly regulate the internalization of TfR: siRNA interference of Eps15, Eps15L1, Itsn1 and Itsn2 reduced TfR internalization to 50% (Teckchandani, Mulkearns et al. 2012). In order to understand the molecular mechanism by which Eps15 and Eps15L1 regulate TfR internalization in MEFs, we performed co-localization studies of Eps15, Eps15L1 and Itsn1 in clathrin-structures, using AP-2 as a marker of CDE. We found that in single Eps15- and Eps15L1-KO cells, the number of AP-2-positive structures was decreased. However, Eps15 (in Eps15L1-KO) or Eps15L1 (in Eps15-KO) and Itsn1 still co-localized with AP-2 in AP-2-positive structures. Since TfR internalization was only mildly impaired in single KO cells, we may speculate that endocytic structures lacking Eps15 or Eps15L1 are still efficiently assembled, probably due to compensatory rearrangement of protein interactions. Instead, in DKO cells, we observed an increase in the number of AP-2-positive structures, and a reduced co-localization of AP-2 with Itsn1. This result suggests that in DKO cells the endocytic structures are not efficiently assembled. High resolution and live imaging studies are required to better clarify perturbations in the formation of clathrin-structures in Eps15/Eps15L1-DKO cells.

The protein levels of Itsn1 were found to be downregulated both in Eps15L1-KO and DKO cells, thus suggesting a possible role of Eps15L1 in the stabilization of Itsn1. Of note, downregulation of Itsn1 protein levels has been observed also in lower organisms null for Eps15 (Koh, Korolchuk et al. 2007, Rose, Malabarba et al. 2007, Wang, Bouhours et al. 2008) and in brain extracts from Eps15L1-KO mice (Alberici et al., unpublished results).

As reported before, the lack of one of the components of the endocytic machinery may cause compensatory rearrangement of protein interactions. By Co-IP analysis, we encountered such a mechanism in Eps15L1-KO cells. In these cells, we found that Itsn1

associated with a higher fraction of the available cellular Eps15 protein. Probably through Eps15 itself, Itsn1 associated also with more molecules of AP-2. Whether such a mechanism exists also in Eps15-KO is still under investigation. We will evaluate whether interaction of other accessory adaptor proteins, such as FCHo1/2 proteins, with the clathrin machinery are rearranged in MEFs lacking Eps15 and/or Eps15L1. Our hypothesis is that interaction of Eps15L1 with FCHo1/2 might increase upon KO of Eps15, thus overcoming the lack of Eps15. The reason to why we postulate an interaction between Eps15L1 and FCHo1/2 is based on previous mass spectrometry analysis in our laboratory, which identified an interaction between Eps15L1 and SGIP1 in the mouse brain, where SGIP1 is a protein that shares a μ-homology domain with FCHo1/2.

5. The redundant role of Eps15 and Eps15L1 in the development of RBCs

We tested whether the role of Eps15 and Eps15L1 in TfR endocytosis had a physiological relevance *in vivo*. In the organism, erythroid cells are the most avid consumers of iron and, because of this, they express high levels of TfR on the membrane. As a consequence, perturbations in proteins involved in iron uptake by TfR primarily affect the development of erythroid cells. In detail, studies in murine models indicate that the complete deletion of TfR is not compatible with life due to erythroid and neural defects (Levy, Jin et al. 1999). Instead, a less severe phenotype is observed in mice in which TfR levels are reduced or proteins involved in the intracellular trafficking of TfR are altered. These mice, indeed, suffer from microcytic hypochromic anemia, a condition characterized by defective maturation of RBCs. Based on these data, we decided to investigate whether erythroid development was affected in cDKO mice ($Eps15^{flp/flp}/Eps15L1^{-/-}/tg^{Tie2Cre}$) as an *in vivo* readout of impaired TfR internalization. In agreement with the *in vitro* finding that Eps15 and Eps15L1 are redundantly required for TfR internalization, we found that cDKO mice

suffered from microcytic hypochromic anemia: they had reduced MCV and high RDW, pale RBCs (indicative of reduced haemoglobin content within them) and high reticulocyte count. Of note, even if to a less extent, also cEps15-KO mice ($Eps15^{flp/flp}/Eps15L1^{+/+}/tg^{Tie2Cre}$) had reduced MCV, as previously observed in constitutive Eps15-KO mice (Pozzi et al., unpublished results). Since the erythroid defects were more severe in cDKO mice, these results indicate that Eps15 and Eps15L1 are redundantly required in erythroid development. Similarly to cDKO mice, data from literature show that also hematopoietic-specific KO mice for the clathrin adaptor protein PICALM suffer from microcytic hypochromic anemia and have a high RDW and an increased number of reticulocytes in the blood (Ishikawa, Maeda et al. 2015). PICALM is essential for the maturation of erythroid cells: indeed, PICALM-KO hematopoietic progenitors barely develop into an erythroid lineage when cultured for three days. This maturation defect can be linked to a role for PICALM in the regulation of TfR internalization: indeed, PICALM-KO splenic erythroblasts are characterized by impaired TfR internalization and, as a consequence, increased amounts of surface-bound Tf. Since the number of CCPs is reduced in PICALM-KO splenic erythroblasts, impaired TfR internalization is due to a role for PICALM in the maturation of CCPs (Ishikawa, Maeda et al. 2015).

Similar to PICALM, Eps15 and Eps15L1 might take part in the endocytic machinery, regulating TfR internalization in erythroid cells. Of note, PICALM contains NPF motifs for the binding to Eps15 proteins. It would be interesting to unravel the interplay among all these proteins in TfR internalization. Moreover, to investigate whether surface levels of TfR correlate with the altered development of Eps15/Eps15L1-DKO erythroid cells, we will perform a FACS analysis for CD71/TfR in these cells.

Even if Eps15 and Eps15L1 redundantly regulate erythroid development, impaired maturation of RBCs is not the major lethality cause of Eps15/Eps15L1-DKO mice as their phenotype is not recapitulated by cDKO mice ($Eps15^{flp/flp}/Eps15L1^{-/-}/tg^{Tie2Cre}$). This observation suggests that defective erythtroid development is, among others, one of the

factors that addictively contribute to the *in vivo* phenotype of DKO mice.

6. Conclusion

From previous and here presented findings we have learned that: i) Eps15L1 plays a non-redundant function in the nervous system (Alberici et al., unpublished results); ii) Eps15 and Eps15L1 contribute to the regulation of the Notch signalling pathway in signal-sending cells in a non-redundant manner; iii) Eps15 and Eps15L1 redundantly regulate VEGFR-2 turnover; iv) Eps15 and Eps15L1 play a redundant role in TfR internalization, possibly through the regulation of the assembly of AP-2-positive structures; v) Eps15 and Eps15L1 are redundantly required *in vivo* for the maturation of erythroid cells, possibly through control of TfR internalization.

All together, these findings suggest that lack of Eps15 and Eps15L1 impacts on several cellular processes that, together with other unexplored processes, might addictively contribute to the phenotypes observed in Eps15/Eps15L1-DKO mice. Based on our results, we can explain the lethality of Eps15/Eps15L1-DKO mice as a combination of perturbed physiological processes.

REFERENCES

Bakowska, J. C., R. Jenkins, J. Pendleton and C. Blackstone (2005). "The Troyer syndrome (SPG20) protein spartin interacts with Eps15." Biochem Biophys Res Commun **334**(4): 1042-1048.

Balconi, G., R. Spagnuolo and E. Dejana (2000). "Development of endothelial cell lines from embryonic stem cells: A tool for studying genetically manipulated endothelial cells in vitro." Arterioscler Thromb Vasc Biol **20**(6): 1443-1451.

Banerjee, A., A. Berezhkovskii and R. Nossal (2012). "Stochastic model of clathrin-coated pit assembly." Biophys J **102**(12): 2725-2730.

Bashkirov, P. V., S. A. Akimov, A. I. Evseev, S. L. Schmid, J. Zimmerberg and V. A. Frolov (2008). "GTPase cycle of dynamin is coupled to membrane squeeze and release, leading to spontaneous fission." Cell **135**(7): 1276-1286.

Behnia, R. and S. Munro (2005). "Organelle identity and the signposts for membrane traffic." Nature **438**(7068): 597-604.

Benmerah, A., M. Bayrou, N. Cerf-Bensussan and A. Dautry-Varsat (1999). "Inhibition of clathrin-coated pit assembly by an Eps15 mutant." J Cell Sci **112 (Pt 9)**: 1303-1311.

Benmerah, A., B. Begue, A. Dautry-Varsat and N. Cerf-Bensussan (1996). "The ear of alpha-adaptin interacts with the COOH-terminal domain of the Eps 15 protein." J Biol Chem **271**(20): 12111-12116.

Benmerah, A., J. Gagnon, B. Begue, B. Megarbane, A. Dautry-Varsat and N. Cerf-Bensussan (1995). "The tyrosine kinase substrate eps15 is constitutively associated with the plasma membrane adaptor AP-2." J Cell Biol **131**(6 Pt 2): 1831-1838.

Benmerah, A., C. Lamaze, B. Begue, S. L. Schmid, A. Dautry-Varsat and N. Cerf-Bensussan (1998). "AP-2/Eps15 interaction is required for receptor-mediated endocytosis." J Cell Biol **140**(5): 1055-1062.

Benmerah, A., V. Poupon, N. Cerf-Bensussan and A. Dautry-Varsat (2000). "Mapping of Eps15 domains involved in its targeting to clathrin-coated pits." J Biol Chem **275**(5): 3288-3295.

Boucrot, E., A. P. Ferreira, L. Almeida-Souza, S. Debard, Y. Vallis, G. Howard, L. Bertot, N. Sauvonnet and H. T. McMahon (2015). "Endophilin marks and controls a clathrin-independent endocytic pathway." Nature **517**(7535): 460-465.

Brodsky, F. M., C. Y. Chen, C. Knuehl, M. C. Towler and D. E. Wakeham (2001). "Biological basket weaving: Formation and function of clathrin-coated vesicles." Annual Review of Cell and Developmental Biology **17**: 517-568.

Calebiro, D., V. O. Nikolaev, M. C. Gagliani, T. de Filippis, C. Dees, C. Tacchetti, L. Persani and M. J. Lohse (2009). "Persistent cAMP-signals triggered by internalized G-protein-coupled receptors." PLoS Biol **7**(8): e1000172.

Carbone, R., S. Fre, G. Iannolo, F. Belleudi, P. Mancini, P. G. Pelicci, M. R. Torrisi and P. P. Di Fiore (1997). "eps15 and eps15R are essential components of the endocytic pathway." Cancer Res **57**(24): 5498-5504.

Chen, H., S. Fre, V. I. Slepnev, M. R. Capua, K. Takei, M. H. Butler, P. P. Di Fiore and P. De Camilli (1998). "Epsin is an EH-domain-binding protein implicated in clathrin-mediated endocytosis." Nature **394**(6695): 793-797.

Chen, H., G. Ko, A. Zatti, G. Di Giacomo, L. Liu, E. Raiteri, E. Perucco, C. Collesi, W. Min, C. Zeiss, P. De Camilli and O. Cremona (2009). "Embryonic arrest at midgestation and disruption of Notch signaling produced by the absence of both epsin 1 and epsin 2 in mice." Proc Natl Acad Sci U S A **106**(33): 13838-13843.

Chen, H., V. I. Slepnev, P. P. Di Fiore and P. De Camilli (1999). "The interaction of epsin and Eps15 with the clathrin adaptor AP-2 is inhibited by mitotic phosphorylation and

enhanced by stimulation-dependent dephosphorylation in nerve terminals." J Biol Chem **274**(6): 3257-3260.
Chi, S., H. Cao, J. Chen and M. A. McNiven (2008). "Eps15 mediates vesicle trafficking from the trans-Golgi network via an interaction with the clathrin adaptor AP-1." Mol Biol Cell **19**(8): 3564-3575.
Chi, S., H. Cao, Y. Wang and M. A. McNiven (2011). "Recycling of the epidermal growth factor receptor is mediated by a novel form of the clathrin adaptor protein Eps15." J Biol Chem **286**(40): 35196-35208.
Cocucci, E., F. Aguet, S. Boulant and T. Kirchhausen (2012). "The first five seconds in the life of a clathrin-coated pit." Cell **150**(3): 495-507.
Coda, L., A. E. Salcini, S. Confalonieri, G. Pelicci, T. Sorkina, A. Sorkin, P. G. Pelicci and P. P. Di Fiore (1998). "Eps15R is a tyrosine kinase substrate with characteristics of a docking protein possibly involved in coated pits-mediated internalization." J Biol Chem **273**(5): 3003-3012.
Confalonieri, S., A. E. Salcini, C. Puri, C. Tacchetti and P. P. Di Fiore (2000). "Tyrosine phosphorylation of Eps15 is required for ligand-regulated, but not constitutive, endocytosis." J Cell Biol **150**(4): 905-912.
Cupers, P., E. ter Haar, W. Boll and T. Kirchhausen (1997). "Parallel dimers and anti-parallel tetramers formed by epidermal growth factor receptor pathway substrate clone 15." J Biol Chem **272**(52): 33430-33434.
D'Souza-Schorey, C. and P. Chavrier (2006). "ARF proteins: roles in membrane traffic and beyond." Nature Reviews Molecular Cell Biology **7**(5): 347-358.
De Camilli, P. and K. Takei (1996). "Molecular mechanisms in synaptic vesicle endocytosis and recycling." Neuron **16**(3): 481-486.
DeWire, S. M., S. Ahn, R. J. Lefkowitz and S. K. Shenoy (2007). "Beta-arrestins and cell signaling." Annu Rev Physiol **69**: 483-510.
Doherty, G. J. and H. T. McMahon (2009). "Mechanisms of Endocytosis." Annual Review of Biochemistry **78**: 857-902.
Doria, M., A. E. Salcini, E. Colombo, T. G. Parslow, P. G. Pelicci and P. P. Di Fiore (1999). "The eps15 homology (EH) domain-based interaction between eps15 and hrb connects the molecular machinery of endocytosis to that of nucleocytosolic transport." J Cell Biol **147**(7): 1379-1384.
Duarte, A., M. Hirashima, R. Benedito, A. Trindade, P. Diniz, E. Bekman, L. Costa, D. Henrique and J. Rossant (2004). "Dosage-sensitive requirement for mouse Dll4 in artery development." Genes Dev **18**(20): 2474-2478.
Duarte, A., M. Hirashima, R. Benedito, A. Trindade, P. Diniz, E. Bekman, L. Costa, D. Henrique and J. Rossant (2004). "Dosage-sensitive requirement for mouse Dll4 in artery development." Genes & development **18**(20): 2474-2478.
Ehrlich, M., W. Boll, A. Van Oijen, R. Hariharan, K. Chandran, M. L. Nibert and T. Kirchhausen (2004). "Endocytosis by random initiation and stabilization of clathrin-coated pits." Cell **118**(5): 591-605.
Fallon, L., C. M. Belanger, A. T. Corera, M. Kontogiannea, E. Regan-Klapisz, F. Moreau, J. Voortman, M. Haber, G. Rouleau, T. Thorarinsdottir, A. Brice, P. M. van Bergen En Henegouwen and E. A. Fon (2006). "A regulated interaction with the UIM protein Eps15 implicates parkin in EGF receptor trafficking and PI(3)K-Akt signalling." Nat Cell Biol **8**(8): 834-842.
Fazioli, F., D. P. Bottaro, L. Minichiello, A. Auricchio, W. T. Wong, O. Segatto and P. P. Difiore (1992). "Identification and Biochemical-Characterization of Novel Putative Substrates for the Epidermal Growth-Factor Receptor Kinase." Journal of Biological Chemistry **267**(8): 5155-5161.
Fazioli, F., L. Minichiello, B. Matoskova, W. T. Wong and P. P. Di Fiore (1993). "eps15, a novel tyrosine kinase substrate, exhibits transforming activity." Mol Cell Biol **13**(9): 5814-5828.

Ferguson, S. M., G. Brasnjo, M. Hayashi, M. Wolfel, C. Collesi, S. Giovedi, A. Raimondi, L. W. Gong, P. Ariel, S. Paradise, E. O'Toole, R. Flavell, O. Cremona, G. Miesenbock, T. A. Ryan and P. De Camilli (2007). "A selective activity-dependent requirement for dynamin 1 in synaptic vesicle endocytosis." Science **316**(5824): 570-574.
Ferguson, S. M., A. Raimondi, S. Paradise, H. Shen, K. Mesaki, A. Ferguson, O. Destaing, G. Ko, J. Takasaki, O. Cremona, O. T. E and P. De Camilli (2009). "Coordinated actions of actin and BAR proteins upstream of dynamin at endocytic clathrin-coated pits." Dev Cell **17**(6): 811-822.
Ferrandon, S., T. N. Feinstein, M. Castro, B. Wang, R. Bouley, J. T. Potts, T. J. Gardella and J. P. Vilardaga (2009). "Sustained cyclic AMP production by parathyroid hormone receptor endocytosis." Nat Chem Biol **5**(10): 734-742.
Gagnon, E., S. Duclos, C. Rondeau, E. Chevet, P. H. Cameron, O. Steele-Mortimer, J. Paiement, J. J. M. Bergeron and M. Desjardins (2002). "Endoplasmic reticulum-mediated phagocytosis is a mechanism of entry into macrophages." Cell **110**(1): 119-131.
Gaidarov, I., F. Santini, R. A. Warren and J. H. Keen (1999). "Spatial control of coated-pit dynamics in living cells." Nat Cell Biol **1**(1): 1-7.
Galvez, T., J. Gilleron, M. Zerial and G. A. O'Sullivan (2012). "SnapShot: Mammalian Rab Proteins in Endocytic Trafficking." Cell **151**(1): 234-U244.
Garlanda, C., C. Parravicini, M. Sironi, M. Derossi, R. W. Decalmanovici, F. Carozzi, F. Bussolino, F. Colotta, A. Mantovani and A. Vecchi (1994). "Progressive Growth in Immunodeficient Mice and Host-Cell Recruitment by Mouse Endothelial-Cells Transformed by Polyoma Middle-Sized T-Antigen - Implications for the Pathogenesis of Opportunistic Vascular Tumors." Proceedings of the National Academy of Sciences of the United States of America **91**(15): 7291-7295.
Geminard, C., A. De Gassart, L. Blanc and M. Vidal (2004). "Degradation of AP2 during reticulocyte maturation enhances binding of hsc70 and Alix to a common site on TFR for sorting into exosomes." Traffic **5**(3): 181-193.
Gerber, H. P., A. McMurtrey, J. Kowalski, M. H. Yan, B. A. Keyt, V. Dixit and N. Ferrara (1998). "Vascular endothelial growth factor regulates endothelial cell survival through the phosphatidylinositol 3 '-kinase Akt signal transduction pathway - Requirement for Flk-1/KDR activation." Journal of Biological Chemistry **273**(46): 30336-30343.
Girao, H., S. Catarino and P. Pereira (2009). "Eps15 interacts with ubiquitinated Cx43 and mediates its internalization." Exp Cell Res **315**(20): 3587-3597.
Gould, G. W. and J. Lippincott-Schwartz (2009). "New roles for endosomes: from vesicular carriers to multi-purpose platforms." Nat Rev Mol Cell Biol **10**(4): 287-292.
Haffner, C., K. Takei, H. Chen, N. Ringstad, A. Hudson, M. H. Butler, A. E. Salcini, P. P. Di Fiore and P. De Camilli (1997). "Synaptojanin 1: localization on coated endocytic intermediates in nerve terminals and interaction of its 170 kDa isoform with Eps15." FEBS Lett **419**(2-3): 175-180.
Haugh, J. M. and T. Meyer (2002). "Active EGF receptors have limited access to Ptdlns(4,5)P-2 in endosomes: implications for phospholipase C and PI 3-kinase signaling." Journal of Cell Science **115**(2): 303-310.
Hayer, A., M. Stoeber, D. Ritz, S. Engel, H. H. Meyer and A. Helenius (2010). "Caveolin-1 is ubiquitinated and targeted to intralumenal vesicles in endolysosomes for degradation." Journal of Cell Biology **191**(3): 615-629.
Henne, W. M., E. Boucrot, M. Meinecke, E. Evergren, Y. Vallis, R. Mittal and H. T. McMahon (2010). "FCHo proteins are nucleators of clathrin-mediated endocytosis." Science **328**(5983): 1281-1284.
Hinrichsen, L., J. Harborth, L. Andrees, K. Weber and E. J. Ungewickell (2003). "Effect of clathrin heavy chain- and alpha-adaptin-specific small inhibitory RNAs on endocytic accessory proteins and receptor trafficking in HeLa cells." J Biol Chem **278**(46): 45160-45170.

Hoeller, D., N. Crosetto, B. Blagoev, C. Raiborg, R. Tikkanen, S. Wagner, K. Kowanetz, R. Breitling, M. Mann, H. Stenmark and I. Dikic (2006). "Regulation of ubiquitin-binding proteins by monoubiquitination." Nat Cell Biol **8**(2): 163-169.
Hollopeter, G., J. J. Lange, Y. Zhang, T. N. Vu, M. Y. Gu, M. Ailion, E. J. Lambie, B. D. Slaughter, J. R. Unruh, L. Florens and E. M. Jorgensen (2014). "The Membrane-Associated Proteins FCHo and SGIP Are Allosteric Activators of the AP2 Clathrin Adaptor Complex." Elife **3**.
Hrabe de Angelis, M., J. McIntyre, 2nd and A. Gossler (1997). "Maintenance of somite borders in mice requires the Delta homologue DII1." Nature **386**(6626): 717-721.
Huang, F., A. Khvorova, W. Marshall and A. Sorkin (2004). "Analysis of clathrin-mediated endocytosis of epidermal growth factor receptor by RNA interference." J Biol Chem **279**(16): 16657-16661.
Hurley, J. H. and P. I. Hanson (2010). "Membrane budding and scission by the ESCRT machinery: it's all in the neck." Nature Reviews Molecular Cell Biology **11**(8): 556-566.
Insall, R. H. and L. M. Machesky (2009). "Actin Dynamics at the Leading Edge: From Simple Machinery to Complex Networks." Developmental Cell **17**(3): 310-322.
Ishikawa, Y., M. Maeda, M. Pasham, F. Aguet, S. K. Tacheva-Grigorova, T. Masuda, H. Yi, S. U. Lee, J. Xu, J. Teruya-Feldstein, M. Ericsson, A. Mullally, J. Heuser, T. Kirchhausen and T. Maeda (2015). "Role of the clathrin adaptor PICALM in normal hematopoiesis and polycythemia vera pathophysiology." Haematologica **100**(4): 439-451.
Jutras, I. and M. Desjardins (2005). "Phagocytosis: At the crossroads of innate and adaptive immunity." Annual Review of Cell and Developmental Biology **21**: 511-527.
Kent, H. M., H. T. McMahon, P. R. Evans, A. Benmerah and D. J. Owen (2002). "Gamma-adaptin appendage domain: structure and binding site for Eps15 and gamma-synergin." Structure **10**(8): 1139-1148.
Kerr, M. C. and R. D. Teasdale (2009). "Defining macropinocytosis." Traffic **10**(4): 364-371.
Kirchhausen, T., K. L. Nathanson, W. Matsui, A. Vaisberg, E. P. Chow, C. Burne, J. H. Keen and A. E. Davis (1989). "Structural and functional division into two domains of the large (100- to 115-kDa) chains of the clathrin-associated protein complex AP-2." Proc Natl Acad Sci U S A **86**(8): 2612-2616.
Kisanuki, Y. Y., R. E. Hammer, J. Miyazaki, S. C. Williams, J. A. Richardson and M. Yanagisawa (2001). "Tie2-Cre transgenic mice: a new model for endothelial cell-lineage analysis in vivo." Dev Biol **230**(2): 230-242.
Koh, T. W., V. I. Korolchuk, Y. P. Wairkar, W. Jiao, E. Evergren, H. L. Pan, Y. Zhou, K. J. T. Venken, O. Shupliakov, I. M. Robinson, C. J. O'Kane and H. J. Bellen (2007). "Eps15 and Dap160 control synaptic vesicle membrane retrieval and synapse development." Journal of Cell Biology **178**(2): 309-322.
Koo, B. K., H. S. Lim, R. Song, M. J. Yoon, K. J. Yoon, J. S. Moon, Y. W. Kim, M. C. Kwon, K. W. Yoo, M. P. Kong, J. Lee, A. B. Chitnis, C. H. Kim and Y. Y. Kong (2005). "Mind bomb 1 is essential for generating functional Notch ligands to activate Notch." Development **132**(15): 3459-3470.
Kopan, R. and M. X. Ilagan (2009). "The canonical Notch signaling pathway: unfolding the activation mechanism." Cell **137**(2): 216-233.
Krebs, L. T., Y. Xue, C. R. Norton, J. R. Shutter, M. Maguire, J. P. Sundberg, D. Gallahan, V. Closson, J. Kitajewski, R. Callahan, G. H. Smith, K. L. Stark and T. Gridley (2000). "Notch signaling is essential for vascular morphogenesis in mice." Genes & development **14**(11): 1343-1352.
Krebs, L. T., Y. Xue, C. R. Norton, J. R. Shutter, M. Maguire, J. P. Sundberg, D. Gallahan, V. Closson, J. Kitajewski, R. Callahan, G. H. Smith, K. L. Stark and T. Gridley (2000). "Notch signaling is essential for vascular morphogenesis in mice." Genes Dev **14**(11): 1343-1352.

Lampugnani, M. G., F. Orsenigo, M. C. Gagliani, C. Tacchetti and E. Dejana (2006). "Vascular endothelial cadherin controls VEGFR-2 internalization and signaling from intracellular compartments." J Cell Biol **174**(4): 593-604.
Lampugnani, M. G., A. Zanetti, M. Corada, T. Takahashi, G. Balconi, F. Breviario, F. Orsenigo, A. Cattelino, R. Kemler, T. O. Daniel and E. Dejana (2003). "Contact inhibition of VEGF-induced proliferation requires vascular endothelial cadherin, beta-catenin, and the phosphatase DEP-1/CD148." Journal of Cell Biology **161**(4): 793-804.
Le Borgne, R. (2006). "Regulation of Notch signalling by endocytosis and endosomal sorting." Current Opinion in Cell Biology **18**(2): 213-222.
Le Borgne, R. (2006). "Regulation of Notch signalling by endocytosis and endosomal sorting." Curr Opin Cell Biol **18**(2): 213-222.
Le Roy, C. and J. L. Wrana (2005). "Signaling and endocytosis: A team effort for cell migration." Developmental Cell **9**(2): 167-168.
Levy, J. E., O. Jin, Y. Fujiwara, F. Kuo and N. C. Andrews (1999). "Transferrin receptor is necessary for development of erythrocytes and the nervous system." Nat Genet **21**(4): 396-399.
Limbourg, F. P., K. Takeshita, F. Radtke, R. T. Bronson, M. T. Chin and J. K. Liao (2005). "Essential role of endothelial Notch1 in angiogenesis." Circulation **111**(14): 1826-1832.
Lundmark, R. and S. R. Carlsson (2003). "Sorting nexin 9 participates in clathrin-mediated endocytosis through interactions with the core components." J Biol Chem **278**(47): 46772-46781.
Ma, L., P. K. Umasankar, A. G. Wrobel, A. Lymar, A. J. McCoy, S. S. Holkar, A. Jha, T. Pradhan-Sundd, S. C. Watkins, D. J. Owen and L. M. Traub (2016). "Transient Fcho1/2.Eps15/R.AP-2 Nanoclusters Prime the AP-2 Clathrin Adaptor for Cargo Binding." Developmental Cell **37**(5): 428-443.
Martina, J. A., C. J. Bonangelino, R. C. Aguilar and J. S. Bonifacino (2001). "Stonin 2: an adaptor-like protein that interacts with components of the endocytic machinery." J Cell Biol **153**(5): 1111-1120.
Massol, R. H., W. Boll, A. M. Griffin and T. Kirchhausen (2006). "A burst of auxilin recruitment determines the onset of clathrin-coated vesicle uncoating." Proc Natl Acad Sci U S A **103**(27): 10265-10270.
Mathie, A. (2007). "Neuronal two-pore-domain potassium channels and their regulation by G protein-coupled receptors." J Physiol **578**(Pt 2): 377-385.
Maurer, M. E. and J. A. Cooper (2006). "The adaptor protein Dab2 sorts LDL receptors into coated pits independently of AP-2 and ARH." Journal of Cell Science **119**(20): 4235-4246.
Mayor, S. and R. E. Pagano (2007). "Pathways of clathrin-independent endocytosis." Nature Reviews Molecular Cell Biology **8**(8): 603-612.
McMahon, H. T. and E. Boucrot (2011). "Molecular mechanism and physiological functions of clathrin-mediated endocytosis." Nature Reviews Molecular Cell Biology **12**(8): 517-533.
Miaczynska, M. and M. Zerial (2002). "Mosaic organization of the endocytic pathway." Experimental Cell Research **272**(1): 8-14.
Miettinen, P. J., J. E. Berger, J. Meneses, Y. Phung, R. A. Pedersen, Z. Werb and R. Derynck (1995). "Epithelial Immaturity and Multiorgan Failure in Mice Lacking Epidermal Growth-Factor Receptor." Nature **376**(6538): 337-341.
Motley, A., N. A. Bright, M. N. Seaman and M. S. Robinson (2003). "Clathrin-mediated endocytosis in AP-2-depleted cells." J Cell Biol **162**(5): 909-918.
Ney, P. A. (2011). "Normal and disordered reticulocyte maturation." Current Opinion in Hematology **18**(3): 152-157.
Norris, F. A., E. Ungewickell and P. W. Majerus (1995). "Inositol hexakisphosphate binds to clathrin assembly protein 3 (AP-3/AP180) and inhibits clathrin cage assembly in vitro." J Biol Chem **270**(1): 214-217.

Pece, S., M. Serresi, E. Santolini, M. Capra, E. Hulleman, V. Galimberti, S. Zurrida, P. Maisonneuve, G. Viale and P. P. Di Fiore (2004). "Loss of negative regulation by Numb over Notch is relevant to human breast carcinogenesis." Journal of Cell Biology **167**(2): 215-221.
Peter, B. J., H. M. Kent, I. G. Mills, Y. Vallis, P. J. Butler, P. R. Evans and H. T. McMahon (2004). "BAR domains as sensors of membrane curvature: the amphiphysin BAR structure." Science **303**(5657): 495-499.
Pilecka, I., M. Banach-Orlowska and M. Miaczynska (2007). "Nuclear functions of endocytic proteins." Eur J Cell Biol **86**(9): 533-547.
Polo, S. and P. P. Di Fiore (2006). "Endocytosis conducts the cell signaling orchestra." Cell **124**(5): 897-900.
Polo, S., S. Sigismund, M. Faretta, M. Guidi, M. R. Capua, G. Bossi, H. Chen, P. De Camilli and P. P. Di Fiore (2002). "A single motif responsible for ubiquitin recognition and monoubiquitination in endocytic proteins." Nature **416**(6879): 451-455.
Ponka, P. and C. N. Lok (1999). "The transferrin receptor: role in health and disease." International Journal of Biochemistry & Cell Biology **31**(10): 1111-1137.
Poupon, V., S. Polo, M. Vecchi, G. Martin, A. Dautry-Varsat, N. Cerf-Bensussan, P. P. Di Fiore and A. Benmerah (2002). "Differential nucleocytoplasmic trafficking between the related endocytic proteins Eps15 and Eps15R." J Biol Chem **277**(11): 8941-8948.
Pozzi, B., S. Amodio, C. Lucano, A. Sciullo, S. Ronzoni, D. Castelletti, T. Adler, I. Treise, I. H. Betsholtz, B. Rathkolb, D. H. Busch, E. Wolf, H. Fuchs, V. Gailus-Durner, M. H. de Angelis, C. Betsholtz, S. Casola, P. P. Di Fiore and N. Offenhauser (2012). "The endocytic adaptor Eps15 controls marginal zone B cell numbers." PLoS One **7**(11): e50818.
Raiborg, C. and H. Stenmark (2009). "The ESCRT machinery in endosomal sorting of ubiquitylated membrane proteins." Nature **458**(7237): 445-452.
Raimondi, A., S. M. Ferguson, X. Lou, M. Armbruster, S. Paradise, S. Giovedi, M. Messa, N. Kono, J. Takasaki, V. Cappello, E. O'Toole, T. A. Ryan and P. De Camilli (2011). "Overlapping role of dynamin isoforms in synaptic vesicle endocytosis." Neuron **70**(6): 1100-1114.
Rodriguez, C. I., F. Buchholz, J. Galloway, R. Sequerra, J. Kasper, R. Ayala, A. F. Stewart and S. M. Dymecki (2000). "High-efficiency deleter mice show that FLPe is an alternative to Cre-loxP." Nat Genet **25**(2): 139-140.
Rose, S., M. G. Malabarba, C. Krag, A. Schultz, H. Tsushima, P. P. Di Fiore and A. E. Salcini (2007). "Caenorhabditis elegans intersectin: A synaptic protein regulating neurotransmission." Molecular Biology of the Cell **18**(12): 5091-5099.
Rossant, J. and L. Howard (2002). "Signaling pathways in vascular development." Annu Rev Cell Dev Biol **18**: 541-573.
Roux, A., K. Uyhazi, A. Frost and P. De Camilli (2006). "GTP-dependent twisting of dynamin implicates constriction and tension in membrane fission." Nature **441**(7092): 528-531.
Roxrud, I., C. Raiborg, N. M. Pedersen, E. Stang and H. Stenmark (2008). "An endosomally localized isoform of Eps15 interacts with Hrs to mediate degradation of epidermal growth factor receptor." J Cell Biol **180**(6): 1205-1218.
Roy, M., W. S. Pear and J. C. Aster (2007). "The multifaceted role of Notch in cancer." Curr Opin Genet Dev **17**(1): 52-59.
Sadowski, P. G., A. J. Groen, P. Dupree and K. S. Lilley (2008). "Sub-cellular localization of membrane proteins." Proteomics **8**(19): 3991-4011.
Saffarian, S., E. Cocucci and T. Kirchhausen (2009). "Distinct dynamics of endocytic clathrin-coated pits and coated plaques." PLoS Biol **7**(9): e1000191.
Salcini, A. E., S. Confalonieri, M. Doria, E. Santolini, E. Tassi, O. Minenkova, G. Cesareni, P. G. Pelicci and P. P. Di Fiore (1997). "Binding specificity and in vivo targets of the EH domain, a novel protein-protein interaction module." Genes Dev **11**(17): 2239-2249.

Salcini, A. E., M. A. Hilliard, A. Croce, S. Arbucci, P. Luzzi, C. Tacchetti, L. Daniell, P. De Camilli, P. G. Pelicci, P. P. Di Fiore and P. Bazzicalupo (2001). "The Eps15 C. elegans homologue EHS-1 is implicated in synaptic vesicle recycling." Nat Cell Biol **3**(8): 755-760.
Savio, M. G., N. Wollscheid, E. Cavallaro, V. Algisi, P. P. Di Fiore, S. Sigismund, E. Maspero and S. Polo (2016). "USP9X Controls EGFR Fate by Deubiquitinating the Endocytic Adaptor Eps15." Curr Biol **26**(2): 173-183.
Schmitt, T. M. and J. C. Zuniga-Pflucker (2002). "Induction of T cell development from hematopoietic progenitor cells by delta-like-1 in vitro." Immunity **17**(6): 749-756.
Schumacher, C., B. S. Knudsen, T. Ohuchi, P. P. Di Fiore, R. H. Glassman and H. Hanafusa (1995). "The SH3 domain of Crk binds specifically to a conserved proline-rich motif in Eps15 and Eps15R." J Biol Chem **270**(25): 15341-15347.
Schwenk, F., U. Baron and K. Rajewsky (1995). "A cre-transgenic mouse strain for the ubiquitous deletion of loxP-flanked gene segments including deletion in germ cells." Nucleic Acids Res **23**(24): 5080-5081.
Scita, G. and P. P. Di Fiore (2010). "The endocytic matrix." Nature **463**(7280): 464-473.
Sengar, A. S., W. Wang, J. Bishay, S. Cohen and S. E. Egan (1999). "The EH and SH3 domain Ese proteins regulate endocytosis by linking to dynamin and Eps15." EMBO J **18**(5): 1159-1171.
Sibilia, M. and E. F. Wagner (1995). "Strain-Dependent Epithelial Defects in Mice Lacking the Egf Receptor (Vol 269, Pg 234, 1995)." Science **269**(5226): 909-909.
Sigismund, S., S. Confalonieri, A. Ciliberto, S. Polo, G. Scita and P. P. Di Fiore (2012). "Endocytosis and signaling: cell logistics shape the eukaryotic cell plan." Physiol Rev **92**(1): 273-366.
Sigismund, S., T. Woelk, C. Puri, E. Maspero, C. Tacchetti, P. Transidico, P. P. Di Fiore and S. Polo (2005). "Clathrin-independent endocytosis of ubiquitinated cargos." Proc Natl Acad Sci U S A **102**(8): 2760-2765.
Sorkin, A. and M. von Zastrow (2009). "Endocytosis and signalling: intertwining molecular networks." Nat Rev Mol Cell Biol **10**(9): 609-622.
Sorkina, T., M. Miranda, K. R. Dionne, B. R. Hoover, N. R. Zahniser and A. Sorkin (2006). "RNA interference screen reveals an essential role of Nedd4-2 in dopamine transporter ubiquitination and endocytosis." J Neurosci **26**(31): 8195-8205.
Sprinzak, D., A. Lakhanpal, L. Lebon, L. A. Santat, M. E. Fontes, G. A. Anderson, J. Garcia-Ojalvo and M. B. Elowitz (2010). "Cis-interactions between Notch and Delta generate mutually exclusive signalling states." Nature **465**(7294): 86-90.
Stenmark, H. (2009). "Rab GTPases as coordinators of vesicle traffic." Nature Reviews Molecular Cell Biology **10**(8): 513-525.
Stenmark, H. (2012). "The Rabs: A family at the root of metazoan evolution." Bmc Biology **10**.
Stimpson, H. E., C. P. Toret, A. T. Cheng, B. S. Pauly and D. G. Drubin (2009). "Early-arriving Syp1p and Ede1p function in endocytic site placement and formation in budding yeast." Mol Biol Cell **20**(22): 4640-4651.
Sundborger, A., C. Soderblom, O. Vorontsova, E. Evergren, J. E. Hinshaw and O. Shupliakov (2011). "An endophilin-dynamin complex promotes budding of clathrin-coated vesicles during synaptic vesicle recycling." J Cell Sci **124**(Pt 1): 133-143.
Swanson, J. A. (2008). "Shaping cups into phagosomes and macropinosomes." Nat Rev Mol Cell Biol **9**(8): 639-649.
Swiatek, P. J., C. E. Lindsell, F. F. del Amo, G. Weinmaster and T. Gridley (1994). "Notch1 is essential for postimplantation development in mice." Genes & development **8**(6): 707-719.
Swiatek, P. J., C. E. Lindsell, F. F. Delamo, G. Weinmaster and T. Gridley (1994). "Notch1 Is Essential for Postimplantation Development in Mice." Genes & Development **8**(6): 707-719.

Takahashi, T., S. Yamaguchi, K. Chida and M. Shibuya (2001). "A single autophosphorylation site on KDR/Flk-1 is essential for VEGF-A-dependent activation of PLC-gamma and DNA synthesis in vascular endothelial cells." Embo Journal **20**(11): 2768-2778.
Tebar, F., S. Confalonieri, R. E. Carter, P. P. Di Fiore and A. Sorkin (1997). "Eps15 is constitutively oligomerized due to homophilic interaction of its coiled-coil region." J Biol Chem **272**(24): 15413-15418.
Tebar, F., T. Sorkina, A. Sorkin, M. Ericsson and T. Kirchhausen (1996). "Eps15 is a component of clathrin-coated pits and vesicles and is located at the rim of coated pits." J Biol Chem **271**(46): 28727-28730.
Teckchandani, A., E. E. Mulkearns, T. W. Randolph, N. Toida and J. A. Cooper (2012). "The clathrin adaptor Dab2 recruits EH domain scaffold proteins to regulate integrin beta 1 endocytosis." Molecular Biology of the Cell **23**(15): 2905-2916.
Threadgill, D. W., A. A. Dlugosz, L. A. Hansen, T. Tennenbaum, U. Lichti, D. Yee, C. Lamantia, T. Mourton, K. Herrup, R. C. Harris, J. A. Barnard, S. H. Yuspa, R. J. Coffey and T. Magnuson (1995). "Targeted Disruption of Mouse Egf Receptor - Effect of Genetic Background on Mutant Phenotype." Science **269**(5221): 230-234.
Torrisi, M. R., L. V. Lotti, F. Belleudi, R. Gradini, A. E. Salcini, S. Confalonieri, P. G. Pelicci and P. P. Di Fiore (1999). "Eps15 is recruited to the plasma membrane upon epidermal growth factor receptor activation and localizes to components of the endocytic pathway during receptor internalization." Mol Biol Cell **10**(2): 417-434.
Tosoni, D., C. Puri, S. Confalonieri, A. E. Salcini, P. De Camilli, C. Tacchetti and P. P. Di Fiore (2005). "TTP specifically regulates the internalization of the transferrin receptor." Cell **123**(5): 875-888.
Traub, L. M. (2009). "Tickets to ride: selecting cargo for clathrin-regulated internalization." Nature Reviews Molecular Cell Biology **10**(9): 583-596.
Tsukazaki, T., T. A. Chiang, A. F. Davison, L. Attisano and J. L. Wrana (1998). "SARA, a FYVE domain protein that recruits Smad2 to the TGFbeta receptor." Cell **95**(6): 779-791.
Uezu, A., A. Horiuchi, K. Kanda, N. Kikuchi, K. Umeda, K. Tsujita, S. Suetsugu, N. Araki, H. Yamamoto, T. Takenawa and H. Nakanishi (2007). "SGIP1 alpha is an endocytic protein that directly interacts with phospholipids and Eps15." Journal of Biological Chemistry **282**(36).
van Bergen En Henegouwen, P. M. (2009). "Eps15: a multifunctional adaptor protein regulating intracellular trafficking." Cell Commun Signal **7**: 24.
vanDelft, S., R. Govers, G. J. Strous, A. J. Verkleij and P. M. P. V. E. Henegouwen (1997). "Epidermal growth factor induces ubiquitination of Eps15." Journal of Biological Chemistry **272**(22): 14013-14016.
Vecchi, M., S. Polo, V. Poupon, J. W. van de Loo, A. Benmerah and P. P. Di Fiore (2001). "Nucleocytoplasmic shuttling of endocytic proteins." J Cell Biol **153**(7): 1511-1517.
Ventura, A., D. G. Kirsch, M. E. McLaughlin, D. A. Tuveson, J. Grimm, L. Lintault, J. Newman, E. E. Reczek, R. Weissleder and T. Jacks (2007). "Restoration of p53 function leads to tumour regression in vivo." Nature **445**(7128): 661-665.
Wang, W., M. Bouhours, E. O. Gracheva, E. H. Liao, K. L. Xu, A. S. Sengar, X. F. Xin, J. Roder, C. Boone, J. E. Richmond, M. Zhen and S. E. Egan (2008). "ITSN-1 controls vesicle recycling at the neuromuscular junction and functions in parallel with DAB-1." Traffic **9**(5): 742-754.
Wendland, B. (2002). "Epsins: adaptors in endocytosis?" Nat Rev Mol Cell Biol **3**(12): 971-977.
Westhoff, B., I. N. Colaluca, G. D'Ario, M. Donzelli, D. Tosoni, S. Volorio, G. Pelosi, L. Spaggiari, G. Mazzarol, G. Viale, S. Pece and P. P. Di Fiore (2009). "Alterations of the Notch pathway in lung cancer." Proceedings of the National Academy of Sciences of the United States of America **106**(52): 22293-22298.

Wong, W. T., C. Schumacher, A. E. Salcini, A. Romano, P. Castagnino, P. G. Pelicci and P. P. Di Fiore (1995). "A protein-binding domain, EH, identified in the receptor tyrosine kinase substrate Eps15 and conserved in evolution." Proc Natl Acad Sci U S A **92**(21): 9530-9534.
Xie, X. H., B. S. Cho and J. A. Fischer (2012). "Drosophila Epsin's role in Notch ligand cells requires three Epsin protein functions: The lipid binding function of the ENTH domain, a single Ubiquitin interaction motif, and a subset of the C-terminal protein binding modules." Developmental Biology **363**(2): 399-412.
Xue, Y., X. Gao, C. E. Lindsell, C. R. Norton, B. Chang, C. Hicks, M. Gendron-Maguire, E. B. Rand, G. Weinmaster and T. Gridley (1999). "Embryonic lethality and vascular defects in mice lacking the Notch ligand Jagged1." Human molecular genetics **8**(5): 723-730.
Xue, Y., X. Gao, C. E. Lindsell, C. R. Norton, B. Chang, C. Hicks, M. Gendron-Maguire, E. B. Rand, G. Weinmaster and T. Gridley (1999). "Embryonic lethality and vascular defects in mice lacking the Notch ligand Jagged1." Hum Mol Genet **8**(5): 723-730.
Yaffe, D. and O. Saxel (1977). "Serial passaging and differentiation of myogenic cells isolated from dystrophic mouse muscle." Nature **270**(5639): 725-727.
Ye, W. and E. M. Lafer (1995). "Clathrin binding and assembly activities of expressed domains of the synapse-specific clathrin assembly protein AP-3." J Biol Chem **270**(18): 10933-10939.
Yuan, W. C., Y. R. Lee, S. Y. Lin, L. Y. Chang, Y. P. Tan, C. C. Hung, J. C. Kuo, C. H. Liu, M. Y. Lin, M. Xu, Z. J. Chen and R. H. Chen (2014). "K33-Linked Polyubiquitination of Coronin 7 by Cul3-KLHL20 Ubiquitin E3 Ligase Regulates Protein Trafficking." Mol Cell **54**(4): 586-600.
Zaremba, S. and J. H. Keen (1985). "Limited proteolytic digestion of coated vesicle assembly polypeptides abolishes reassembly activity." J Cell Biochem **28**(1): 47-58.
Zhu, B. M., S. K. McLaughlin, R. Na, J. Liu, Y. Cui, C. Martin, A. Kimura, G. W. Robinson, N. C. Andrews and L. Hennighausen (2008). "Hematopoietic-specific Stat5-null mice display microcytic hypochromic anemia associated with reduced transferrin receptor gene expression." Blood **112**(5): 2071-2080.
Zilian, O., C. Saner, L. Hagedorn, H. Y. Lee, E. Sauberli, U. Suter, L. Sommer and M. Aguet (2001). "Multiple roles of mouse Numb in tuning developmental cell fates." Current biology : CB **11**(7): 494-501.
Zilian, O., C. Saner, L. Hagedorn, H. Y. Lee, E. Sauberli, U. Suter, L. Sommer and M. Aguet (2001). "Multiple roles of mouse Numb in tuning developmental cell fates." Curr Biol **11**(7): 494-501.